

**NASA
Reference
Publication
1234**

January 1990

Nimbus 7 Solar Backscatter
Ultraviolet (SBUV) Ozone
Products User's Guide

Albert J. Fleig, R. D. McPeters,
P. K. Bhartia, Barry M. Schlesinger,
Richard P. Cebula, K. F. Klenk,
Steven L. Taylor, and Donald F. Heath

(NASA-RP-1234) NIMBUS 7 SOLAR BACKSCATTER
ULTRAVIOLET (SBUV) OZONE PRODUCTS USER'S
GUIDE (NASA) 117 D CSCL 04A

N90-17227

Unclas

H1/46 0256777



**NASA
Reference
Publication
1234**

1990

**Nimbus 7 Solar Backscatter
Ultraviolet (SBUV) Ozone
Products User's Guide**

Albert J. Fleig and R. D. McPeters
*Goddard Space Flight Center
Greenbelt, Maryland*

P. K. Bhartia, Barry M. Schlesinger,
Richard P. Cebula, K. F. Klenk,
and Steven L. Taylor
*ST Systems Corporation (STX)
Lanham, Maryland*

Donald F. Heath
*Goddard Space Flight Center
Greenbelt, Maryland*



National Aeronautics and
Space Administration
Office of Management
Scientific and Technical
Information Division

PREFACE

This User's Guide describes ozone data products obtained from measurements by the Solar Backscatter Ultraviolet (SBUV) instrument on Nimbus-7 from 31 October 1978 through 12 February 1987. Because of changes in the instrument's performance, the quality of the ozone data degrades beginning 13 February 1987, and the later data are not included in the data set discussed in this guide.

The HDSBUV, CPOZ, and ZMT tapes described in this User's Guide were prepared by the Ozone Processing Team of NASA/Goddard Space Flight Center. Please acknowledge the Ozone Processing Team (OPT) as the source of the data whenever reporting on results obtained using data from these tapes. The members of the OPT contributing to this effort were Albert J. Fleig (manager), P. K. Bhartia, Richard P. Cebula, Donald F. Heath, K. F. Klenk, K. D. Lee, R. D. McPeters, and Charles G. Wellemeyer.

TABLE OF CONTENTS

<u>Section</u>	<u>Page</u>
PREFACE	iii
1 INTRODUCTION	1
2 HISTORICAL BACKGROUND	3
2.1 Processing History	3
2.2 Documentation History	3
2.3 Changes Between Version 4.0 and Version 5.0	4
2.4 Experiment Team	6
2.5 Ozone Processing Team (OPT)	6
3 OVERVIEW	7
3.1 Instrument	7
3.2 Algorithm	8
3.3 Data Uncertainties and Limitations	8
3.4 Data Quality Flags	9
3.5 Tape Content	12
4 THEORETICAL FOUNDATION	15
4.1 Physical Origins of Backscattered Radiation	15
4.2 Albedos	16
5 INSTRUMENT	19
5.1 Detailed Description	19
5.2 Wavelength Calibration	20
5.3 Albedo Calibration Function	20
6 ALGORITHM	27
6.1 Albedo Measurements	27
6.2 Computation of Albedos	27
6.3 Computation of Reflectivity	29
6.4 Estimation of Surface Pressure	29
6.5 Total Ozone	30
6.5.1 Application of Tables	30
6.5.2 Best Ozone	31
6.5.3 Validity Checks	31
6.6 Profile Ozone	32
6.6.1 <i>A Priori</i> Information	33
6.6.2 Measurement Errors	34
6.6.3 Calculation of Albedos	34
6.6.4 Inversion	35
6.6.5 Validity Checks	36

7	GENERAL UNCERTAINTIES	37
7.1	Accuracy and Precision of SBUV Albedo	37
7.2	Relation Between Albedo Errors and Ozone Errors	37
7.3	Input Physics	38
7.4	Profile Resolution	39
7.4.1	Perturbation Studies	40
7.4.2	Averaging Kernels	43
7.5	Long-term Drift	45
7.6	Comparison with Other Ozone Measurements	46
8	PROBLEMS LOCALIZED IN SPACE AND TIME	51
8.1	Contamination from El Chichon	51
8.2	Problems with Antarctic Ozone Low	52
8.3	Solar Eclipses	52
9	TAPE FORMATS	55
9.1	High-Density SBUV (HDSBUV) Tape	55
9.1.1	Overall Structure	55
9.1.2	Detailed Description	56
9.2	Compressed Ozone (CPOZ) Tape	73
9.2.1	Overall Structure	73
9.2.2	Detailed Format	75
9.3	Zonal Means Tape (ZMT)	82
9.3.1	Overall Structure	82
9.3.2	Detailed Format	84
	REFERENCES	91
	RELATED LITERATURE	95
	ACRONYMS, INITIALS, AND ABBREVIATIONS	97
	<u>Appendixes</u>	
A	DEFINITION OF SBUV PROFILE LAYERS AND LEVELS	99
B	FORTRAN PROGRAMS TO READ HDSBUV, CPOZ AND ZMT TAPES	101
C	COEFFICIENTS FOR TEMPERATURE DEPENDENCE OF OZONE ABSORPTION; ATMOSPHERIC TEMPERATURE PROFILES	107
D	CLIMATOLOGICAL OZONE PROFILES USED FOR TOTAL OZONE	109
E	<i>A PRIORI</i> INFORMATION	111
F	INVENTORY OF HDSBUV TAPES	115
G	DATA AVAILABILITY AND COST	117

LIST OF FIGURES

<u>Figure</u>		<u>Page</u>
2.1	Effect of Absorption Coefficient Changes on Ozone Profile	5
4.1	Single Scattering Contribution Function	18
5.1	(Top) Accumulated Solar Exposure as a Function of Time. (Bottom) SBUV irradiance of 273 nm, normalized to value on first day of measurement	22
7.1	Effect on Retrieved Ozone of 10 percent Gaussian Change, Centered at 3.0 mbar with 10 km Full-width at Half-maximum	41
7.2	Effect on Retrieved Ozone of 5 percent Gaussian Change, Centered at 3.0 mbar with 5 km Full width at Half-maximum	42
7.3	SBUV Averaging Kernels	44
9.1	CPOZ Tape Structure - Overview	74
9.2	ZMT Structure - Overview	83

LIST OF TABLES

<u>Table</u>		<u>Page</u>
3.1	Overview of Uncertainties	9
3.2	HDSBUV Data Quality Flags	10
3.3	CPOZ Data Quality Flags	11
5.1	SBUV Wavelength Calibration	20
5.2	Calibration Constants	24
6.1	Absorption and Scattering Coefficients	28
7.1	Effect of 1 Percent Change in Albedos at All Wavelengths on Derived Mid-latitude Ozone	38
7.2	Time-Invariant Errors in Retrieved Ozone	39
7.3	Random Errors	40
7.4	Properties of Averaging Kernels	45
7.5	Experimental Uncertainties in Determining Long-term Ozone Trend	46
7.6	Bias between SBUV and Conventional Ozone Sensors	48
7.7	Drift between SBUV and Conventional Ozone Sensors	50
8.1	Percent Change in Average Profile Ozone Over Antarctica	53
8.2	Solar Eclipses	54
A.1	Standard Layers Used for Ozone Profiles	100

SECTION 1

INTRODUCTION

This document is a guide to the ozone data products obtained from the measurements by the Solar Backscatter Ultraviolet (SBUV) instrument aboard the Nimbus-7 satellite. It describes in detail the structure and content of three products: the High-Density SBUV (HDSBUV) tape, the Compressed Ozone (CPOZ) tape, and the Zonal Means Tape (ZMT). Sample software that reads the tapes appears in Appendix B. This document also discusses data quality. The derivation of the ozone values, their uncertainties, and the results of studies comparing SBUV results with those of other measurements are described. Several changes have been made in the procedures used to derive ozone values. The current version of the algorithm is designated version 5. Version 5 tapes are identified from a description in the tape standard header file. The Version 5 tapes supersede all previous versions and are the only tapes that should be used in future studies based upon SBUV data. This document supersedes previous documents describing earlier versions of the tapes.

Nimbus-7 was launched 24 October 1978; measurements began a week later. The data on the tapes cover the period from 31 October 1978 through 12 February 1987. In November 1985, some changes were introduced into the processing and validation procedure. These changes reduced the time interval between the measurements and the archival of the derived products. An instrument problem beginning 13 February 1987 resulted in a significant decline in the data quality, and, for that reason, it was decided to terminate this data set on 12 February 1987.

SBUV measures the solar irradiance and the radiance backscattered by the Earth's atmosphere in 12 selected wavelength bands in the ultraviolet. Given these radiances and irradiances, total column ozone (also referred to as total ozone), and the vertical distribution of ozone (also referred to as the ozone profile) are obtained using retrieval algorithms. SBUV views the nadir, with contiguous fields of view of 200×200 kilometers. The ozone measured for each day consists of 200 km wide strips, 26° apart in longitude. There are 13 or 14 orbits each day.

Section 2 relates this document and the data products it describes to previous documents and data products, listing the earlier versions and the changes between the current data products and the previous products. There are changes in both the derivation of the ozone values and in the format of the tapes. The changes that began in November 1985 also are described in Section 2. Section 3 provides a general overview of the SBUV instrument, the algorithm, the uncertainties in the results, and other basic information required to properly use the tapes. Section 3 is designed for the user who wants a basic understanding of the products, but who does not wish to go into details. Such a user may wish to skip Sections 4 through 8. Section 4 presents an outline of those aspects of the theory of scattering of solar radiation by the Earth's atmosphere applicable to the retrieval of ozone profiles from backscattered radiances. In Section 5, the instrument, its calibration and the characterization of its changes with time are discussed. The algorithms for retrieval of total ozone and profile ozone are described in Section 6. Section 7 describes the overall uncertainties in the ozone data and how they are estimated. Section 8 discusses two sources of uncertainty that affect limited time intervals and geographical coverage. Detailed descriptions of the tape formats appear in Section 9. Appendix A provides details of the location in pressure and altitude of the levels and layers for which data appear on the tapes. Appendix B provides sample FORTRAN programs that can be used to read the tapes. Appendixes C through E tabulate information used in the algorithm for ozone retrieval. Appendix F contains an inventory of tapes, listing the number of files on each and the time span covered. Appendix G describes how tapes may be obtained.

SECTION 2

HISTORICAL BACKGROUND

2.1 Processing History

The first 6 years of ozone data (31 October 1978 - 3 November 1984) processed using the procedures described in this document were archived at the National Space Science Data Center (NSSDC) in January 1986; data for later times have been archived as they were processed and validated. The values were generated using Version 5 of the processing software. Previous results available from the NSSDC were processed using Version 4, the only other version for which data have been archived. Several improvements have been made to the data quality, both in the algorithm and the instrument characterization. Version 5 data should be used for any future studies based upon SBUV data. The differences between Versions 4 and 5 are described in Section 2.3. The ozone profiles and total ozone values derived from the two versions of the software generally agree within 10 percent, but the difference is a function of both latitude and height.

In November 1985, the processing procedure changed. The purpose of the change was to reduce the time between a measurement and the release of the ozone values based on it. The aspect with the most significant effect on data quality was a change in the derivation of the solar irradiance. In the original procedure, solar irradiance was measured daily, but, starting November 1985, it was measured weekly, using linear interpolation to derive values for the days in between. At the shortest wavelength used by SBUV, the solar irradiance may vary by as much as 0.5 percent over the 27-day synodic rotation period of the Sun, because of the rotation of active regions. Under the new procedures, the solar irradiances used in the ozone retrieval will not reflect this variation. The higher levels of the ozone profiles will be affected, in the sense that the ozone values may be underestimated when the solar irradiance is at its maximum in the 27-day cycle and overestimated when the solar irradiance is at minimum. Use of the data after November 1985 for investigations of the relation between ozone and short-term solar variability is not recommended.

The other principal change in the procedure concerns the validation studies required before data were released. Originally, data were not released until they had been compared with measurements from ground stations. Because the ground-based data may not be available until several months after the measurements are made, this step caused a significant delay. Releasing data is no longer dependent on completed studies.

On 13 February 1987, an instrument problem developed, which produced a significant decline in the data quality. The number of measurements flagged because the chopper used to permit dark current measurements was not in synchronization increased significantly. Examination of selected ozone data following the onset of this problem revealed a sharp increase in the scatter of the profile ozone values; a systematic change cannot be ruled out. Because of this problem, the data set described in this document ends before the problem developed; the last day is 12 February 1987. Any decisions regarding release of later data will follow an assessment of the effect of the instrument problem on the ozone values.

2.2 Documentation History

The basic tapes used in deriving all other tape products are the Raw Unit Tapes (RUT). These tapes contain uncalibrated irradiance and radiance data, housekeeping data, calibration information, instrument field-of-view (FOV) location, and solar ephemeris information from SBUV. RUTs also contain information on clouds, terrain pressure, and snow-ice thickness. These tapes are discussed in a user's guide (Fleig *et al.*, 1983), which describes the experiment, instrument calibration, operating schedules and data coverage, data quality assessment, and tape formats applicable to the first two years of these tapes. Most, but not all of the information in

that user's guide remains valid. But the section on in-orbit instrument performance in particular has been superseded.

In June 1982, a user's guide to the first year of SBUV data (Fleig *et al.*, 1982) was produced, to accompany the release of that data. In addition to describing the format of the released tape, the OZONE-S, that user's guide described the algorithm used to retrieve ozone values and provided a brief outline of the theoretical foundations. The discussion in that document has served as a basis for the description of the algorithm in the present guide. Continued observation revealed that, contrary to the assumptions made at the time the first year of data had been archived, the reflectivity of the diffuser plate deployed when measuring solar irradiance was changing with time. An addendum to the first year's user's guide, produced in August 1982, discussed the effect of the failure to correct for the change in diffuser reflectivity. When two years of data became available, a user's guide to derivative products (Fleig *et al.*, 1984) was produced. This document discussed the changes in instrument sensitivity as they were understood at that time.

As the baseline of time available for deriving the instrument calibration increased, additional improvements in the characterization of the changes with time became possible. By the time 4 years of data were ready to be archived, a revised characterization function had been developed. In addition, El Chichon erupted, and provisions were needed to explain the effects of aerosol contamination on ozone retrievals. There had also been some changes in the tape format. These issues were addressed in a third and fourth year addendum (NASA, 1984) to the first year's user's guide. This document also contained a table of corrections for the effects of revisions in the instrument characterization on the first 2 years of data.

The present user's guide is intended to supersede all previous documents on the ozone tape products (Fleig *et al.*, 1982, 1984; NASA, 1984), but not the entire RUT user's guide (Fleig *et al.*, 1983).

Tape specifications for the Version 5 Compressed Ozone (CPOZ) tapes were provided to the NSSDC to accompany the tapes (NASA, 1986). The tape formats included there have been incorporated into Section 9.2, and the supplemental discussion in the CPOZ specifications document has also been adapted into this guide.

2.3 Changes Between Version 4.0 and Version 5.0

There are a number of differences between the processing that generated the currently archived Version 5 data set and the previously archived Version 4 data set. These changes were in the analysis of the change of the instrument sensitivity with time, in the values of physical constants used for the retrievals, in the retrieval algorithm, and in the tape formats.

The presence of a larger baseline of data has permitted significant improvements in the instrument characterization. Some of these changes were discussed in the third and fourth year addendum (NASA, 1984). The reprocessed data set incorporates all these changes and uses one consistent calibration starting with the launch of the instrument. The procedure used in deriving the instrument calibration is described in detail in Section 5.

New values for the ozone absorption coefficients have been incorporated into the revised algorithm. These coefficients are based on recent measurements of ozone cross-sections at the U.S. National Bureau of Standards (Paur and Bass, 1985) and were recommended for use in ozone measurement by the International Ozone Commission in its August 1984 meeting at Halkidiki, Greece. As a result of these changes, the long standing bias between SBUV and Dobson total ozone measurements has been reduced to less than 2 percent and is now within the combined experimental error of the two measurements. In addition, the new cross-sections have improved the consistency between radiances in the different SBUV bands, removing an apparent anomaly at 301.9 nm that had prevented use of this band for ozone retrievals. The effects of absorption coefficient changes on the ozone profile are dependent on solar zenith angle, as shown in Figure 2.1. The change in ozone absorption coefficients is the most significant improvement between Versions 4 and 5.

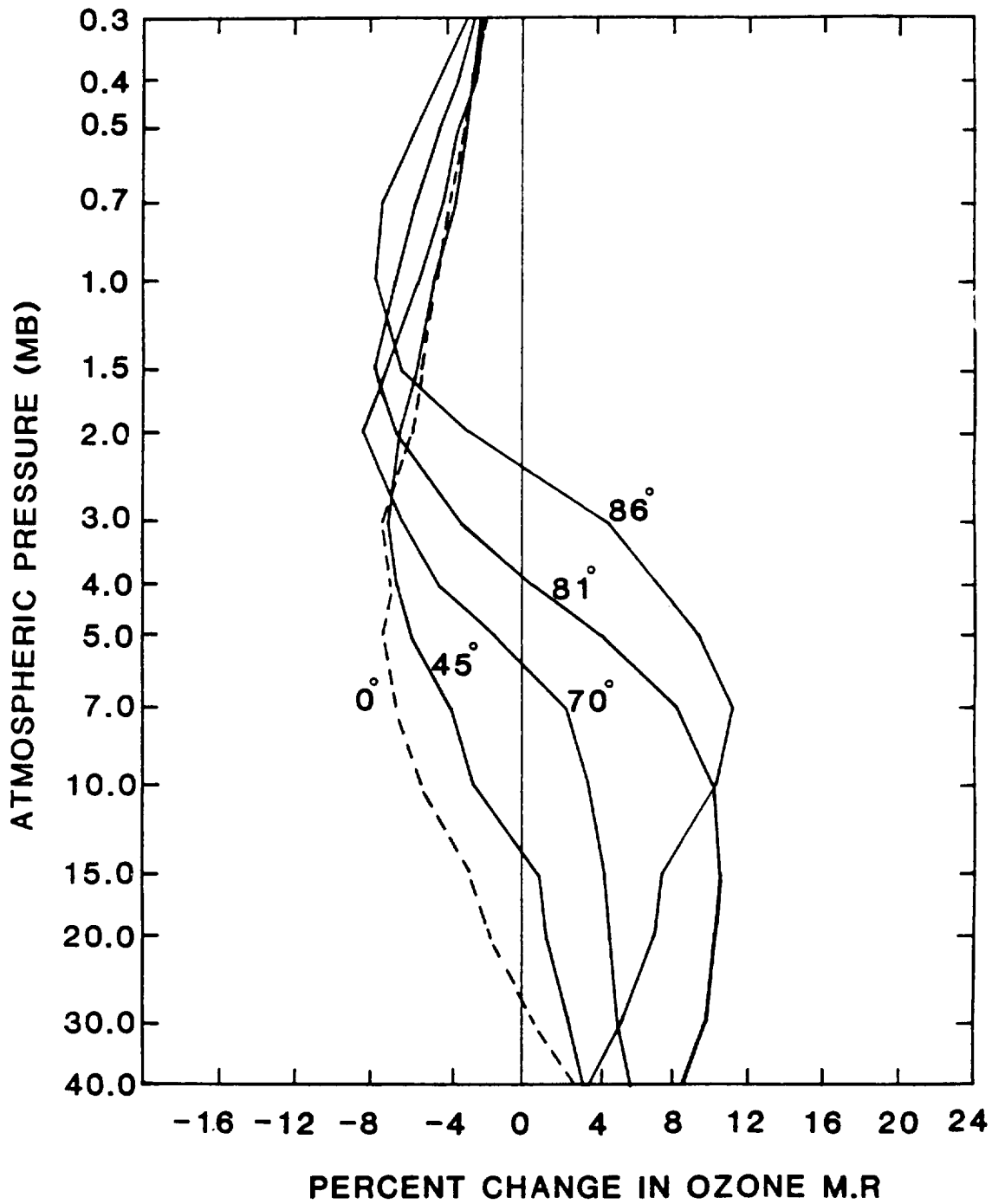


Figure 2.1. Effect of absorption coefficient changes on ozone profile, for selected solar zenith angles.

Small changes in the Rayleigh scattering coefficients have also been made to incorporate some recently published data (Bates, 1984). Table 6.1 contains the new ozone absorption and Rayleigh scattering coefficients at the SBUV wavelengths.

Several changes have been made in the retrieval algorithm:

- a. An improved *a priori* profile and associated covariance matrix.
- b. Use of the 301.9 nm wavelength band in profile retrieval.
- c. Extension of the maximum solar zenith angle for ozone retrieval from 85.7° to 88°.
- d. Use of a new wavelength pair for total ozone.
- e. A modification of the scheme used to obtain the adopted Best ozone value from the values for the three pairs.
- f. Revision to the data flagging schemes.

The effects of these changes are generally small except in the lower stratosphere or at high latitude. The Version 5 data quality for either of these conditions should be significantly improved over that for Version 4. A detailed discussion of the Version 5 algorithm appears in Section 6.

The tape formats have been modified as a result of the changes in the algorithm and in response to user requests. The most important change is that ozone mixing ratios are reported at three additional pressure levels: 50 mbar, 70 mbar, and 100 mbar, for a total of 19 levels from 0.3 mbar to 100 mbar. The layers and levels used on the tape are listed in Appendix A. In addition, the total ozone and profile data quality flags have been redefined. These flags now provide considerably more information about the data quality and allow the user to select slightly contaminated or less reliable data if necessary. However, users must now pay careful attention to the meaning of these flags in order to avoid inadvertently selecting bad data. Section 3.4 provides detailed definitions for the flags and recommendations as to which should be accepted.

2.4 Experiment Team

The combined SBUV/TOMS instrument has been supported by the Nimbus Experiment Team (NET). The regular NET members were D. F. Heath, Chairman, A. J. Krueger, C. L. Mateer, A. J. Miller, D. Cunnold, A. E. Green, A. Belmont, and W. L. Imhof. In addition, A. J. Fleig, R. D. McPeters, A. Kaveeshwar, K. F. Klenk, P. K. Bhartia, and H. Park were nominated by the NET to be Associate Members. The SBUV instrument was built by Beckman Instruments, Inc., of Anaheim, California.

2.5 Ozone Processing Team (OPT)

Algorithm development, evaluation of instrument performance, ground-truth validation, and data production were carried out by A. J. Fleig, R. D. McPeters, A. Kaveeshwar, K. F. Klenk, P. K. Bhartia, H. Park, K. D. Lee, C. G. Wellemeyer, and R. P. Cebula of the Ozone Processing Team (OPT). The OPT was managed by A. J. Fleig and supported by individuals from ST Systems Corporation and NASA/Goddard Space Flight Center.

SECTION 3

OVERVIEW

3.1 Instrument

The SBUV experiment on board the Nimbus-7 satellite is designed to measure the total column ozone and the vertical distribution of ozone in a column beneath the satellite. The instrument is an improved version of the Backscatter Ultraviolet (BUV) experiment that flew on board Nimbus-4. It contains a tandem Ebert-Fastie double monochromator with a highly linear detector system that allows it to measure ultraviolet radiation over a dynamic range of seven orders of magnitude, and a filter photometer. The satellite normally measures radiation reflected from the Earth's atmosphere directly beneath it. To measure the solar irradiance, a ground aluminum diffuser plate is deployed to reflect sunlight into the instrument. Both Earth radiance and solar irradiance can be measured in either of two modes. In *step scan* mode, the primary mode of operation, the instrument steps through 12 wavelength bands, selected for their applicability to ozone measurement, in the wavelength region between 250 nm and 340 nm. In *continuous scan* mode, the instrument measures the incoming radiation between 160 nm and 400 nm at 0.2 nm intervals.

Several improvements over the BUV instrument design have been incorporated into the SBUV instrument. The following are the principal changes:

- a. A mechanical chopper that allows measurement of the signal when the instrument is shielded from radiation, permitting elimination of the effects of charged particles and subtraction of dark current.
- b. Exposure of the diffuser plate to the Sun for only a few minutes a day rather than continuously, thereby substantially reducing the rate of degradation.
- c. Addition of continuous scan mode.

The normal operation of the instrument is measurement of Earth radiance in step scan mode. Normally, once a day, at the northern terminator of an orbit, operation switches to solar irradiance measurement in continuous scan mode. There were some periods during which solar irradiance was measured at the northern terminator of every orbit rather than once a day. During the early years of the satellite lifetime, SBUV was scheduled to operate on a cycle of 3 days on, one off, because of limits on satellite power. This schedule was not firmly established until spring 1979, and even after that time there were occasional departures from the schedule. By the summer of 1983, the failure of other experiments on the satellite had reduced their power demands, and the practice of turning SBUV off every fourth day was discontinued.

Once a week, solar irradiance is measured in step scan mode, at the same wavelengths as the Earth radiance. Also, approximately every 24 days, the instrument is dedicated to continuous scan measurements of Earth radiance. On these days, there may not be any ozone values available, or only a small number of values near midnight GMT at either the start or end of the day.

Ozone values are derived from the ratio of backscattered Earth radiance to incoming solar irradiance, the albedo. The only difference between the system used to measure Earth radiance and that used to measure solar irradiance is the deployment of the diffuser plate when solar irradiance is being measured; the other optical components are identical. Therefore, the only change in the instrument that can cause a change of the albedo with time is a change in the reflectivity of the diffuser plate. Changes in any other aspect of the optical system will affect both radiance and irradiance in the same way; their effect will cancel when the albedo is calculated from the ratio of radiance to irradiance. A more detailed description of the instrument and its calibration appears in Section 5.

3.2 Algorithm

The retrieval of total ozone is based on a table lookup and interpolation process (Klenk *et al.*, 1982). A table that gives backscattered radiance as a function of total ozone, solar zenith angle, surface pressure, surface reflectivity, and latitude is constructed. Given the computed radiances for the latitude, surface pressure, reflectivity and solar zenith angle of each radiance measurement, the total ozone value for the scan can be derived by interpolation in the table.

The wavelength dependence of the backscattered radiance for the eight shortest wavelengths measured by the experiment is a function of the ozone profile. However, this profile cannot be derived directly from the measured radiances. Because the radiances are integrals of contributions from various levels, the ozone profile solution consistent with a set of radiance measurements is not unique. Some constraints are needed in order to find the mathematical solution that represents physical reality. The profile algorithm uses an optimum statistical method (Rodgers 1976; Klenk *et al.*, 1983) to obtain profiles from the measured radiances and from *a priori* information that includes a first guess profile and an estimate of its variance, the estimated errors in the measurements, and the correlations between profile variance and errors of measurement at different levels. The *a priori* information provides a constraint on which of the solutions consistent with the measurements is to be accepted, and the optimum method governs the way in which the constraint is applied. Section 6 describes the algorithms for both total ozone and ozone profiles in greater detail.

3.3 Data Uncertainties and Limitations

The ozone values derived from the SBUV measurements have three types of uncertainties: uncertainties in the basic measurements, uncertainties in the physical quantities needed to retrieve ozone values from the measurements, and uncertainties in the mathematical procedure used to derive ozone values from the measurements. In addition, the limits on the inherent information content of the measurements must always be considered in studying the ozone values derived from SBUV. This section summarizes the essential points. Section 7 discusses these uncertainties in detail.

Table 3.1 summarizes the overall uncertainties. The time dependent drift shown is the drift of SBUV derived ozone against ozone values reported by the ground-based ozone monitoring network. The comparisons between the SBUV and ground-based measurements are presented in more detail in Section 7.6. Given the uncertainties in the measurements from the ground network, the "true" drift of the SBUV could be a factor of 1.5 greater or smaller than the numbers shown. Studies are continuing to improve these estimates.

The total ozone value derived from SBUV is the integrated amount of ozone from the top of the atmosphere down to the average altitude of the earth's surface in the instrument's instantaneous field of view. When clouds are present, the instrument cannot detect the ozone below them. In such cases, the reported total ozone includes an estimated ozone amount in the atmosphere below the clouds. This estimation procedure is described in section 6.4. It is also worthwhile to note that even in the absence of clouds, the backscattered radiances are relatively insensitive to the ozone near the surface. Therefore, the SBUV derived "total ozone" will not respond fully to fluctuations in the ozone concentration near the surface. This issue is discussed by Klenk *et al.*, (1982).

The SBUV ozone profiles are reported in two forms. The primary results from the algorithm are layer ozone amounts in Umkehr layers, defined in Table A.1, which, except for the lowest and the highest layers, are roughly 5 km in height. For the convenience of the users, the ozone values are also reported as ozone mixing ratios at 19 pressure levels.

In either case, it is important to note that the inherent vertical resolution of the measurements is about 8 km between the altitudes of 30-50 km. Below 30 km the resolution degrades rapidly. Below 20 km the SBUV has little structural information about the ozone profile; the primary information consists of the layer amount of ozone between 20 km and the

Table 3.1
Overview of Uncertainties

Type of Error	Level				
	1 mbar	3 mbar	10 mbar	30 mbar	Total
Random (rms)	5%	3%	5%	10%	2%
Absolute (bias)	7%	5%	5%	6%	3%
Time-dependent (drift) over 8 years	10%	8%	5%	3%	3%

reflecting surface. Above 50 km the information provided is generally not useful except at high solar zenith angles. Very close to the terminator the range of validity extends up to 60 km. The limited vertical resolution of the backscatter ultraviolet technique must be considered in studies of the ozone vertical profiles derived from SBUV. Perturbations in the ozone profile that extend over an altitude range greater than the SBUV's inherent vertical resolution will generally be reported faithfully. Perturbations that are more limited in altitude range will be underestimated in magnitude and broadened in altitude. Also, some shape distortion may occur for narrow perturbations. These issues are discussed in more detail in Section 7.4.

3.4 Data Quality Flags

The data quality flags describe the quality of the retrieved ozone values. The flag values appear in words 26 (THIR total ozone flag), 40 (non-THIR total ozone flag), and 157 (profile flag) of the data record of the HDSBUV tape, and in word 10 of the data record on the CPOZ tape. The data quality flags on the HDSBUV tape are two-digit integers and the flag on the CPOZ tape is a three-digit integer. The units digit describes the optical path length, warns of a discrepancy between ozone values derived from different wavelength pairs, or, on the HDSBUV tape, explains why good ozone values could not be retrieved from the scan. The tens digit on the CPOZ flag indicates the presence or absence of contamination by volcanic aerosols. The tens digit on the HDSBUV flags and the hundreds digit on the CPOZ flag signify whether the measurement was made on the ascending or descending part of the orbit. The total ozone flags are discussed in detail in Section 6.5.3 and the profile flags in Section 6.6.5. Table 3.2 summarizes the significance of each flag on the HDSBUV tape, and Table 3.3 provides a similar summary for the CPOZ tape.

Total ozone data quality degrades as the optical path of the ultraviolet radiation through the atmosphere increases. For the purpose of setting the CPOZ and HDSBUV total ozone data flag indicators the path length is characterized by the product of air mass and total column ozone, in units of atm-cm. In the SBUV viewing geometry, for a typical 350 matm-cm column ozone amount, low path would represent all measurements with solar zenith angles less than 72.3°, high path would include measurements between 72.3° and 83.6°, and very high path would extend up to 88°. Data are not processed for solar zenith angles greater than 88°. A value of 4 for the units digit indicates that the differences among the three total ozone values derived independently from the three wavelength pairs are outside a selected tolerance. Flag 4 rarely occurs at small solar zenith angles. However, at large solar zenith angles, a user may wish to accept total ozone values with a data quality flag of 4 if noisy data are preferable to no data at all. Such situations

Table 3.2
HDSBUV Data Quality Flags

<u>Code</u>	<u>Total Ozone (Words 26, 40)</u>	<u>Profile (Word 157)</u>
Units Digit		
0	Low path (air mass x total ozone ≤ 1.5 atm-cm)	Good profile
1	High path (1.5 atm-cm < air mass x total ozone ≤ 3.5 atm-cm)	Ozone for 3 lowest layers deviates from climatology; probable volcanic contamination
2	Very high path (air mass x total ozone > 3.5 atm-cm)	Profile total ozone inconsistent with Best ozone from total ozone algorithm
3	Spare	Large final residue
4	Large disagreement among A,B,C pair total ozone	Initial residue > 60%
5	Best total ozone and profile total ozone inconsistent	C (equation 25) outside 0.5-3.0 mbar
6	Spare	σ (equation 25) outside 0.3-0.8 mbar
7	Photometer and monochromator reflectivity differ by more than 0.15	Reflectivity outside range - 0.05 to 1.05, or changes by more than 0.05 between consecutive wavelengths
8	Reflectivity outside - 0.05 to 1.05 range	No Best total ozone available
9	Derived total ozone outside range of tables	Bad counts or missing measurements
Tens digit		
0x	Ascending part of orbit	
1x	Descending part of orbit	

Table 3.3
CPOZ Data Quality Flags

Units Digit

- 0 Low path (air mass x total ozone \leq 1.5 atm-cm)
- 1 High path (1.5 atm-cm < air mass x total ozone \leq 3.5 atm-cm)
- 2 Very high path (3.5 atm-cm < air mass x total ozone)
- 4 Large disagreement among A, B, C pair values

Tens Digit

- 0x Acceptable ozone profile
- 1x Significant volcanic aerosol contamination present;
some contamination of surrounding areas likely

Hundreds Digit

- 0xx Ascending part of orbit (80°S to 80°N)
- 1xx Descending part of orbit (80°N to 80°S)

normally occur near the winter solstice. When the latitude of the terminator approaches 67°, there may be no total ozone measurements close to the terminator with flags less than 4.

High altitude volcanic aerosols affect ozone profile values near the altitude where the aerosols are located. The magnitude of the error depends strongly on the altitude of the aerosol layer; aerosols at altitudes below 20 km have practically no effect on the SBUV ozone measurement.

For about six months after the April 1982 eruption of the volcano El Chichon, a large fraction of the SBUV data in the northern tropics is flagged for volcano contamination. During this period, those SBUV profile data for altitudes below the 5 mbar pressure level with a tens digit volcano contamination flag of 1 in word 10 of the CPOZ tape or a units digit lower level anomaly flag value of 1 in word 157 of the HDSBUV tape should not be used for analysis. Some surrounding data, even if not flagged, should also be rejected. *Data for altitudes above the 5 mbar pressure level and the total ozone measurements are not affected by the presence of aerosols.* For further discussion see Section 8.1.

Although profile ozone values are returned for HDSBUV profile flag values greater than 1, these flag values mark problems with the retrieval and use of these data is not recommended.

Finally, the tens digit of the HDSBUV flag and the hundreds digit on the CPOZ flag distinguish SBUV data taken during the ascending part of the Nimbus-7 orbit (as the satellite moves from 80°S to 80°N) from data taken during the descending part (80°N to 80°S). During most of the descending part of the orbit, the subsatellite point is in darkness, and no ozone

measurements are possible. However, at high latitudes near the summer pole, in the regions of midnight sun, data will be obtained twice at the same latitude: once from the normal midday ascending orbit measurement, and once from the nightside descending orbit measurement. The data from the descending part of the orbit will have a larger solar zenith angle and path length than that for the ascending part of the orbit at the same latitude; they will, in general, be noisier and less accurate. We recommend that data with a flag value for the descending part of orbit normally not be used for analysis. The exception to this rule is for lower mesospheric ozone (0.3 to 1 mbar) derived from SBUV. The radiance weighting functions shift to higher altitudes for higher solar zenith angles, and, therefore, for these higher levels, the descending data will be of better quality than the ascending data.

To summarize, the best compromise between coverage and data quality is obtained for the CPOZ data if one accepts flags 0-2 and 10-12 for total ozone and flags 0 through 14 for ozone profiles above the altitude of the 5 mbar pressure level; for profiles below the altitude of 5 mbar only flags 0-2 should be accepted, and data from areas surrounding regions with flag 10-14 values should be considered suspect. For HDSBUV, the best mix of data quality and completeness of coverage is attained by accepting total ozone flags 0-2 for total ozone data, profile flags 0-1 at 5 mbar and higher altitudes, and profile flag 0 only for the profile from the 5 mbar level to the ground.

3.5 Tape Content

Three kinds of tape products are archived at the National Space Science Data Center: the High Density SBUV (HDSBUV) tape, the Compressed Ozone (CPOZ) tape, and the Zonal Means Tape (ZMT).

The HDSBUV tape is the most detailed compilation of information from the SBUV experiment and the process of retrieving ozone values. The tape includes instrument field-of-view location, solar ephemeris information, calibrated albedos, numerous quantities that are calculated during the derivation of the ozone values, and the derived total ozone and ozone profiles. Only users who are interested in the details of the ozone derivation will find all the information on this tape useful.

The first record on each data file of an HDSBUV tape includes date, time, latitude and longitude of the first scan on the file, solar irradiance for the day, count-to-radiance conversion factors, instrument wavelengths, ozone absorption coefficients, and indicators of which of the possible processing options have been exercised. Each data record includes subsatellite latitude and longitude, solar zenith angle, albedos, cloud information based upon Temperature-Humidity Infrared Radiometer (THIR) measurements, total ozone values from each of the wavelength pairs used, and reflectivities. Each data record also includes auxiliary quantities that can be used to evaluate the accuracy of the results, ozone mixing ratios at selected levels and ozone contents of selected layers, reflectivities for the wavelengths used, quantities that can be used to evaluate the uncertainty in the profiles, and a volcanic aerosol contamination index. A full description of the HDSBUV tape appears in Section 9.1.

The CPOZ tape contains ozone values for all individual measurements made by the SBUV instrument, uncertainties, location, and selected physical data used in deriving the ozone values. The information on it is stripped from the HDSBUV tape. Users who are interested in the complete ozone data set, but not in the fine details of the process of derivation, will find this tape to be the most useful of the products.

The first record on each data file of a CPOZ tape includes the date, time, orbit number, and subsatellite latitude at the start of each scan, the instrument wavelengths, the solar irradiance at each wavelength, the ozone absorption coefficients at each wavelength, and the count to radiance conversion for a particular gain range at each wavelength. A data record includes the latitude, longitude and solar zenith angle for each scan, a data quality flag, volcano contamination index, albedos, total ozone value, ozone amounts in 12 layers, their uncertainties, and mixing ratios at 19 selected pressure levels. The layers are defined precisely in Appendix A and the levels on page 68. Section 9.2 describes the tape in detail.

A ZMT includes daily, weekly, monthly, and three-month seasonal averages for mixing ratios at 19 selected pressure levels and for total ozone. The ozone averages are for zones of 10-degree width centered at the equator and at 10-degree intervals from it. A ZMT also includes the standard deviation of the zonal average and the highest and lowest values used in computing the average. Zonal mean reflectivity, standard deviation, and maximum and minimum values are also present on the tape. ZMT specifications appear in Section 9.3.

Zonal averages for a given period are obtained by averaging all measurements with appropriate data quality flags for that period (i.e., monthly averages are averages of all measurements in the month, not of daily averages). The decision as to which data quality flags should be accepted follows the recommendations of Section 3.4. The standard deviation is obtained during the calculation of this average. The standard deviation of a daily average includes contributions from both random variability and longitudinal scatter. That for periods longer than a day will have an additional component due to actual changes in ozone with time. Unavailability of averages over periods of a week and longer, marked by zero values for ozone and standard deviation, occurs almost always in polar winter night regions, where the sun is at too large a zenith angle or is below the horizon during the reporting period. In latitude zones crossed by the line of maximum zenith angle during a particular month or season the average on the tape may not be derived from data over the entire month or season but only a part of it.

SECTION 4

THEORETICAL FOUNDATION

4.1 Physical Origins of Backscattered Radiation

To interpret the radiance measurements made by the SBUV instrument requires an understanding of how the Earth's atmosphere scatters ultraviolet radiation as a function of solar zenith angle. Incoming solar radiation undergoes absorption and scattering by atmospheric constituents such as ozone, Rayleigh scattering, and scattering by aerosols. Radiation that penetrates to the troposphere is scattered by clouds, and radiation that reaches the ground is scattered by surfaces of widely differing reflectivity. The wavelengths chosen for measurements by SBUV were selected because of their high ozone absorption. At all of these wavelengths absorption by other atmospheric components is normally negligible compared to that of ozone. However, at 255 nm, nitrogen oxide γ -band emission has a non-negligible contribution, and this wavelength has, therefore, not been used in SBUV ozone retrievals. The ozone absorption coefficients differ from band to band, increasing as the wavelength decreases. Consequently, as wavelength decreases, significant absorption occurs at progressively higher levels in the atmosphere. Although in principle the backscattered intensity at a given wavelength depends upon the entire ozone profile $x(p)$ from the top of the atmosphere to the surface, in practice it is sensitive only to the profile for a restricted range in altitudes. Consequently, measurements of backscattered radiation at shorter wavelengths yield information on the ozone profile at higher levels of the atmosphere than measurements at longer wavelengths.

At wavelengths shorter than about 295 nm, solar radiation is almost completely absorbed above the ozone density peak at 20-25 km. Because the intensity of the backscattered radiation at these wavelengths is determined solely by the ozone profile above the peak, it can be used to derive that part of the ozone profile. At these wavelengths, tropospheric features, including clouds, aerosols and terrain height, do not affect the radiation scattering and can be ignored. The computation of atmospheric scattering for the shorter wavelengths is easier than it is for the longer wavelengths.

Between 295 nm and 310 nm, scattering takes place over a wide range of altitudes. The backscattered intensity depends upon the height of the ozone peak as well as the ozone amount below the peak. Radiation at these wavelengths thus provides profile information near and below the ozone peak.

For wavelengths longer than 310 nm, the backscattered radiance consists primarily of solar radiation that penetrates the stratosphere and is reflected back by the dense tropospheric air, clouds, aerosols and the Earth's surface; scattering takes place predominantly in the troposphere. For these wavelengths, the backscattered intensity is determined primarily by the total optical depth of the atmosphere above the scattering layer; details of vertical variation in the optical depth function $\tau_{\lambda}(p)$ become largely unimportant. The amount of ozone below the scattering layer is small and can be estimated with sufficient accuracy to permit derivation of total column ozone. Because most of the ozone is in the stratosphere, the principal effect of the total atmospheric ozone is to attenuate both the solar flux going to the troposphere and the component reflected back to the satellite. This separation of the absorbers in the stratosphere (i.e., ozone) and the "reflector" in the troposphere (i.e., atmospheric scattering, clouds and Earth surface) causes backscattered radiances longer than 310 nm to depend weakly on the distribution of ozone in the stratosphere.

Derivation of atmospheric ozone content from measurements of the backscattered radiance requires a treatment of scattering from the Earth's surface, by clouds, and by other aerosols. These scattering processes are not isotropic; the scattered light depends upon both incident angle and viewing angle. In principle, then, the reflectivity is a function of solar zenith angle. Studies by Dave (1978) and by Fraser and Ahmad (1978) show that, in practice, the contribution of clouds and aerosols to the backscattered intensity can be treated by assuming that radiation is reflected from a particular pressure level called the "scene pressure" with an effective "scene

reflectivity" R. Thus, in addition to deriving a reflectivity for the albedo calculations, a pressure level for the effective reflecting surface must be defined for each instantaneous field of view (IFOV).

4.2 Albedos

The calculation of albedos follows the formulation of Dave (1964). We define the backscattered albedo as the ratio of the radiance backscattered from the Earth/atmosphere to the solar irradiance incident on the top of the atmosphere. Consider an atmosphere bounded below by a Lambertian surface of reflectivity R. For unit incident solar irradiance at a solar zenith angle of θ_0 , the intensity I of the radiation scattered toward the zenith can be expressed as

$$I(\theta_0, R, \tau) = I_0(\theta_0, \tau) + RI_s(\theta_0, \tau)f_1(\tau)/[1-Rf_2(\tau)], \quad (1)$$

where the two terms on the right hand side represent the atmospheric and surface contributions to the backscattered radiation, respectively. I_s is the intensity of direct and diffuse radiation reaching the surface, f_1 is the fraction of reflected radiation directed towards the zenith, and f_2 is the fraction of reflected radiation scattered back to the surface. These quantities are complex functions of θ_0 and $\tau_\lambda(p)$; the latter represents the optical depth of the atmosphere at wavelength λ as a function of the atmospheric pressure p. The product of I_s and f_1 is often combined into one term designated as T. For an atmosphere containing only Rayleigh scatterers and ozone, $\tau_\lambda(p)$ can be written as $\tau_\lambda(p) = \alpha_\lambda x(p) + \beta_\lambda p$, where, $x(p)$ is the column ozone amount above a pressure p, α_λ is the ozone absorption coefficient, and β_λ is the Rayleigh scattering coefficient averaged over the instrument bandpass centered at λ .

At wavelengths below 290 nm, little solar radiation penetrates below 30 km, permitting surface, cloud, and aerosol effects to be ignored; since radiation is scattered from a region of the atmosphere which is optically thin for scattering, multiple scattering effects may also be ignored. For such cases the backscattered intensity I in (1) can be explicitly written to a high degree of accuracy as

$$I_\lambda = (1/4\pi)F_\lambda\beta_\lambda P(\cos\theta_0) \int \exp [-s(\alpha_\lambda x + \beta_\lambda p)] dp. \quad (2)$$

This expression for I_λ is commonly described as the single scattering radiance.

The Rayleigh phase function $P(\cos\theta_0)$, assuming a depolarization factor of .035 (Bates, 1984), can be written as

$$P(\cos\theta_0) = .7629 (1 + 0.932 \cos^2\theta_0). \quad (3)$$

The slant path (air mass) s can be approximated by $1+\sec(\theta_0)$ at low solar zenith angles (60°), or by the Chapman (1931) function at moderate solar zenith angles ($<80^\circ$). For solar zenith angles greater than 80° , s must be treated as a function of p, calculated by ray-tracing.

It is convenient to describe the ratio of backscattered to incident radiation in terms of a parameter Q_λ , defined by the following expression:

$$Q_\lambda = \{4\pi/[(\beta_\lambda P(\cos\theta_0))]\} (I_\lambda/F_\lambda). \quad (4)$$

For the single scattering case defined by (2),

$$Q_\lambda = \int C_\lambda(p) d(\log p), \quad (5)$$

where

$$C_\lambda(p) = \delta Q_\lambda / \delta \log p = p \exp [-s(\alpha_\lambda x + \beta_\lambda p)]. \quad (6)$$

Q_λ , which is the product of the single scattering albedo and physical and numerical constants, has the dimensions of pressure. Its value is typically close to the pressure near which most of the radiation at wavelength λ is backscattered. $C_\lambda(p)$ is called the contribution function. It defines the shape of the scattering layer and is plotted in Figure 4.1 for the SBUV wavelength bands (see Table 5.1). The contribution function derived in (6) completely describes the scattering layer only for wavelengths shorter than 290 nm.

For longer wavelengths, in addition to the single scattering component described by (2), there is an additional component of the backscattered radiation originating in the dense troposphere and at the Earth's surface. This additional component is described as multiple scattering and reflectivity (MSR). The position p_{\max} of the peak of the contribution function is derived by setting $dC_\lambda/dp = 0$, which gives

$$\beta_\lambda s p_{\max} + \alpha_\lambda s \, dx/d \log p = 1. \quad (7)$$

This result shows that, in general, there can be two peaks in the contribution function, one determined by the strength of ozone absorption at a given wavelength ($\alpha_\lambda s$), the other by the optical path for Rayleigh scattering ($\beta_\lambda s$). The former peak occurs where the partial pressure of ozone in the atmosphere ($dx/d \log p$) attains a value equal to $(\alpha_\lambda s)^{-1}$ and the latter peak is at a pressure equal to $(\beta_\lambda s)^{-1}$. For the shorter SBUV wavelengths the former peak dominates the latter, lower tropospheric peak because of the strong attenuation of the ultraviolet light near the ozone peak. However, at moderately absorbing wavelengths near 300 nm, both peaks can have equal strength, as seen in Figure 4.1.

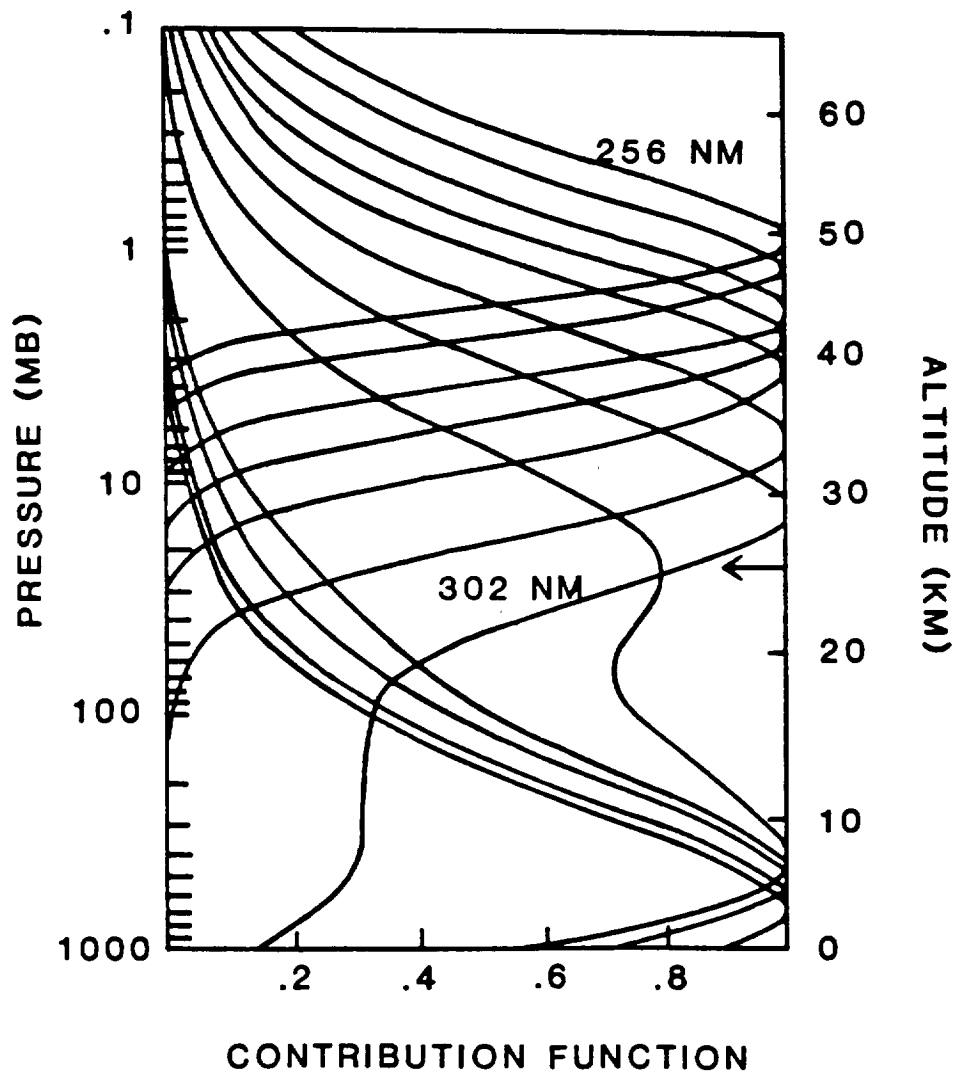


Figure 4.1. Single scattering contribution function.

SECTION 5

INSTRUMENT

5.1 Detailed Description

Descriptions in greater detail of the instrument and its calibration appear elsewhere (Heath *et al.*, 1975; Cebula *et al.*, 1988). This section, some of which has been adapted from the latter paper, will discuss those aspects useful for understanding the ozone data.

The double monochromator and the photometer discussed in Section 3.1 are mounted to look in the nadir direction with coincident fields of view of $11.3^\circ \times 11.3^\circ$. As the satellite moves in its Sun-synchronous, retrograde orbit, the instantaneous field of view (IFOV) traces out 200 km wide swaths on the ground, separated by 26-degree longitude intervals between successive orbits. The satellite footprint moves at a speed of roughly 6 km/sec. The SBUV has five operating modes which determine data processing sequences, data formats and the SBUV wavelength cam operation:

- a. Step scan mode.
- b. Wavelength calibration mode.
- c. Cage cam mode.
- d. Continuous scan mode.
- e. Scan off mode.

The primary operating mode of the SBUV is step scan mode. In this mode, the SBUV instrument measures photometric responses at each of the 12 wavelength channels listed in Table 5.1 with a 1 nm bandwidth. The wavelength cam is sequentially driven from the 339.9 nm to the 255.6 nm position. The first measurement occurs 0.88 second after the start of the scan. After reaching each wavelength position, the cam stops and a 1-second integration is performed. The cam then advances to the next position, requiring approximately 0.5 second. The cycle repeats until all 12 wavelength positions have been covered (in 18 seconds). After completing the last measurement, the cam continues until the cage position is reached. The entire sequence requires 32 seconds and is repeated until a different mode command is issued. The step scan measurements of backscattered Earth radiance are used to obtain the radiances from which albedos are derived.

For every monochromator measurement in the step scan mode, the photometer takes a simultaneous measurement in a fixed band centered at 343 nm with a 3.0 nm bandwidth. The photometer measures the effective UV reflectivity of the surface in the IFOV, monitoring reflectivity variations as the subsatellite scene changes during the course of a scan.

In continuous scan mode, the SBUV instrument scans from 160 nm to 400 nm in 0.2 nm increments, sampling data at 80 millisecond intervals. One complete wavelength scan in this mode requires 112 seconds (seven VIP major frames). During the first major frame, the SBUV wavelength cam advances to the beginning of the spectral region; the complete data sampling is done during the next six major frames. The solar irradiance used in calculating the albedo is based on continuous scan mode measurements, as discussed in Section 5.3.

For the wavelength calibration mode, the mercury-argon lamp is turned on and the diffuser plate deployed to reflect light from the lamp into the instrument. The physical scan operation is similar to that of step scan mode, although the wavelengths are different. Wavelength calibration is discussed in greater detail in the following section.

Additional details and descriptions of the other modes are provided in the RUT User's Guide (Fleig *et al.*, 1983).

Because of signal contamination by charged particles, BUUV on Nimbus-4 was unable to measure ozone values when the satellite was passing through the South Atlantic Anomaly. To eliminate this problem, an optical chopping system was incorporated into SBUV. The system operates at a frequency of 25 Hz. The background measured during the dark time of the chopped signal is subtracted from the signal obtained when the instrument is exposed to ultraviolet radiation. This subtraction thus eliminates contributions to the signal from charged particle contamination and enables the SBUV instrument to obtain ozone measurements over the South Atlantic Anomaly. It also provides a straightforward correction for dark current.

5.2 Wavelength Calibration

Scans of the mercury-argon lamp for wavelength calibration are normally made about twice a week. The wavelength scale is based upon observations of the position of six selected mercury lines, five of which are in the section of the spectrum used in deriving albedos for ozone retrieval, and on observations of the Ca II H and K lines from the solar irradiance measurements. The derived wavelengths are based on measurements made during the period 11 August - 5 November 1983. Changes in the wavelength scale are monitored through observations of the position of four of the mercury lines, three in the region of the spectrum used in ozone retrieval. Some drift in the instrument wavelength scale, probably the result of cam wear, has been observed. Table 5.1 shows the derived rate of drift at each of the 12 step wavelengths used in the ozone measurement, along with the values of the wavelengths as they are used in the retrieval software. One thousand orbits correspond to approximately two months. The uncertainty of these wavelength drifts is very small, less than 0.01 nm over six years. The absolute wavelengths at launch are not known as accurately as the wavelength drifts. To determine absolute wavelengths, the grating angle was measured in the laboratory using a micrometer with the cam positioned at each of the 12 machined steps corresponding to the 12 wavelengths. The estimated uncertainty of this procedure is ± 0.05 nm.

Table 5.1
SBUV Wavelength Calibration

Prelaunch Vacuum Wavelength (nm)	Wavelength Drift (nm per 1000 orbits)
255.65	-4.73×10^{-4}
273.61	-6.54×10^{-4}
283.10	-7.49×10^{-4}
287.70	-7.96×10^{-4}
292.29	-8.42×10^{-4}
297.59	-8.95×10^{-4}
301.97	-9.39×10^{-4}
305.87	-9.79×10^{-4}
312.56	-1.05×10^{-3}
317.56	-1.10×10^{-3}
331.26	-1.23×10^{-3}
339.89	-1.32×10^{-3}
343.3 (Photometer)	(Not measured)

5.3 Albedo Calibration Function

The albedo calibration function supplies a correction to the measured albedos for those changes in the instrument sensitivity that affect the albedo measurement. This function is

determined from the instrument output in the solar irradiance measurement mode. Changes in the instrument output have five possible sources of origin:

- a. Changes in the gain or detection efficiency of the photomultiplier tube (PMT).
- b. Changes in the gain of the electronic amplifiers.
- c. Changes in the transmissivity of the optical components of the system.
- d. Variations in the solar irradiance.
- e. Changes in the reflectivity of the diffuser plate.

The first four of these changes affect both the irradiance and the radiance measurements and together constitute the function $f_\lambda(t)$, called the albedo calibration function. Only changes in the diffuser plate affect the albedo.

The instrument count C_λ in the irradiance mode can be written as follows:

$$C_\lambda(t)/C_{o\lambda} = f_\lambda(t)[R_\lambda(\alpha,\beta,t)/R_{o\lambda}(\alpha,\beta)][d_o^2/d^2(t)], \quad (8)$$

where R_λ is the diffuser reflectivity, α is the solar elevation relative to the diffuser plate, β is the solar azimuth relative to the diffuser plate, and d is the Earth-Sun distance in astronomical units (a.u.). The zero subscript signifies values for the first day of solar measurement. The diffuser reflectivity is an explicit function of time and of the direction of incidence of sunlight on the diffuser plate. The dependence of the reflectivity on the solar elevation and azimuth is described as the goniometric properties of the diffuser plate. The form of (8) shows that only variations in the intrinsic solar irradiance are included in f_λ ; the variations in the count rate due to changes in the Earth-Sun distance appear explicitly in (8). The instrument count c_λ in the radiance mode is given by the following expression:

$$c_\lambda(t)/c_{o\lambda} = [I_\lambda(t)/I_{o\lambda}]f_\lambda(t)[F_{o\lambda}/F_\lambda(t)][d_o^2/d^2(t)], \quad (9)$$

where I_λ represents the measured radiance, and F_λ the solar flux incident at the Earth. The measured radiance varies with the incident solar irradiance and, therefore, that contribution to $f_\lambda(t)$ is divided out.

Because the ozone values are derived from the albedos (I/F), it is convenient to rewrite (9) in the following form:

$$[I_\lambda(t)/F_\lambda(t)] = [I_{o\lambda}/F_{o\lambda}][c_\lambda(t)/c_{o\lambda}]/\{f_\lambda(t)[d_o^2/d^2(t)]\}. \quad (10)$$

To compute $f_\lambda(t)$ from (8) requires the functional form of $R(\alpha,\beta,t)$. Diffuser degradation is believed to arise when surface contaminants deposited on the diffuser either before launch or in flight are made opaque by exposure to sunlight. The process is analogous to the exposure of a photographic plate and is described by the same mathematical formulation. The diffuser degradation rate parameter r_λ is defined by the expression:

$$r_\lambda = -1/R_\lambda \cdot \delta R_\lambda / \delta E, \quad (11)$$

where E is the total hours of solar exposure received by the diffuser plate since launch. Figure 5.1 shows E as a function of time; the irradiance output of the instrument at 273.5 nm is also shown. Note that the instrument output is anticorrelated with the accumulated exposure.

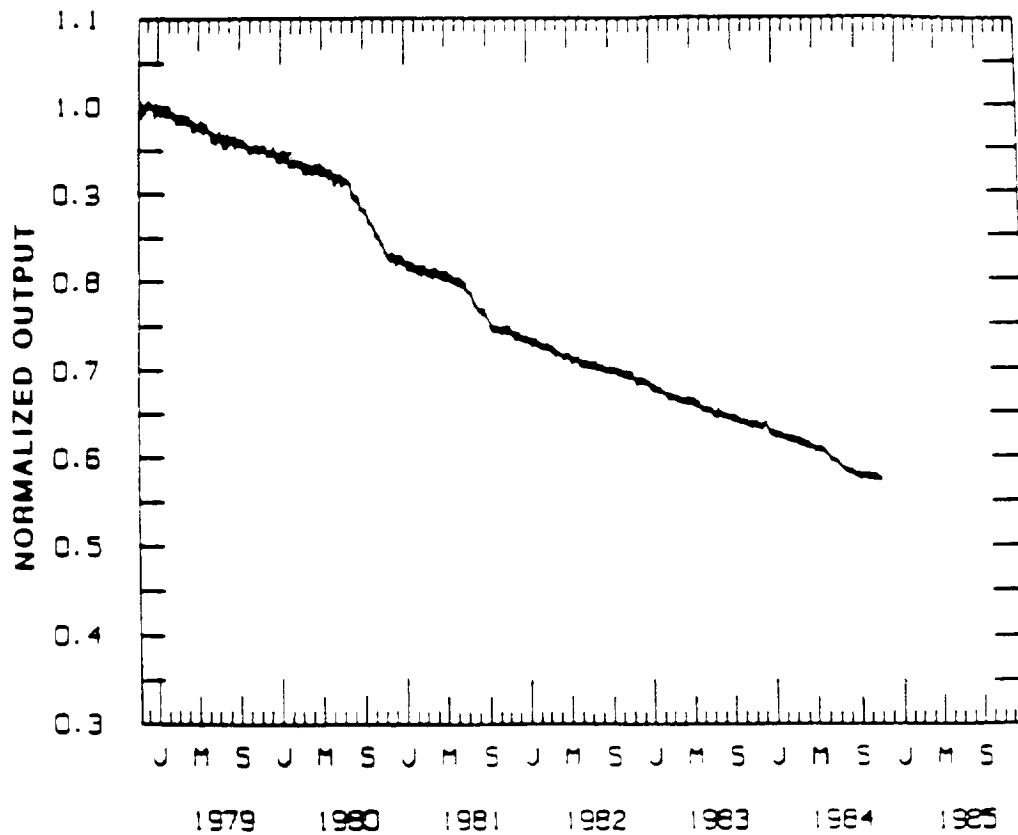
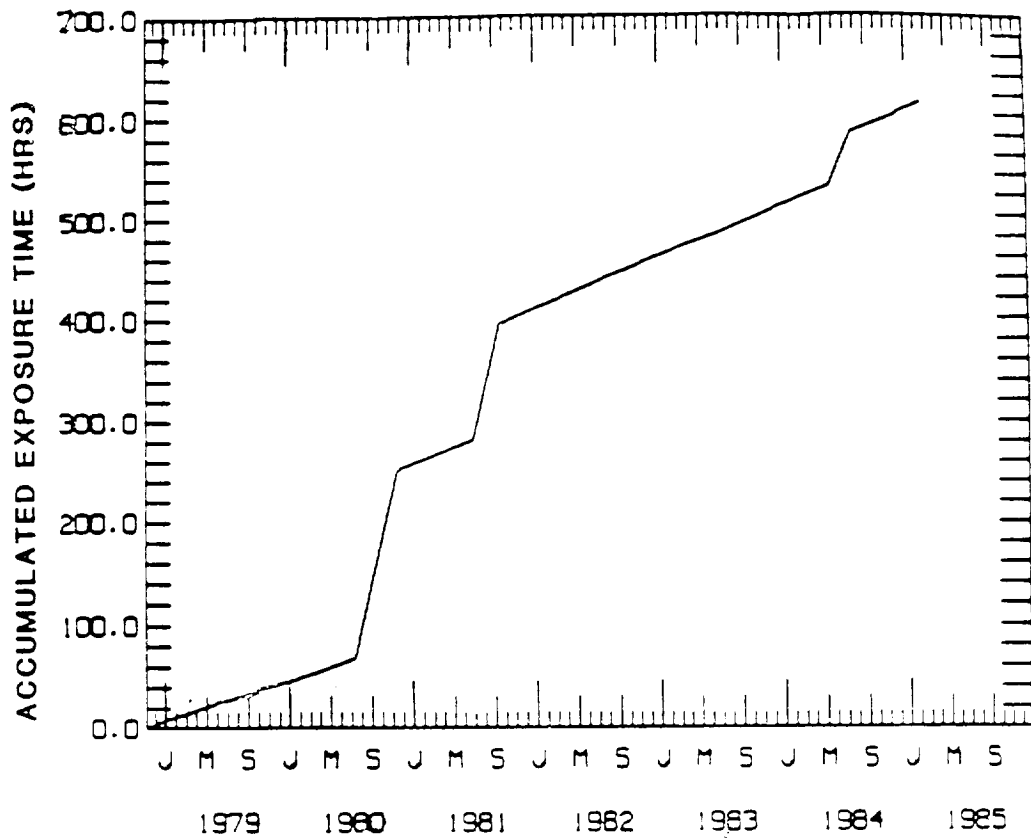


Figure 5.1. (Top) Accumulated solar exposure as a function of time. (Bottom) SBUV irradiance of 273.5 nm, normalized to value on first day of measurement.

The following assumptions were therefore used to derive r_λ :

- (1) The fractional change in diffuser reflectivity is proportional to the amount of additional solar exposure given to it (i.e., r_λ is constant).
- (2) The diffuser degrades only when exposed to the Sun and remains stable in the dark.
- (3) The scattering phase function of the diffuser (dependence of R_λ on α and β) does not change as a result of degradation.

These three assumptions allow us to integrate (11) to write

$$R_\lambda(\alpha, \beta, t) = R_{0\lambda}(\alpha, \beta) \exp[-r_\lambda E(t)]. \quad (12)$$

The albedo $I_{0\lambda}/F_{0\lambda}$ on the first day of measurement is given by

$$I_{0\lambda}/F_{0\lambda} = (k_{0\lambda} c_{0\lambda}) / (K_{0\lambda} C_{0\lambda}), \quad (13)$$

where $k_{0\lambda}$ is the count-to-physical-units calibration factor for radiance and $K_{0\lambda}$ is that for irradiance on the first day of solar measurement.

Combining (8), (10), (12), and (13) yields

$$I_\lambda/F_\lambda = [c_\lambda(t)/C_\lambda(t)] / (k_{0\lambda}/K_{0\lambda}) \exp[-r_\lambda E(t)]. \quad (14)$$

This equation shows all the fundamental quantities needed to determine albedo I/F from SBUV measurements under the assumptions used to derive r_λ : counts measured by the instrument in radiance and irradiance measuring modes, calibration constants for these modes, and the rate of diffuser degradation. Strictly speaking, the calibration constants, $k_{0\lambda}$ and $K_{0\lambda}$, refer only to the first day of solar measurement; however, no loss of accuracy results if the pre-launch values of these constants, given in Table 5.2, are used in (14). Any change in instrument throughput affects both $k_{0\lambda}$ and $K_{0\lambda}$ in a similar way, and, given the assumption that the diffuser degrades only when exposed, the diffuser reflectivity, which affects $K_{0\lambda}$ but not $k_{0\lambda}$, would not have changed from its prelaunch value until its first exposure to the Sun on the first day of solar measurement.

Table 5.2 contains the diffuser degradation constants r_λ . They were obtained from SBUV irradiance measurements made in the continuous scan mode over the time period 15 July 1980 - 17 September 1981. Included in this 430-day period are two intervals lasting a total of 206 days during which the instrument output changed primarily due to rapid degradation in the diffuser plate, while other changes in the instrument or changes in the solar flux were relatively small and could be approximated. Cebula *et al.*, (1988) describe this procedure in detail, including the validation of the three assumptions made in deriving the diffuser degradation model.

Though (14) can in principle be used directly to obtain I/F from the calibration constants given in Table 5.2, this procedure was not used operationally. Irradiance is measured in the step scan mode (the operational ozone measurement mode) only once a week. Because instrument calibration may change significantly from day to day, weekly measurements are not sufficiently frequent to characterize the instrument accurately. In addition, during periods of strong rotational modulation, the solar irradiance at the two shortest wavelengths used in the ozone measurements may vary non-negligibly over periods of less than one week. Therefore, daily irradiance measurements made in the continuous scan mode have been used to derive the albedo correction function $f_\lambda(t)$, using (8). I/F can then be operationally calculated by substituting this value of $f_\lambda(t)$ into (10).

Table 5.2
Calibration Constants

No.	Wavelength (nm)	Solar Flux at 1 AU (watt/cm ³)	Prelaunch Radiance Calibration Constant * (watt/cm ³ / ster/count)	Prelaunch Irradiance Calibration Constant * (watt/cm ³ / ster/count)	Diffuser Degradation Constants (hrs ⁻¹)
1	255.65	75.486	5.102 x 10 ⁻⁵	2.333 x 10 ⁻⁴	5.8113 x 10 ⁻⁴
2	273.61	185.12	5.506 x 10 ⁻⁵	2.811 x 10 ⁻⁴	4.4232 x 10 ⁻⁴
3	283.10	312.90	5.978 x 10 ⁻⁵	3.377 x 10 ⁻⁴	4.4813 x 10 ⁻⁴
4	287.70	320.63	6.157 x 10 ⁻⁵	3.429 x 10 ⁻⁴	4.2734 x 10 ⁻⁴
5	292.29	524.50	6.274 x 10 ⁻⁵	3.499 x 10 ⁻⁴	4.0737 x 10 ⁻⁴
6	297.59	504.86	6.352 x 10 ⁻⁵	3.529 x 10 ⁻⁴	3.8543 x 10 ⁻⁴
7	301.97	436.41	6.366 x 10 ⁻⁵	3.551 x 10 ⁻⁴	3.6014 x 10 ⁻⁴
8	305.87	562.60	6.347 x 10 ⁻⁵	3.545 x 10 ⁻⁴	3.5619 x 10 ⁻⁴
9	312.56	665.48	6.268 x 10 ⁻⁵	3.513 x 10 ⁻⁴	3.3520 x 10 ⁻⁴
10	317.56	767.06	6.188 x 10 ⁻⁵	3.442 x 10 ⁻⁴	3.2150 x 10 ⁻⁴
11	331.26	979.86	5.203 x 10 ⁻⁵	3.209 x 10 ⁻⁴	3.8985 x 10 ⁻⁴
12	339.89	1035.3	4.463 x 10 ⁻⁵	3.020 x 10 ⁻⁴	2.7230 x 10 ⁻⁴
13	343.30	964.29	1.853 x 10 ⁻³	1.011 x 10 ⁻²	2.6509 x 10 ⁻⁴

* Gain Range 2

NOTE: (1 watt/cm³) = 10⁻¹ ergs/sec - cm² - Å⁰

Starting in November 1985, the procedure used to calculate the albedo calibration function was modified, as part of the effort to streamline the data processing system and reduce the time between data acquisition and data availability. Under the original procedure described above, the albedo calibration function was calculated only until three months before the end of solar irradiance data. Otherwise, as the length of the SBUV data base grew, step discontinuities would appear at the boundaries between sections of the albedo calibration function calculated at different times. Additionally, because the diffuser degradation correction was based on observation of the accumulated exposure time for the SBUV/TOMS solar diffuser plate, any gap in the data base would result in an error in this correction. Hence, the processing was delayed until a complete data record was available.

Two changes were made to the instrument calibration system. First, in the revised subsystem, when a day does not have a solar irradiance measurement, the solar irradiances used in computing the albedo calibration function are calculated by linear interpolation between the bracketing solar measurements, eliminating the need for several extra months of data beyond the period for which albedo calibration functions are to be calculated. Comparison of sample albedo calibration functions calculated using the original cubic spline interpolation and the revised linear interpolation showed differences of 0.2 percent or less. The second change is that in the revised system, the diffuser exposure time is based on a prediction rather than on an actual measurement. This procedure allows albedo calibration functions to be calculated and ozone data to be processed even if there are gaps in the data base.

Comparison of the difference between the predicted and actual diffuser solar exposure times at the end of 8 years of instrument operation (1 year of operation under the revised system) indicated that use of the predictive diffuser exposure time introduced a 0.03 percent relative error

into the ratio of the A-Pair (331 nm, 313 nm) albedo calibration functions. The relative errors introduced into the B-Pair (331 nm, 318 nm) and C-Pair (331 nm, 340 nm) albedo calibration functions were approximately 0.02 percent and 0.01 percent, respectively. The resultant estimated systematic bias introduced into the total ozone retrieval by error in the predictive diffuser exposure time is less than 0.14 percent at the end of the eighth year of operation.

The absolute error in the albedo calibration function introduced by the use of predictive exposure time ranges from 0.19 percent at 340 nm to 0.34 percent at 274 nm. This error is proportional to the diffuser correction, $\exp(-r\lambda E)$.

At the shortest wavelengths, the streamlined processing introduces a new limit on the utility of the data for measuring short term ozone variations. When active regions are present on the Sun, the solar irradiance observed at the Earth may vary as the Sun rotates. In the streamlined processing system, because there are gaps in the time series of measurements, the solar irradiances used to derive albedos may not reflect these variations. There will then be a potential error in the albedo the size of the irradiance variations. At solar maximum, these variations can be as large as 0.8 percent at 274 nm; around 0.5 percent at 283 nm, 288 nm, and 302 nm; and 0.1 to 0.3 percent for 292 nm, 298 nm, 306 nm, and 312 nm. SBUV spectral scan solar irradiance measurements, available from the NSSDC on the SBUV spectral scan (SUNC) tape, show solar variations no more than one-fourth as large during the period when the streamlined processing system has been used. Because the streamlined system does not track solar irradiance variations precisely, small periodic artifacts may be produced in the ozone time series. Use of ozone data processed using the streamlined systems to study ozone variations associated with solar ultraviolet variability is not recommended.

The effect of albedo errors on the derived ozone profile is a complex function of altitude and is discussed in detail in Section 7.2. The effect of the error caused by the use of predictive exposure time is about 0.6 percent at 1 mbar and is smaller at lower altitudes.

The Ozone Trends Panel (Watson et al., 1988) carefully evaluated the SBUV instrument and data and concluded that there was a drift in total ozone between SBUV/TOMS and the ground stations of about 2 to 3% between October 1978 and October 1985, and that this drift was likely caused by extra uncharacterized degradation of the diffuser plate. We agree with this conclusion. In particular, assumption 2 (page 23), which is key to separating changes in the monochromator from changes in the diffuser plate, appears to be in error. The assumption was very nearly correct for the period before mid-1982 but was more and more in error after 1982, leading to significant error in derived total ozone. Long term trends in the archived SBUV ozone data should be evaluated with caution.

SECTION 6

ALGORITHM

6.1 Albedo Measurements

The algorithm operates on the albedos whose derivation from the raw counts has been described in Section 5. Albedos are available for all 12 wavelengths listed in Table 5.1. The albedo at 255.6 nm is not used in the derivation of ozone profiles because McPeters (1980) has shown that the radiance at this wavelength is contaminated by emission in the 255.1 nm NO band. For application of the algorithm, the measured albedos are converted to two functional forms:

- a. the Q-Value:

$$Q_{\lambda} = \{4\pi/[\beta_p(\cos \theta)]\}(I_{\lambda}/F_{\lambda}). \quad (\text{same as equation 4})$$

- b. the N-Value:

$$N_{\lambda} = -100 \times \log_{10} (I_{\lambda}/F_{\lambda}). \quad (15)$$

6.2 Computation of Albedos

For the 292 nm and longer SBUV wavelengths, software using successive iterations of the radiative transfer equation (Dave, 1964) is used to compute theoretical SBUV albedos. This calculation requires the following information:

- a. Ozone absorption coefficients α_{λ} as a function of temperature for the SBUV wavelength bands.
- b. Rayleigh scattering coefficients β_{λ} .
- c. Standard temperature profiles.
- d. Standard ozone profiles.
- e. Surface pressure at the lower boundary of the atmosphere.
- f. Solar zenith angle.

The resultant albedos are stored in the look-up tables used by the total ozone algorithm and the multiple scattering and reflectivity (MSR) correction table used by the profile algorithm.

The effective ozone absorption coefficient is computed separately for each step scan wavelength band as a function of temperature and Rayleigh scattering. Table 6.1 gives the ozone absorption coefficients at nominal temperatures and the Rayleigh scattering coefficients. As discussed in Section 5.2, the actual wavelengths measured by the SBUV instrument drift with time. As the measured wavelength changes, the appropriate absorption coefficient will also change. A correction for this change has been incorporated in the software implementing the algorithm. The size of this correction appears in Table 6.1. Note that although the percentage corrections at the two longest SBUV wavelengths appear to be significant, the actual change in absorption coefficient is small, because there is no significant ozone absorption at these wavelengths.

A function is fit to the dependence of the measured absorption coefficients on temperature (Paur and Bass, 1985). The regression equations used are tabulated in Appendix C. Using this function with the standard temperature profiles (Environmental Science Services Administration *et al.*, 1966), ozone absorption coefficients for the SBUV wavelengths are derived at different altitudes.

Seventeen standard ozone profiles have been constructed, from an ozone climatology based on past satellite results for altitudes above the 16 mbar level and on balloon ozonesonde measurements for lower altitudes. The shape of a profile for a given total ozone value depends upon latitude. Profiles are constructed for three latitude bands: low-latitude (15°), mid-latitude (45°), and high latitude (75°). These profiles are given in Appendix D.

Given the wavelength, total ozone and ozone profile, surface pressure, and solar zenith angle, the quantities I_0 , I_s , f_1 , and f_2 of equation (1) are calculated. For the tables used in the algorithm, these terms are computed for the eight longest monochromator wavelengths and the photometer wavelength, for all 17 standard profiles, and two reflecting surface pressure levels (1.0 atm and 0.4 atm). For each of these cases, I_0 and I_s are calculated for ten choices of solar zenith angle, with a finer grid for higher zenith angles; f_1 and f_2 do not depend on zenith angle. As discussed in Section 4.1, the amount of second order and higher scattering and surface reflection for wavelengths shorter than 292 nm is negligible. At these wavelengths, I_0 is computed using a simpler formulation that considers only single scattering.

Table 6.1
Absorption and Scattering Coefficients

Wavelength (nm)	Effective Ozone Absorption Coefficient* (atm-cm) ⁻¹	Absorption Coefficient Drift (**)	Rayleigh Scattering Coefficient (atm ⁻¹)
255.7	309.7	-0.14	2.4573
273.6	169.9	-0.80	1.8131
283.1	79.88	-0.76	1.5660
287.7	48.33	-1.3	1.4597
292.3	27.82	-1.2	1.3627
297.6	13.66	-1.4	1.2605
302.0	7.462	-1.2	1.1831
305.9	4.281	-1.0	1.1194
312.9	1.632	-1.6	1.0198
317.6	0.8684	-0.8	0.9527
331.3	0.1397	-3.5	0.7956
339.9	0.0248	5.4	0.7134
343.3 (photometer)	0.0191	Not Applicable	0.6864

* Calculated at a nominal temperature; see Appendix C for absorption coefficient dependence on temperature.

** Percent change in absorption coefficient per 1 nm change in wavelength.

6.3 Computation of Reflectivity

As discussed in Section 4.1, the contribution of clouds and aerosols to the backscattered intensity is treated by assuming that radiation is reflected with a single effective reflectivity from a particular pressure level. In the SBUV ozone retrieval algorithm, reflectivity is estimated using the radiances from the longest SBUV monochromator wavelength band at 339.8 nm, and from the 12 photometer measurements at 343 nm, each of which is coincident with the monochromator measurement at one wavelength. In this wavelength region, the reflectivity is weakly sensitive to the ozone amount; a change in ozone of 50 matm-cm affects the reflectivity by less than one percent. To incorporate the ozone dependence into the calculated reflectivity, an iterative procedure is used. An estimated reflectivity is calculated using a climatological ozone value. Using this estimated reflectivity, an estimated total ozone is derived. The reflectivity is then recomputed, using the estimated total ozone. This reflectivity is then used in the final total ozone derivation.

The purpose of the photometer is to monitor scene changes. Reflectivities are derived from monochromator measurements only at 339.8 nm. As the instrument steps from one wavelength to the next, the satellite footprint is moving over the ground at a speed of approximately 6 km/sec. Consequently, when the instrument is measuring at another wavelength, the subsatellite scene reflectivity may no longer be what it was when measurements were being made at 339.8 nm. The photometer measurements are used to monitor the changes in scene reflectivity between 339.8 nm monochromator measurements in the derivation of the reflectivity for measurements at the other wavelengths.

Solving (1) for reflectivity R gives

$$R = (I - I_0) / [I_s f_1 + (I - I_0) f_2]. \quad (16)$$

With I_0 , I_s and f_2 from the tables for the respective wavelengths, reflectivities are computed for surfaces at pressures of 1.0 and 0.4 atm.

6.4 Estimation of Surface Pressure

In the derivation of ozone values, an effective IFOV surface pressure, P_0 , is estimated from the terrain pressure P_t and the estimated cloud top pressure P_c , using the following expression:

$$P_0 = (1 - w)P_c + wP_t. \quad (17)$$

The weighting function w is based on the measured surface reflectivity. A higher reflectivity generally implies greater cloudiness. Normally, when snow or ice is not present, w is set to unity for $R < 0.2$, to zero for $R > 0.6$, and is obtained by linear interpolation as a function of R for intermediate reflectivities.

A different method is used to obtain effective surface pressure when there is evidence for snow or ice in the IFOV. Snow or ice thickness data from around the globe are collected by the Air Force Global Weather Center and mapped on a polar stereographic projection. These data have been mapped onto a $1^\circ \times 1^\circ$ latitude-longitude grid and used to determine the presence or absence of snow in the SBUV IFOV. When snow or ice is present, it is assumed that, despite the high reflectivity, there is only a 50 percent probability that clouds are present. The effective pressure is then obtained by averaging the value of P_0 obtained from (17) with the terrain pressure.

The cloud-top pressure is estimated in two ways. When measurements by the Temperature Humidity Infrared Radiometer (THIR) on Nimbus-7 are available, the cloud-top pressure can be

based on co-located THIR infrared measurements. Cloud-top pressure is also estimated from an empirical climatology based on studies using THIR measurements:

$$P_c(\text{atm}) = 0.3 + 0.15[1 - \cos(2 \times \text{lat})]. \quad (18)$$

When THIR measurements are available, total ozone values retrieved using THIR-derived cloud-top pressures appear on the HDSBUV and CPOZ tapes. Total ozone values derived using the empirical climatology appear on the HDSBUV and CPOZ tapes for all FOV's, whether or not there is a THIR-based value for the same FOV.

The average terrain heights are available from the National Oceanic and Atmospheric Administration National Meteorological Center (NOAA/NMC), given in km for 2.5° x 2.5° latitude and longitude cells. These heights are converted to units of pressure and interpolated to the SBUV IFOV's to establish the surface pressure at the point on the Earth's surface directly below the satellite.

6.5 Total Ozone

When measured and computed albedos are compared in the determination of total ozone, the albedos for individual wavelengths are not compared directly. Albedo ratios, called pair values, are calculated. A pair value is the ratio of the albedo at a longer wavelength that is relatively insensitive to ozone to that for a shorter, ozone sensitive wavelength. The use of albedo ratios reduces the effect of wavelength-independent uncertainties in the monochromator calibration.

From the ozone values derived from the individual pairs, a "Best" ozone value is selected or computed, based on the sensitivity to ozone, profile shape and wavelength separation of the values from each individual pair. When THIR data are available, a "THIR Best" total ozone value is also obtained.

6.5.1 Application of Tables

As discussed in Section 6.1, the measured albedos are expressed in terms of N-values, which are proportional to the logarithm of the albedo. A ratio of albedos then becomes a difference of N-values. Three pairs are defined:

$$\begin{aligned} \text{A-Pair} &= N_{313} - N_{331} \\ \text{B-Pair} &= N_{318} - N_{331} \\ \text{C-Pair} &= N_{331} - N_{340} \end{aligned}$$

For each of the above N-value differences or pairs, four estimates of total ozone values are calculated. Values of total ozone above 1 atm are derived for reflecting surfaces at 1.0 atm and 0.4 atm. For each of these pressures, ozone values are derived from the two standard latitudes surrounding the actual latitude of the measurements. In each case, N-values for the solar zenith angle of the measurement and the given latitude and pressure level are computed from the table values of I_0 , I_s , and f_2 . These N-values produce table-derived pair N-value differences for total ozone values at 50 matm-cm intervals. Ozone between the terrain height and actual pressure level is subtracted using the amount of ozone between 0.4 and 1.0 atm in the standard profile as a basis, assuming that cumulative ozone is linear with log pressure at these levels. Interpolation of the measured N-value pair difference in the table-derived N-value pairs produces total ozone values for each latitude and pressure. The total ozone values for the two pressures are combined using (17). The ozone value for the latitude of the measurements is derived by linear interpolation in latitude between the values for the two bordering standard latitudes. Between 15° and the equator, only the profile set for 15° is used; poleward of 75°, only the 75° profile set is used. An average reflectivity is calculated in the same manner and stored on the tapes.

6.5.2 Best Ozone

The Best ozone is a weighted average of the total ozone values derived from the A-, B- and C-pairs:

$$\text{Best} = (W_A f_A \Omega_A + W_B f_B \Omega_B + W_C f_C \Omega_C) / (W_A + W_B + W_C), \quad (19)$$

where the adjustment factors f_A , f_B , and f_C have been selected to remove existing biases between the ozone values derived from the different pairs. These biases have been derived from the ozone values yielded by different pairs in the regions where both provide information, near a zenith angle of 45° for the A- and B-pairs and near 75° for the B- and C-pairs. By convention, the adjustment f_A for the A-pair is defined to be unity. The adjustment factor f_C , which corrects for the bias between the A- and C-pairs, is derived from the measured adjustment factor for the C-pair relative to that for the B-pair (f_C/B) by the following expression:

$$f_C = f_B f_{C/B}. \quad (20)$$

For SBUV, $f_B=0.98$, and $f_C=1.10$.

The weight W for each individual pair is derived from the following sensitivity factors:

s_1 = sensitivity of the pair N-value to changes in total ozone ($dN/d\Omega$),

s_2 = sensitivity of the pair ozone to the wavelength dependence of the reflectivity (assumed to be inversely proportional to the separation of the two pair wavelengths),

s_3 = sensitivity of the pair ozone to the ozone profile shape (assumed to be proportional to s_1 divided by the sensitivity that would be derived using Beer's law if all the radiation were scattered from the ground). The Beer's law sensitivity is proportional to the difference between the ozone absorption coefficients at the two pair wavelengths),

using the expression

$$W = s_1^2 s_2^2 s_3^2. \quad (21)$$

The overall weighting factor for a given pair is then given by the following expression:

$$W = (\delta\lambda)^{-2} (\delta\alpha)^{-2} (dN/d\Omega)^4, \quad (22)$$

where $\delta\lambda$ is the separation of the two pair wavelengths, and $\delta\alpha$ is the difference between the absorption coefficients at the two pair wavelengths.

6.5.3 Validity Checks

The algorithm performs several validity checks for maintaining data quality. Before measured radiances are accepted for use in ozone determination, the solar zenith angle, satellite attitude, and instrument status are checked to ensure the suitability of the radiances and other geophysical input to the algorithm. This section describes the quality checks performed on the derived reflectivity and Best ozone to identify invalid ozone values caused by either bad input data that passed preprocessing checks or by limitations of the ozone algorithm. The data quality for each sample is identified by a data quality flag. The total ozone flag is in word 26 of the HDSBUV tape for THIR total ozone and word 40 for non-THIR total ozone. The CPOZ tape contains one flag for both total ozone and profiles, in word 10. Note that the individual pair values, which also are stored on the HDSBUV tape, are neither checked nor modified.

The computed Best ozone for each pair must be within the range of the radiance tables. For 15° and lower latitudes, the range is 0.15 atm-cm to 0.35 atm-cm, between 15° and 45°, the range is 0.15 atm-cm to 0.60 atm-cm; and above 45°, it is 0.15 atm-cm to 0.65 atm-cm. If the derived Best ozone is outside the range of the tables, it is set to -999., and the units digit of the HDSBUV total ozone error flag is set to 9.

Next, checks are made on the reflectivity. The reflectivity must be no less than -0.05 and no greater than +1.05. If the reflectivity is outside this range, the Best ozone is set to -999., and the HDSBUV error flag is set to 8. In addition, the 343 nm photometer reflectivity is compared with the 339.8 nm monochromator reflectivity. If the two differ by more than 0.15, the Best ozone is set to -999., and the HDSBUV quality flag is set to 7. Such differences in the two reflectivity values may occur as a result of sporadic problems with the instrument or data transmission.

The Best ozone is then compared with the total ozone returned by the profile algorithm. If the two ozone values differ by more than 3 standard deviations, usually about 1.5 percent, the quality flag is set to 5 and Best ozone is set to -999. The ozone profile is still derived in this case.

Flags 5-9 are not used on the CPOZ tape.

If the data pass flags 9, 8, 7 and 5, the ozone path is calculated in units of atm-cm:

$$\text{ozone path} = \text{BEST} \times (1 + \sec \theta_0). \quad (23)$$

The consistency between Best ozone and the A-, B-, or C-pair is then checked; the pair used in the comparison is the one with the largest weighting factor, as given by (22). The quality flag is set to 4 if inconsistency exists, and Best ozone is set to -999. Data that pass flag 4 are assigned a flag value of 0, 1, or 2 as determined by the ozone path:

<u>Ozone Path</u>	<u>Quality Flag</u>	<u>Pair Used in Flag 4 Consistency Check</u>
1.5	0	A
1.5 - 3.5	1	B
3.5	2	C

Values of 0-4 have the same meaning for the HDSBUV total ozone data flag and the CPOZ data flag.

The tens digit in CPOZ error quality flags is reserved for an indicator of aerosol contamination. Total ozone retrieved from SBUV is not affected by aerosols.

If the data were taken on the descending (north to south) part of the orbit, the value 10 is added to a HDSBUV flag value, and the value 100 is added for the CPOZ tape.

6.6 Profile Ozone

Ozone profiles are derived from the measured albedos using an optimum statistical inversion technique (Rodgers, 1976; Klenk *et al.*, 1983). Because the retrieval of an ozone profile is an attempt to derive a continuous function from a limited number of its integrals, the solution is not unique. An additional constraint, called *a priori* information, is needed to select the particular solution most likely to represent physical reality from among the possible mathematical solutions. Generally, the *a priori* information can be mathematical restrictions on the form of the solution, constraints derived from the physics of the problem, independent information on the solution, or other assumptions. The retrieved profile is thus constructed from both the *a priori* information and the measured albedos. Because the *a priori* information is an integral part of the profile construction, it is sometimes referred to as "virtual measurements."

The *a priori* information used in the inversion algorithm for the SBUV ozone profile includes a "first guess" profile derived from the best available ozone climatology. The albedos that such an ozone profile would yield are calculated. The differences between the albedos calculated

from the first guess profile and the measured albedos are then used to provide a new set of profile values that are more nearly consistent with both the measured albedos and the first guess profile.

Application of the optimum statistical technique requires not only the measurements and *a priori* profiles but also an assessment of their uncertainty or variance. In the case of the albedo, the uncertainty is characterized by the errors of measurement. The method also requires the covariance of the errors of measurement, to determine how dependent the errors at one wavelength are on the errors at another. For the *a priori* information, the variances and covariances are obtained in the development of the climatology.

The derived ozone profile data are provided in two formats. In the first format, the ozone content is given in units of matm-cm (Dobson Units) for each of 12 layers. These layers extend from the Earth's surface to the top of the atmosphere, with widths of approximately 5 km. The second format is mass mixing ratio in units of micrograms per gram, at specified pressure levels from 100 mbar to 0.3 mbar. Volume mixing ratios in parts per million (ppmv) can be obtained by dividing the mass mixing ratio by 1.657. Details of the two formats are presented in Appendix A.

6.6.1 *A Priori* Information

The *a priori* information used by the inversion method consists of a first guess profile as a function of latitude, time of year and total ozone, and its variances and covariances. The ozone climatology used to construct the *a priori* information has been obtained from the best available satellite and balloon ozonesonde measurements.

For the 16 mbar pressure level and higher altitudes, the climatology is based primarily on previous satellite measurements. When ozone values were first derived from the Nimbus 4 BUUV measurements, the climatological profiles used (Bhartia *et al.*, 1981) were based upon ozonesonde data at pressure levels below 20 mbar and an exponential form for the profile at levels well above the mixing ratio maximum, derived from BUUV observations at 274 nm and 283 nm. The higher and lower level profiles were joined by a cubic spline. For the first processing of the SBUV data, the first guess profiles for Umkehr layers 6-12 were based on a functional fit to the results from the original processing of BUUV data, assuming an annual cycle with a sinusoidal variation and amplitude proportional to $[1-\cos(2 \times \text{lat})]$. For the current, Version 5, processing of the SBUV data, first guess profiles for Umkehr layers 6-12 were obtained by fitting a sinusoidal annual variation to the results of the previous processing of SBUV measurements.

At lower altitudes, ozonesonde measurements have been used to construct the first guess profiles. Most of these soundings are concentrated in the middle latitudes and northern hemisphere. The most recent ozonesonde data used were from 1982 measurements.

The first guess profiles are in the form of analytic expressions for the variation of ozone in each specified latitude band and each ozone layer defined in Appendix A. Below 63 mbar (layers 1-3), the first guess ozone is given as a quadratic function of total ozone. Above 16 mbar (layers 6-12), a sinusoidal annual variation is used. The first guess profile from 63 mbar to 16 mbar (layers 4 and 5) is obtained by performing a log-log cubic interpolation in cumulative ozone as a function of atmospheric pressure to the values for layers 2, 3, 6, and 7. This interpolation generally yields a smooth transition between the upper and lower profile segments. The measured SBUV Best total ozone provides an added constraint; total ozone for the constructed first guess must be the same as the measured total ozone. The total ozone value used in deriving the profile differs in one respect from the Best ozone value described in Section 6.5. The derived value of Best ozone represents total ozone above the actual terrain height. The value of total ozone used for profiling, while obtained from the retrieved Best ozone, represents total ozone above the 1000 mbar pressure level and thus may differ from Best ozone at some

locations. Total ozone above 1000 mbar for profiling is approximated from Best ozone by adding $10(1-P_t)/3$ Dobson units, where P_t is the terrain pressure, equivalent to assuming 20 Dobson units of ozone uniformly distributed below 0.4 atm. Both values appear on the HDSBUV tape.

Appendix E provides the equations and coefficients used to construct a first guess for each latitude band, total ozone, and time of year.

The *a priori* profile covariance matrix is constructed on the basis of a statistical analysis of the climatological data. For layers 1-5, the covariance of the Hohenpeissenberg data set about the fit values was used. For layers 6-12, the same process was applied to the SBUV data set, but with modifications to allow for the difference between the covariance of an ensemble of real profiles and an ensemble of climatological profiles. The off-diagonal elements linking layers in the separate sets were estimated subjectively. A single covariance matrix is used for all latitude and time conditions. Matrix values are presented in Appendix E.

The *a priori* information is based on the climatology that was available at the time of preparation. Thus, the information can be expected to be representative only of the best available ozone climatology. Changes in ozone that are different from any seen during the period on which the climatology is based are not represented by the *a priori* information. An example of such a change is the sharp drop in Antarctic early spring ozone that has been especially pronounced since 1982. Section 8.2 discusses the possible errors that may have resulted from the use of an incorrect first guess for the Antarctic spring.

6.6.2 Measurement Errors

A measurement covariance matrix is based on the uncertainties in both the measured and calculated Q-values. For the SBUV retrievals, in addition to the 0.5 percent errors in the measured radiance and the 1.5 percent error in total ozone, the measurement error covariance matrix includes contributions from all errors in quantities that enter into the calculations of the multiple scattering correction and of the albedo that would be generated by the assumed profile. In particular, there is an allowance for a contribution from the errors in the ozone absorption coefficients that arise from variations in atmospheric temperature, about 0.5 percent. The contributions from errors in surface reflectivity and surface pressure are not included but are believed to be small.

6.6.3 Calculation of Albedos

The theoretical albedo used in profile retrieval is the sum of two parts:

- a. Single scattered radiance.
- b. The sum of multiply scattered radiance and that reflected from the surface (MSR).

The single scattered radiance is computed using equation (2). The MSR radiance is obtained from a look-up table. The same quantities are calculated for the MSR tables as for the total ozone tables (i.e., I_0 , I_s , and f_2), except that I_0 for MSR includes only the difference between the results of scattering to all orders and those of single scattering. The MSR thus contains only the sum of the theoretical radiance from second order and higher scattering and the component reflected from the surface.

MSR is a significant component only at wavelengths longer than 290 nm. MSR is weakly dependent on profile shape (Taylor *et al.*, 1980), but strongly dependent on total ozone, surface reflectivity, and solar zenith angle. The reason is that the stratosphere acts principally as an attenuator on the wavelengths that are multiply scattered - the longer wavelengths. Thus, the MSR component of the wavelengths used for profiling has the same overall characteristics as the full radiances used for total ozone.

As for total ozone, there are profile MSR tables for three standard latitudes: low-latitude (15°), mid-latitude (45°), and high latitude (75°). Values for intermediate latitudes are obtained by linearly interpolating in latitude between the Q-values for the adjacent standard latitudes.

As part of the interpolation process for determining the MSR Q-values, the sensitivity of MSR Q-values to total ozone is calculated for each of the longer profile wavelengths. This sensitivity is used to calculate the variances and covariances associated with the MSR component for the measurement covariance matrix.

6.6.4 Inversion

The unknown ozone profile is represented by a vector \mathbf{x} , whose components are the values for ozone content for each of the 12 layers. The single scattering integral equation, (5), is linearized by expanding in a Taylor series about the first guess profile \mathbf{x}' , and dropping second and higher order terms in the expansion. The resulting expression is suitable for an iterative profile solution and may be written in the following form:

$$[\ln Q(\mathbf{x})]_l = [\ln Q(\mathbf{x}')]_l + \sum_k (\partial \ln Q_l / \partial \ln x_k)_{\mathbf{x}'} (\ln x_k - \ln x'_k), \quad (24)$$

where

- Q = Q-value as defined in (4)
- \mathbf{x} = solution ozone
- \mathbf{x}' = ozone profile from previous iteration
- k = layer index
- l = wavelength index.

The partial derivative coefficients in the second term on the right hand side are calculated using the ozone profile for the previous iteration and constitute the weighting function. They measure the sensitivity of the radiance at a particular wavelength to changes in ozone in the different layers in the profile. In vector format, this equation becomes

$$\mathbf{y} = \mathbf{y}_n + \mathbf{K}_n(\mathbf{x} - \mathbf{x}_n), \quad (25)$$

where

- \mathbf{x} = vector of $\ln x_k$ values for solution ozone profile
- \mathbf{x}_n = vector of $\ln x_k$ values for ozone profile for iteration n
- \mathbf{y} = vector of measured values for $\ln Q_l$
- \mathbf{y}_n = vector of values for $\ln Q_l$ calculated from \mathbf{x}_n
- \mathbf{K}_n = matrix of values of weighting function $(\partial \ln Q_l / \partial \ln x_k)$.

A solution profile is computed using the *a priori* and error information from the equation

$$\mathbf{x}_{n+1} = \mathbf{x}_0 + \mathbf{S}_x \mathbf{K}_n^T [\mathbf{K}_n \mathbf{S}_x \mathbf{K}_n^T + \mathbf{S}_e]^{-1} [\mathbf{y} - \mathbf{y}_n - \mathbf{K}_n(\mathbf{x}_0 - \mathbf{x}_n)], \quad (26)$$

where

- \mathbf{S}_e = measurement covariance matrix
- \mathbf{S}_x = *a priori* covariance matrix
- \mathbf{x}_0 = *a priori* profile.

Convergence is determined by the size of $\mathbf{x}_{n+1} - \mathbf{x}_n$.

6.6.5 Validity Checks

Several checks are made to identify scans with missing or grossly abnormal values. If a scan fails any one of these checks, a profile error code of 4 through 9 is assigned and no profile is reported. This error code appears in word 157 of the HDSBUV tape.

If measurements are missing at any wavelength used in the profile calculations, a profile error code of 9 is assigned. If a Best ozone value has not been computed in the total ozone algorithm, then a profile error code of 8 is assigned. Next, the reflectivity for the six longest wavelengths, those that are multiply scattered, is checked. If the monochromator reflectivity for any of these wavelengths is outside the range (-0.05, +1.05), or if the cumulative reflectivity change averages greater than 0.05 between adjacent step scan positions, then a profile error code of 7 is assigned. Such values for reflectivity usually indicate defective data.

The algorithm uses the 274 nm and 283 nm Q-values to calculate values for C, the cumulative ozone above 1 mbar, and σ , the ratio of the atmospheric scale height to the ozone scale height, assuming that the cumulative ozone x is a function of the pressure p (McPeters, 1980):

$$x = C p^{1/\sigma}. \quad (27)$$

If σ is outside the range from 0.3 to 0.8, a profile error code of 6 is assigned. If C is greater than 3.0 matm-cm or less than 0.5 matm-cm, a profile error code of 5 is assigned.

The observed Q-values are compared with the initial Q-values calculated from the *a priori* profile, and residues r are calculated. A residue is defined by the following equation:

$$r = 100(Q_{\text{obs}} - Q_{\text{calc}})/Q_{\text{calc}} \quad (28)$$

where Q_{obs} are the Q-values derived from the observed radiances, and Q_{calc} are the Q-values derived from an assumed profile, in this case, the first guess. If this initial residue is larger than 60 percent, a profile error code of 4 is assigned. If the scan passes all checks described thus far in this section, the ozone profile is computed and additional checks are made. A final residue is derived, using the computed profile to derive Q_{calc} of (28), and compared with the standard deviation (σ) of the observed measurements, obtained as the square root of the diagonal term of the measurement error covariance matrix. If the final residue is larger than 3σ , an error code of 3 is assigned. If total ozone returned by the profile algorithm differs by more than 3σ from the total ozone for profiling, derived as described in 6.6.1 from the Best total ozone returned by the total ozone algorithm, an error code of 2 is assigned. If the ozone derived for the three lowest altitude layers differs by more than 5σ from the climatology-derived initial estimate for those layers, an error code of 1, signifying lower-level anomaly, is assigned on the HDSBUV tape, and a value of 10, signifying aerosol contamination, is added to the CPOZ error flag. Aerosol contamination is discussed in greater detail in Section 8.1.

A profile that passes all these tests is considered a good profile and is assigned an HDSBUV profile error code of 0. For descending orbit (north to south) data, a value of 10 is added to the HDSBUV error flag and a value of 100 is added to the CPOZ error flag.

SECTION 7

GENERAL UNCERTAINTIES

7.1 Accuracy and Precision of SBUV Albedo

The accuracy of the albedo derived from SBUV measurements depends on the accuracy of the pre-launch radiance and irradiance calibration constants. The accuracy of the pre-launch calibration depends, in turn, primarily upon the radiometric accuracy (± 3 percent) of the standard calibration lamp supplied by the National Bureau of Standards (NBS); in addition, the accuracy of the radiance calibration constants depends upon the accuracy with which the reflecting properties of an NBS-calibrated, BaSO₄-coated standard albedo plate are known. The ratio of radiance and irradiance calibration constants appearing in equation (14), however, is not affected by the lamp calibration and is known to better than ± 3 percent.

The accuracy of the calibration of the long-term albedo relative to the first day of measurement depends primarily on the accuracy in characterizing time-dependent changes in the diffuser plate. Cebula *et al.*, (1988) described the methods used to maintain the diffuser plate calibration. They estimated that the total change in diffuser reflectivity after 600 hours of solar exposure in 6 years of operation was known to approximately ± 2 percent. At the end of the data archival period (12 February 1987) the total diffuser solar exposure is approximately 770 hours. Assessments of the long-term drift in the SBUV (Fleig *et al.*, 1986) and TOMS total ozone (Fleig *et al.*, 1988) and the SBUV profile ozone retrievals (Fleig *et al.*, in preparation) suggest that the calibration of the diffuser plate is well known through mid-1982 and somewhat less well known thereafter. Analysis of calibration validation experiments conducted in the 1985-1987 time-frame suggests that the accuracy of the long-term diffuser plate characterization is wavelength-dependent. It is now estimated that after 8 years of in-orbit operation the change in diffuser plate reflectivity is known to within ± 2 percent at 340 nm, the uncertainty increasing to ± 6 percent at 274 nm.

In addition to changes in sensitivity, uncertainties in the instrument wavelength scale can lead to uncertainties in the retrieved ozone. The algorithm is based on the assumption that the instrument measures radiances and irradiances at known wavelengths and bandpasses. If the wavelengths of measurement are not those specified, then the relation between ozone and backscattered radiation will not be that assumed by the algorithm, leading to an error in the retrieved ozone.

In summary, it is estimated that the albedo calibration of the SBUV instrument is accurate to ± 3 percent at all wavelengths immediately after launch and may have drifted by up to ± 2 percent at 340 nm; the drift increases with decreasing wavelength to ± 6 percent at 274 nm. The precision of the SBUV albedo measurement is greater than 0.5 percent at all wavelengths.

7.2 Relation Between Albedo Errors and Ozone Errors

Table 7.1 shows how a positive 1 percent error in all measured albedos affects the derived profile and total ozone in the mid-latitudes. The effect on the total ozone (minus 0.3 percent) is relatively small compared to the effect on the profile above 10 mbar (minus 1 to 2 percent).

When the albedo increases, the derived ozone is expected to decrease, in the same way as it does in the higher altitudes of the profile and for total ozone, as shown in Table 7.1. However, at lower profile altitudes, ozone increases for higher albedos. The increase occurs because the computed profile is constrained to a profile-derived total ozone. Because the change in profile-derived total ozone is less than the overall change in ozone in the higher altitudes of the profile, the profile algorithm compensates for this difference by adding some ozone in the lower levels of the profile (levels below the maximum concentration).

Table 7.1
Effect of 1 Percent Change in Albedos at All Wavelengths on Derived
Mid-latitude Ozone

Pressure (mbar)	Effect on Derived Ozone (percent)
0.3	-1.20
0.4	-1.43
0.5	-1.60
0.7	-1.81
1.0	-1.92
1.5	-1.87
2.0	-1.70
3.0	-1.36
4.0	-1.16
5.0	-1.04
7.0	-0.91
10.0	-0.82
15.0	-0.62
20.0	-0.38
30.0	0.03
40.0	0.35
50.0	0.54
70.0	0.56
100.0	0.25
Total Ozone	-0.3

Table 7.2 summarizes the estimated absolute errors in the derived ozone profile. Such errors do not change with time. These errors are provided as a function of error source and altitude. Line 3 shows the error in ozone resulting from the uncertainty in the wavelength calibration of the instrument, as discussed in Section 7.1. Line 4 shows the error resulting from the uncertainty in the prelaunch radiometric calibration. Random errors are summarized in Table 7.3. Line 1 shows the altitude dependence of the uncertainty in ozone arising from instrument noise. In all cases, the uncertainty in ozone at a given altitude depends upon the wavelengths used in determining the ozone for that altitude, the uncertainty in the measurement at those wavelengths, and the sensitivity of the retrieved ozone to a change in the albedo at that wavelength.

7.3 Input Physics

Calculation of the absorption and scattering of atmospheric radiation by ozone and the other constituents of the atmosphere requires knowledge of the ozone absorption and Rayleigh scattering coefficients. The values used in the algorithm are obtained from laboratory measurements. Any uncertainty in the laboratory values will propagate through the algorithm to produce a systematic error in the derived ozone. Lines 1 and 2 of Table 7.2 show the altitude dependence of the effect of these uncertainties. In addition, the absorptivity of ozone is a function of the temperature. As the temperature changes, the absorption coefficient may change from that assumed in the algorithm, producing an error in retrieved ozone. The size of this error is shown in line 2 of Table 7.3.

Table 7.2
Time-Invariant Errors in Retrieved Ozone

Error Source	Ozone Mixing Ratio Error (%) ^(a)				Total Ozone
	1 mb	3 mb	10 mb	30 mb	
1. Rayleigh Scattering Coefficient ^(c)	1.5	1.5	1	0.5	0.3
2. Ozone Absorption Cross-Section ^(b, c)	3	3	3	3	3
3. Wavelength Calibration	0.5	0.6	0.7	0.7	0.7
4. Radiometric Calibration	5	3	2	2	1
5. Retrieval Error ^(c)	3	2	4	5	1
Root Sum of Squares of sources 1 through 5	7	5	5.5	6	3

Notes:

- a. Possible error in mid-latitude profiles (1σ confidence) from each error source is listed.
- b. This error applies only to SBUV comparisons with non-UV instruments. Within ultraviolet, errors should be less than 1%.
- c. These errors may be ignored when comparing similar SBUV instruments on different satellites.

7.4 Profile Resolution

The vertical resolution of the ozone profiles retrieved from SBUV depends upon the width of the radiance weighting functions and, to a lesser extent, on the separation between the weighting functions. The weighting functions of the five shortest SBUV wavelengths (255 nm to 292 nm) have values of full width at half maximum (FWHM) of about 10 km and peaks separated by 2-3 km. The longer wavelengths have wider weighting functions, whose FWHMs range from 15 km to 25 km, and whose peak separations increase to 5 km. These fundamental properties of the weighting functions, determined by the selection of wavelengths, the physics of radiative transfer and the vertical distribution of ozone in the Earth's atmosphere, limit the amount of information the measured radiances can provide regarding the vertical distribution of ozone.

Table 7.3
Random Errors

Error Source	1 mb	Ozone Mixing Ratio Error (%)			Total Ozone
		3 mb	10 mb	30 mb	
1. Instrument Noise	1	1	2	2	0.5
2. Atmospheric Temperature	0.5	1	1	1	1
3. Retrieval Error	5	3.5	4	10	2
(Sum σ^2) ^{1/2} of sources 1 through 3	5	4	5	10	2

Notes:

Errors listed are rms values for typical mid-latitude measurements. During winter months or under disturbed atmospheric conditions errors 2 and 3 may be larger by a factor of 2.

Vertical resolution of SBUV-derived profiles is 10 km. Listed errors are applicable only at this resolution (see also Section 7.4).

Two approaches have been taken in estimating the resolution of the profiles derived from the SBUV algorithm. In one, the response of the algorithm to a very narrow perturbation in the atmosphere is calculated. In the other, the profiling system is treated as operating on the atmospheric properties as a bandpass filter, called the averaging kernel.

7.4.1 Perturbation Studies

In these studies, a perturbation is applied to the atmospheric ozone profile, the albedos that would be produced by the perturbed profile are calculated, and the algorithm is applied to these albedos to retrieve a profile in the same way as it would be applied to measured albedos. The retrieved profile is compared with the profile used to calculate the albedos. Figures 7.1 and 7.2 show the results of two such calculations. In both cases, the change in ozone has a Gaussian shape and is centered at the 3 mbar level. The solid line shows the percentage difference between the perturbed and unperturbed profile; the dashed line shows the ratio of the retrieved profile to the unperturbed profile. The agreement between the two is a measure of how well the algorithm can reproduce the structure represented by the perturbation. Figure 7.1 shows the results of a study where the maximum change is 10% and the FWHM is 10 km; Figure 7.2 shows the results for a perturbation with the same maximum amplitude but with a FWHM only half as wide.

These figures show that, while the algorithm can still retrieve a change in ozone in the appropriate region of the atmosphere, the agreement between the altitude dependence of the retrieved and assumed ozone changes is markedly poorer for the 5 km FWHM perturbation.

BUMP ANALYSIS - 10 KM FWHM

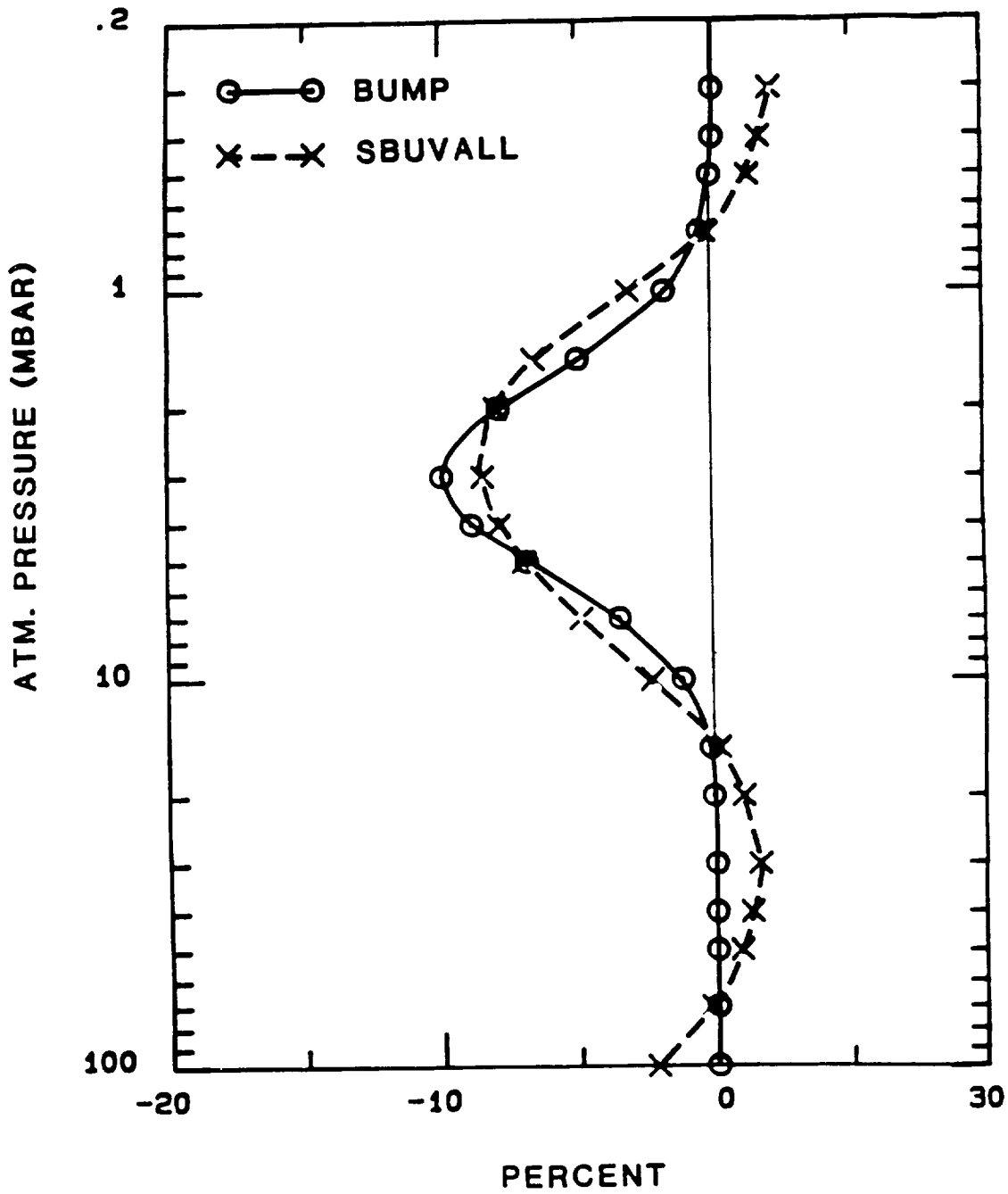


Figure 7.1. Effect on retrieved ozone of 10% Gaussian change, centered at 3.0 mbar with 10 km full-width at half-maximum.

BUMP ANALYSIS - 5 KM FWHM

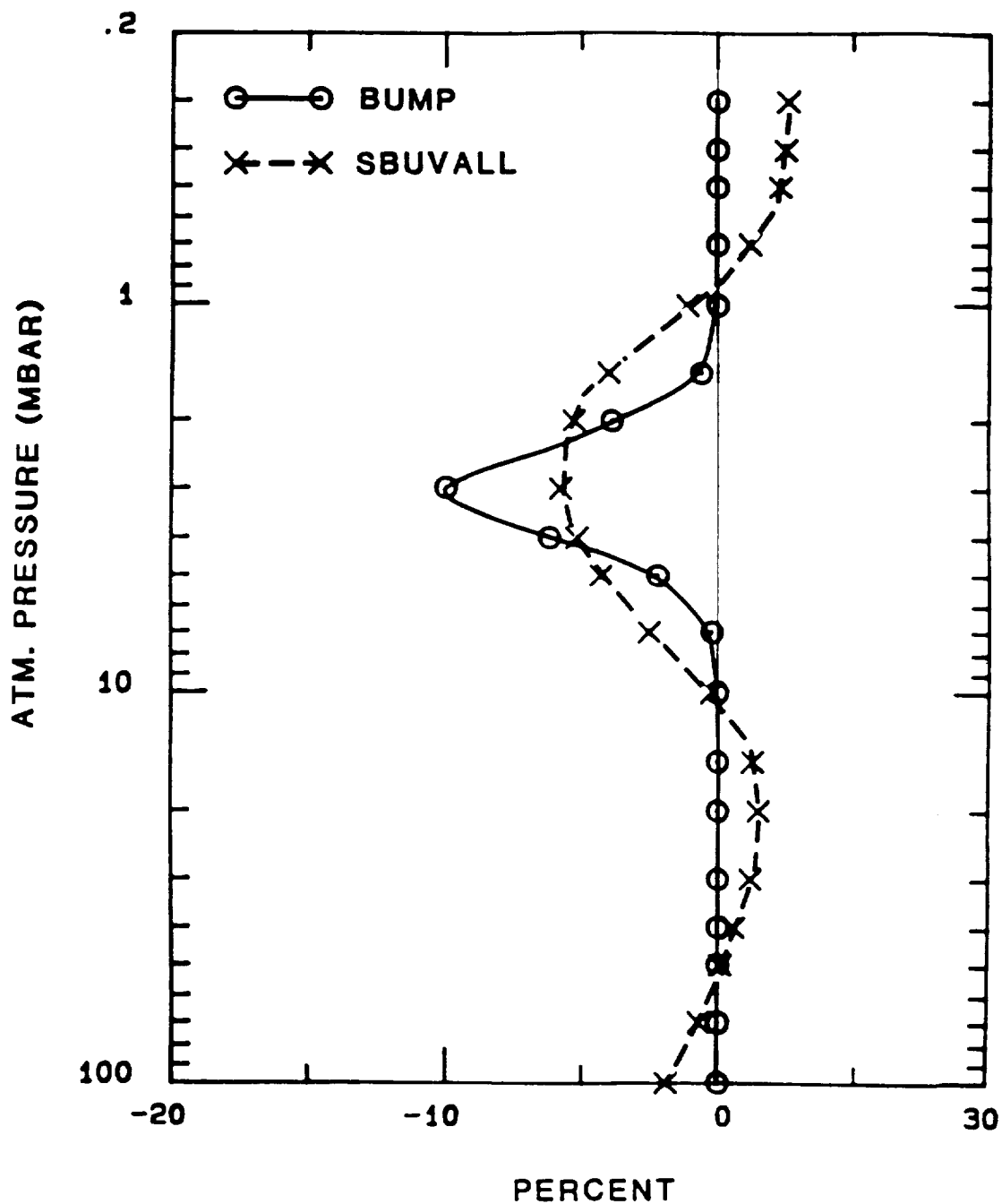


Figure 7.2. Effect on retrieved ozone of 5% Gaussian change, centered at 3.0 mbar with 5 km full-width at half-maximum.

7.4.2 Averaging Kernels

In the averaging kernel approach the profiling system is regarded as a bandpass filter, called the averaging kernel. The profile retrieved by the algorithm in this concept is the convolution of the averaging kernel with the actual ozone profile. The FWHM of this filter defines the resolution of the profiling system. Other properties of the averaging kernel are also analogous to those of a typical bandpass filter, such as an asymmetric bandpass or out-of-band response.

Figure 7.3 is a plot of these kernels at selected pressure levels. The results shown are for a measurement made near the equinox in mid-latitudes, but results for other situations are similar, except at very high solar zenith angles, where all the kernels shift upward by up to 5 km. Table 7.4 summarizes the properties of the averaging kernels at the 19 pressure levels at which SBUV mixing ratios are reported. The peak or mode is the pressure, in mbar, at which the averaging kernel has its maximum value. The error of the peak is the difference in *kilometers* between the actual height of each pressure level and the height where the averaging kernel has its peak value. Positive values signify that the actual height of the pressure level is above that of the peak of the averaging kernel for that level.

Because of these differences between the location of the mode of the averaging kernel and the pressure level, a change in ozone that affects a region of the atmosphere on the order of or smaller than the FWHM given in Table 7.4 will be reported at the wrong altitude. The mode error is the maximum possible error of this kind that can occur. The out-of-band to in-band ratio is the ratio of the fraction of the system response not located between the two zeros surrounding the mode to that between the two zeros. A large out-of-band fraction for a level means that changes at levels far away from a given pressure level may affect the derived results for that level.

In general, the averaging kernels between 0.7 mbar and 20 mbar have "reasonable" properties; the likelihood that SBUV will report misleading information between these altitudes is small. At higher solar zenith angles (> 80 degrees) the upper limit moves up to 0.3 mbar. Outside these limits, the resolution of the SBUV ozone profiles depends strongly on the validity of the *a priori* assumptions made in the retrievals.

For the upper levels (0.3 mbar to 1 mbar), the key *a priori* assumption is that the ozone profiles have a constant scale height (in pressure units); i.e., $\log p(\text{O}_3)/\log p$ is constant, where $p(\text{O}_3)$ is the ozone partial pressure and p is the atmospheric pressure. In the lower levels, the key *a priori* assumption in the algorithm is that the fractional variance of the ozone in layer 2 is almost 2 orders of magnitude larger than that in layer 5, fractional variances of other intermediate layers falling in between. The ozone balloonsondes show this behavior very clearly for short-term to mid-term (seasonal) variations in ozone. For longer term variations, however, the validity of these assumptions is not certain. Current photochemical theories do suggest that the changes in layer 5 (around 20 mb) are likely to be the smallest.

The SBUV results in the 20 mb to 100 mb range agree extremely well with balloonsonde results and, therefore, may be usable for those scientific studies where a high degree of accuracy is not desirable or when no other source of reliable information -- such as the study of global ozone fields, meridional transport, or estimation of ultraviolet flux at different altitudes in the atmosphere -- is available. For studies requiring a high degree of accuracy, such as studies of long-term trends in ozone, users are advised to study the sum of ozone in layers 2, 3, and 4 rather than the reported ozone mixing ratios in the 20 mb to 100 mb range. Error studies show that the *a priori* information largely determines how ozone is distributed among the three layers, whereas the instrumental measurements determine the sum of the ozone amounts in the three layers.

The estimated systematic errors in ozone due to the retrieval process are given in line 3 of Table 7.2; the random errors appear in line 3 of Table 7.3.

Mid 325 DU, 45 SZA

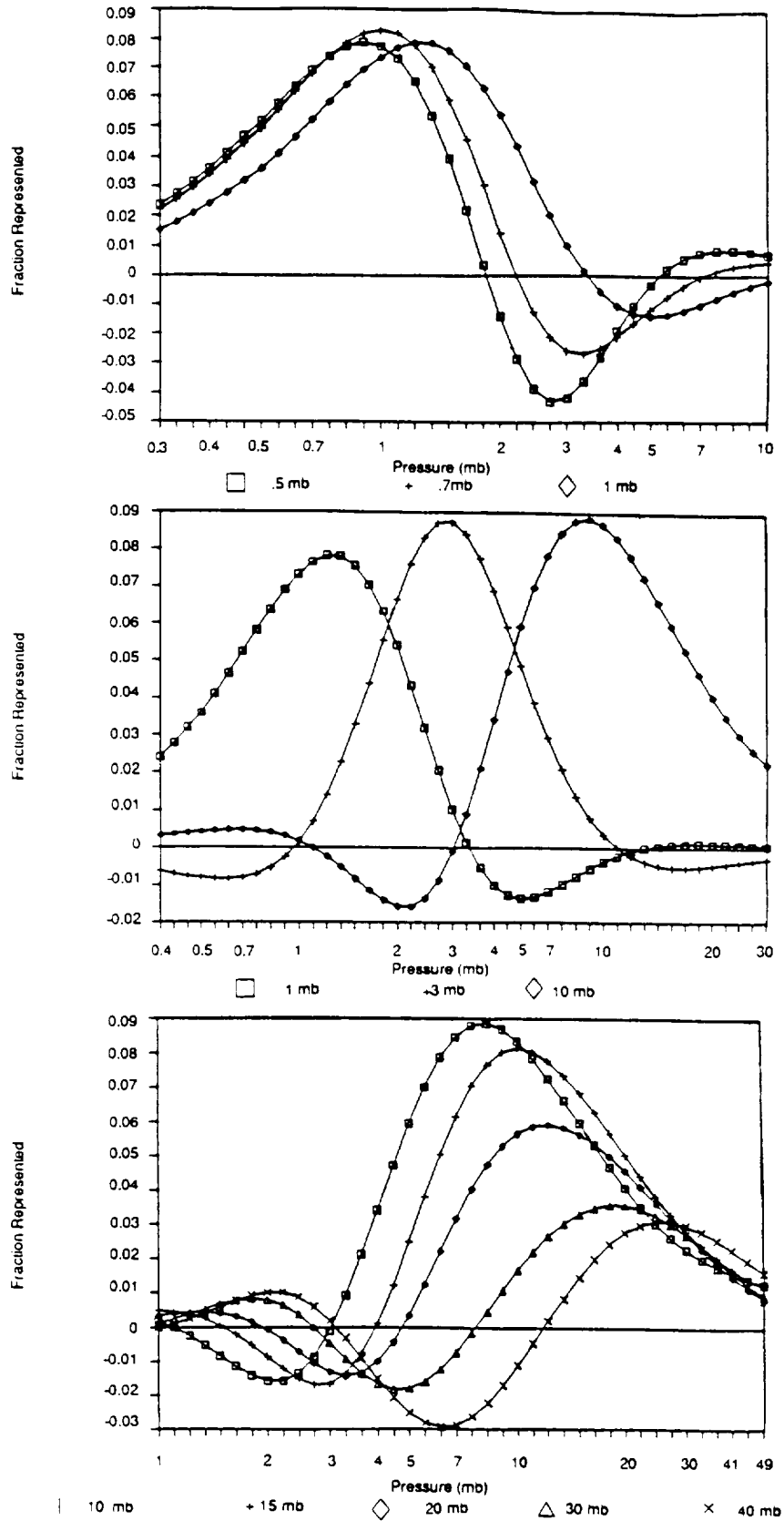


Figure 7.3. SBUV Averaging Kernels.

Table 7.4
Properties of Averaging Kernels

Pressure (mb)	Peak (mb)	Error of Peak (km)	FWHM (km)	Out-of-Band/ In-band
0.3	.8	6.8	8.2	.35
0.4	.9	5.6	8.7	.26
0.5	.9	4.1	8.7	.21
0.7	1.0	2.5	9.6	.13
1.0	1.3	1.8	10.2	.08
1.5	2.0	2.0	8.5	.12
2.0	2.4	1.3	7.6	.13
3.0	3.0	0.0	7.9	.16
4.0	3.8	-0.4	8.4	.11
5.0	4.5	-0.7	7.9	.06
7.0	6	-1.1	8.7	.06
10.0	8	-1.5	10.0	.06
15.0	10	-2.8	9.7	.07
20.0	12	-3.5	9.8	.14
30.0	20	-2.8	8.9	.47
40.0	25	-3.3	8.3	.67
50.0	30	-3.5	9.0	.37
70.0	40	-3.9	10.8	.18
100.0	45	-5.5	11.2	-

7.5 Long-Term Drift

Table 7.5 presents the estimates of uncertainty in determining long-term trends. Two of the sources of uncertainty are instrumental effects discussed in Section 7.1: a possible change with time in the wavelength measured at a given monochromator step scan position, and a possible change in the correct radiometric calibration constants. Estimates of the size of these effects appear in the first two lines of Table 7.5. A third source of uncertainty arises from a possible long-term temperature change and its effect on ozone absorptivity. This effect is discussed in Section 7.3. The possible time-dependent error is estimated on line 3. The remaining two sources of error in Table 7.5 are associated with possible changes in ozone in layers where SBUV cannot measure ozone directly.

The algorithm for retrieving profiles requires that the sum of the amounts of ozone in individual layers, calculated from measurements at the shorter, profiling wavelengths, equal an independently measured total ozone value. However, the radiances used to derive the ozone profile by SBUV are not sensitive to changes in tropospheric ozone. Should tropospheric ozone change, derived total ozone will change, but the radiances will be relatively unaffected. In such a case, the algorithm will assume the wrong total amount of ozone in the layers it is calculating. This ozone deficit or excess will appear in the profile, at the highest pressures or lowest altitudes. This error is listed on line 4 of Table 7.5. The wavelengths at which SBUV measures albedo do not provide enough information to monitor changes in ozone above 0.3 mbar. Nevertheless, if ozone in these layers changes, there will be a slight effect on the albedos at the shortest wavelengths, and, therefore, on the ozone derived at higher pressure. Line 5 shows the magnitude of this effect. The errors in the changes of ozone with time estimated in lines 3, 4, and 5 of Table 7.5 are errors that would be produced by plausible changes in temperature, tropospheric ozone, or ozone above 0.3 mbar. If independent measurements of any of these

quantities were available, they could be used to correct the ozone values derived from SBUV and eliminate that source of uncertainty in the trend.

Table 7.5
Experimental Uncertainties In Measuring Long-Term Ozone Trend

Error Source	Ozone Mixing Ratio Error (%)				Total Ozone
	1 mb	3 mb	10 mb	30 mb	
1. Wavelength Calibration	.2/T	.4/T	.4/T	.4/T	.4/T
2. Radiometric Calibration	10/T	10/T	8/T	5/T	3/T
3. Atmospheric Temperature	.02/°K	.05/°K	.1/°K	.15/°K	.15/°K
4. Tropospheric Ozone		.01% Change			.05%
5. Ozone Above 0.3 mb	.1%		.01% Change		

Notes:

The value of T in error sources 1 and 2 is equal to the number of years of instrument data used for analysis. For SBUV, T is 8 years. The values given apply to mid-latitude retrievals.

Errors 3, 4, and 5 are given as an ozone error due to changes in the relevant atmospheric parameter. If these changes are known from external sources, SBUV ozone values can be corrected using these numbers.

7.6 Comparison with Other Ozone Measurements

The bottom line of Table 7.2 presents an estimate of the combined absolute errors in derived total and profile ozone from all the estimated major error sources, for mid-latitude profiles. The estimated errors from the five listed individual sources are combined using the law of variance (root sum of the squares or RSS) to obtain an overall estimate for the error. The estimates, presented in Table 7.3, of the random errors in individual SBUV measurements should be considered only when SBUV data for individual data points or a small number of data points are compared with other measurements.

The largest error source for total ozone is the uncertainty of the ozone absorption cross-section. However, when SBUV ozone values are being compared with those from other ultraviolet instruments that use the same cross-section, for example the Dobson total ozone measurements, this error does not apply. Neglecting the cross-section error, the estimated (one standard deviation) overall error is 1.6 percent.

The estimated overall absolute errors for the profile are larger than for total ozone, because the radiometric calibration and the retrieval error (or algorithm error) are considerably larger for the profile. The radiometric calibration error is small for total ozone because the total ozone algorithm uses pairs of measured albedos to compute ozone. However, the profile algorithm uses the individually measured albedos.

Table 7.6 presents the biases obtained from comparisons between measurements by SBUV and those by other ozone sensors. Total ozone values measured by SBUV are compared with those measured from the ground by the network of Dobson and M83 stations. The SBUV ozone profiles are compared with Umkehr measurements from the surface, balloon ozonesondes, and radiance-measuring rockets and photometers.

All the comparisons reported here were made using ozone amounts in Umkehr layers. Appendix A provides a definition of the Umkehr layers. Data from other sensors were converted to this format. SBUV data are matched with data from other sensors using the following criteria. SBUV and ground station data must be from the same day. The center of the SBUV field of view must be within 1° of the latitude of the station. The maximum permissible longitude separation varies from 2° for total ozone to 5° for layers 1 through 4, and 10° for the higher layers. These window choices have proven empirically to represent the best compromise between the need for a window that is large enough to provide a sufficient quantity of data to minimize random error and a window that is small enough to minimize systematic errors resulting from changes in ozone with longitude.

To condense the large volume of comparison data into a few meaningful, easily comprehensible quantities, the following linear regression was used:

$$\Delta = b + dt + a_1 \cos 2\pi t + a_2 \sin 2\pi t + a_3 \cos 4\pi t + a_4 \sin 4\pi t, \quad (29)$$

where

$$\Delta = 100 \times (\text{SBUV} - \text{OTHER SENSOR}) / \text{SBUV}$$

t = Time in years measured from the starting day of SBUV measurements, 1 November 1978

b = Intercept of the regression line at t=0, representing the initial bias

d = Drift between SBUV and other sensor in %/year.

The last four terms in the regression model are used if the regression algorithm determines them to be significant. They represent possible seasonal dependence in the bias between SBUV and another sensor.

This regression model has been fitted to the SBUV-ground difference for each individual station. Only those stations with more than 50 matches with SBUV over the six years are included: 66 Dobson, 19 M83, 17 Umkehr (5 in layers 1-4), and 10 ozonesonde stations (11 in layer 5).

The Dobson network has not adopted the new NBS ozone absorption cross-sections used by SBUV. If the Dobson measurements were reduced using the new cross-sections, the bias between SBUV and Dobson would be estimated to decrease by 2-3 percent. In addition, there is an estimated 1.5 percent systematic uncertainty in SBUV alone. The combination of these effects could easily explain the observed initial bias between SBUV and Dobson.

The profile comparisons show no systematic pattern from one sensor to another except in the 10 mbar to 20 mbar range, where SBUV is systematically lower than the other sensors. The bias relative to Umkehr oscillates with altitude. However, little importance should be attached to the Umkehr biases until the Umkehr data have been reprocessed using the new NBS cross-sections.

In the determination of the biases for both the total ozone and the profile, the uncertainties are dominated by the station-to-station variabilities in the data rather than the number of data points. Thus, the inconsistencies between stations and between sensors limit the accuracy and precision with which the SBUV data can be validated.

Table 7.6
Bias Between SBUV and Conventional Ozone Sensors

%Bias (SBUV - Other Sensor)⁽¹⁾

Umkehr Layer Number	Pressure At Layer Midpoint (mb)	Conventional Ozonesondes		Umkehr ⁽³⁾		UV Rocket	UV Photometer
		(Nov 78)	(Oct 84)	(Nov 78)	(Oct 84)		
9	1.4	-	-	-2	9	-12	-
8	2.8	-	-	3	5	-7	-
7	5.6	-	-	0	-2	-7	2
6	11	-1	-7	-11	-12	-13	-9
5	22	-7	-9	-10	-8	-10	-4
4	45	-3	0	13	15	-	-3
3	90	7	13	14	13	-	11
2	180	10	4	-5	-29	-	-
0 + 1	507	-4	-13	-4	-17	-	-
Total Ozone				-2.0 ⁽²⁾	-4.2 ⁽²⁾		

Note:

- (1) For Umkehr and conventional ozonesondes, bias is projected to the beginning and end of data period using linear regression. Rocket bias is based on 18 Wallops Island ROCOZ flights made between August 1983 and October 1984. UV photometer bias is the average of four instruments flown from Palestine, Texas on 21 March 1984.
- (2) Dobson. The Dobson network has not adopted NBS ozone cross-sections. If it were to do so, Dobson total ozone would decrease by 4%, changing the SBUV/Dobson bias to +2% in November 1978 and -0.2% in October 1984.
- (3) Umkehr data for 1-1/2 years following the eruption of El Chichon are not used.

Table 7.7 presents the observed drift between SBUV and Dobson, ozonesondes and Umkehr, based on 8 years of measurements. The drift between SBUV and Dobson is approximately 3 percent over 8 years. One contribution to such a drift could be the change in tropospheric ozone observed at ozonesonde stations (e.g., Logan and Kirchhoff, 1986). Whether this change is global or represents only a local increase of photochemical pollution in the urban areas where most of those stations are located is not known. For a global change, the observed increase of about 10 percent in tropospheric ozone during the SBUV measurement period would generate an algorithm-related drift of -0.5 percent for the period. If the change is local, however, the Dobson, ozonesonde, and Umkehr values will not be truly representative of atmospheric ozone but will contain a local, pollution-induced error. This effect is far too small, however, to explain the entire observed drift in total ozone.

The Umkehr technique can be highly sensitive to the presence of atmospheric aerosols (Deluisi, 1979). A new Umkehr data set, corrected for the impact of aerosols on the Umkehr retrieval, has recently become available (Deluisi, private communication). It includes only five stations, in northern mid-latitudes. Table 7.7 shows that, in the upper layers, there are statistically significant drifts between SBUV and this corrected Umkehr data set, on the order of 5-8% over the 8 years of data. In the lower layers, the vertical resolution of both instruments degrades considerably, and only combined values for multiple layers are meaningful. The drift of SBUV relative to Umkehr for the combined layers 2-4 is -0.3 ± 0.2 %/year.

The drift between SBUV and ozonesondes is not significant in most layers; however, the statistical uncertainties in estimating this drift (3 percent to 8 percent over 8 years) are rather large -- on the order of the estimated uncertainty from SBUV.

In summary, there appears to be a significant, calibration-related drift in the SBUV total ozone and upper level ozone profile values relative to those from ground-based measurements. The SBUV results can be approximately normalized to the long-term behavior of the ground network using drift correction factors derived from Table 7.7. The ground truth comparisons are too noisy to resolve any latitude dependence or non-linear time dependence in the SBUV-ground differences.

Table 7.7
Drift Between SBUV and Conventional
Ozone Sensors

Umkehr Layer No.	Drift in %/year	
	SBUV-Ozonesondes	SBUV-Umkehr
9	-	-0.8 ± 0.4
8	-	-1.0 ± 0.2
7	-	-0.7 ± 0.2
6	-0.7 ± 1.0	-0.6 ± 0.1
5	-0.3 ± 0.3	-0.3 ± 0.1
4	0.4 ± 0.7	0.4 ± 0.2
3	0.4 ± 1.0	-0.7 ± 0.4
2	-1.7 ± 0.8	-4.1 ± 0.8
0 + 1	-2.8 ± 1.8	-0.2 ± 1.1
Total Ozone (SBUV-Dobson)	-0.38 ± 0.13	

Note: Uncertainties represent 95% confidence limits.

SECTION 8

PROBLEMS LOCALIZED IN SPACE AND TIME

8.1 Contamination From El Chichon

The three eruptions of El Chichon in southern Mexico between 28 March and 6 April 1982 injected significant amounts of sulfur-containing gas and dust into the tropical stratosphere. The principal sulfur gas was SO₂, which changes in time to H₂SO₄ aerosol.

When gaseous SO₂ is present, it absorbs in several bands in the 290 nm to 320 nm range, some of which coincide with wavelengths used by SBUV to measure ozone. When aerosols form, enhanced scattering is expected, in particular at the 297.5 nm, 301.9 nm, and to a lesser extent, at the 305.8 nm wavelengths used to measure ozone. Thus, in the first days after the eruption, the data reflect these two opposite effects. Some tropical areas show the increased radiances from aerosol scattering, while others show the decreased values caused by SO₂ absorption. By early June only anomalous increased radiances occur in the data, as the SO₂ gas is converted entirely to aerosol. Thus, the only relatively long-term effects of El Chichon on the SBUV data are increased radiances caused by aerosol scattering.

Because the effect of aerosol on the longer wavelengths used to determine total ozone is relatively small, the accuracy of derived total ozone is not significantly affected, even when stratospheric aerosol levels are highest. The use of ratios of albedos for pairs of wavelengths further reduces the impact of any anomalous increase in radiance from the aerosols. On the other hand, the anomalous increased radiances at the three ozone measurement wavelengths listed above significantly affect the accuracy of the ozone profile. For these increases in radiance, the profile algorithm derives a significant decrease in ozone in the middle stratosphere, where most of the ozone resides. The profile from the altitudes of the 5 mbar pressure level downward is affected. Because the algorithm requires that the sum of the ozone amounts equal total ozone, and because total ozone is practically unaffected, the profile algorithm is forced to increase the ozone at some other layer. This increase occurs where the derived ozone is least sensitive to the measured albedos, in Umkehr layers 1-3, from 64 mbar to the surface. Because the normal ozone content of these layers is low, the distortion of the albedos by aerosol produces a very large anomalous increase in the profile ozone for Umkehr layers 1-3. Thus, the profile algorithm can detect the presence of very small amounts of stratospheric aerosols by monitoring the anomalous increases in ozone for Umkehr layers 1-3.

The degree to which tropospheric ozone for a particular profile deviates from the values expected from climatology is described by the Volcano Contamination Index (VCI). The VCI is expressed in units of the climatological standard deviation of the tropospheric ozone value for a given latitude. For example, a VCI of 5.0 represents a profile with a tropospheric ozone value 5.0 standard deviations larger than the climatological average.

When the VCI is 5.0 or greater, the profile error flag is set (i.e., word 257 of the HDSBUV tape is set equal to either 1 or 11, and 10 is added to word 10 of the CPOZ tape). This error flag does not screen all the data contaminated by aerosol but only that which is most significantly affected. *Unflagged data, in particular unflagged data with VCI between 2 and 5, can still have significant aerosol contamination.* Consequently, ozone profiles with values of the VCI between 2 and 5 should be rejected if they are in the neighborhood of profiles with a VCI greater than 5. In addition, ozone profiles from other extended regions where the VCI is consistently above 2 should also be considered suspect.

The VCI derived for an aerosol layer of a given optical thickness is very sensitive to the height of the layer. Calculated simulations show that aerosols below 20 km would be indistinguishable from normal tropospheric clouds. Thus, even when significant aerosol is present, it has relatively little impact on the profile if it is sufficiently low in the atmosphere.

Krueger (1985) describes a function related to the amount of SO₂ present that is denoted as the SO₂ Index (SOI). This index can be expressed as the following function of the N-values for SBUV:

$$\text{SOI} = [32.21N_{340} - 60.88N_{331} + 51.69N_{318} - 23.03N_{312} - 1.8 - 59.3s\Omega - 47.6(s\Omega)^2 + 59.3\Omega]/s, \quad (29)$$

where s is slant path $1/\cos\theta_0$, Ω is Best ozone, and θ_0 is solar zenith angle. The SOI appears on the HDSBUV tape as word 46. It does not appear on the CPOZ tape or the ZMT. The SOI was stored on the HDSBUV tape because it has proved useful in deriving SO₂ amounts from TOMS data; however, examination of selected scans has shown that the SOI from SBUV is not a reliable measure of atmospheric SO₂.

8.2 Problems with Antarctic Ozone Low

Each year since the first year of SBUV measurements, ozone over Antarctica has decreased significantly during the first 40 days after the spring equinox (21 September). For example, at the 80° S latitude band, total ozone during this 40-day period in 1979 ranged from 260 matm-cm to 360 matm-cm but in 1983 decreased to a range of 200 to 235 matm-cm. The springtime ozone decrease has become even more pronounced in later years. Each year, after the 40-day period, total ozone returns to values relatively close to the 1979 values for the same season.

The SBUV algorithm uses historical ozonesonde data for the construction of the total ozone and profile "look-up" albedo tables and of the profile first guess. Because of the lack of ozonesonde data at high latitudes in the southern hemisphere, corresponding northern hemisphere data were used. Limited data from high latitudes in the southern hemisphere had suggested that there was no significant difference between the two hemispheres. The ozonesonde data did not contain profiles with ozone less than 270 matm-cm. Thus, during the 40-day periods when the ozone is very low, the SBUV total ozone and the profile multiple scattering correction are derived from extrapolations of the albedo tables significantly beyond the historical range of climatological data. Likewise, the profile first guess is derived from extrapolations of historical ozonesonde data.

At the time the archived data were generated, only limited ozonesonde data from Antarctica during these 40-day periods were available for the SBUV lifetime (Chubachi, 1985). Such data and the results of special studies of the SBUV-measured albedos suggest that, while the error from extrapolation of the albedo tables is relatively small compared with the decrease in ozone observed from SBUV, the error from extrapolation of the profile first guess is large. Table 8.1 shows the percent change in the average ozone profile for the 80°S latitude band from the period of 1-15 October 1979, to the period 1-15 October 1984, as obtained from the archived data set. Also shown in Table 8.1 is the percentage change in ozone for the same period from two special studies using different first guesses. The results from the two special studies differ relatively little from each other. However, for layer 7 and below, there are significant differences between the archived data and changes derived from the special studies. McPeters *et al.* (1986) also demonstrate the effect of changes in the *a priori* profile on the retrieved ozone profile during times of low Antarctic ozone.

8.3 Solar Eclipses

When the Sun is eclipsed, the decrease in incoming solar irradiance leads to a decrease in the backscattered Earth radiance, as the actual albedo is not affected. However, because the solar irradiance used to calculate the albedo for ozone retrieval is derived from measurements of the uneclipsed Sun, the albedo derived using it will not be correct during times of eclipse. Consequently, ozone values are not retrieved for periods of time and ranges of latitude where

Table 8.1
 Percent Change in Average Ozone Profile Over Antarctica (80° South) 1-15 October
 1979 to 1-15 October 1984

SBUV Layer	Layer Center Pressure (mbar)	Special Studies		
		Archived Data	First Guess A*	First Guess B**
1	0.18	-11	-17	-11
2	0.35	-15	-16	-15
3	0.70	-19	-18	-19
4	1.4	-21	-19	-21
5	2.8	-18	-18	-19
6	5.6	-14	-16	-16
7	11	-10	-17	-18
8	22	-38	-25	-27
9	45	-47	-31	-30
10	89	-7	-31	-30
11	179	-40	-28	-24
12	506	-12	-21	-24

* Profile first guess based on study of change in SBUV measured albedos.

** Profile first guess based on ozonesonde data from Syowa station (69° South); 1979-1983 data.

the radiances are affected by a solar eclipse. Table 8.2 lists the days, times, and regions of the Earth involved. In actual production, the information in this table is part of the input stream for the job run and is used by the software to exclude the listed periods and regions.

Table 8.2
Solar Eclipses

Year	Date	Day of Year (Number)	Start Time (GMT seconds)	End Time	Northern Limit	Southern Limit
1979	February 26	57	53160	68634	83° N	3° N
1979	August 22	234	53754	71346	4° S	79° S
1980	February 16	47	22554	41520	62° N	40° S
1980	August 10	223	58482	79800	40° N	55° S
1981	February 4-5	35-36	70068	02952	5° N	90° S
1981	July 31	212	84278	22824	90° N	5° N
1982	January 25	25	10188	23658	30° S	90° S
1982	June 21	172	37668	49176	18° S	68° S
1982	July 20	201	62322	72546	90° N	40° N
1982	December 15	349	26514	42042	68° N	9° N
1983	June 11	162	07770	26148	30° N	68° S
1983	December 4	338	34860	55194	69° N	35° S
1984	May 30	151	50008	70506	83° N	29° S
1984	November 22-23	327-328	72804	05598	30° N	85° S
1985	May 19	139	69208	85338	90° N	12° N
1985	November 12	316	43722	58326	40° S	90° S
1986	April 9	99	14940	30720	0°	90° S
1986	October 30	283	61020	76440	90° N	5° S
1987	March 29	88	36120	56160	45° N	90° S
1987	September 23	266	00840	22080	90° N	50° S
1988	March 17-18	77-78	84240	16308	90° N	80° S
1989	March 7	66	58608	71892	17° N	75° N
1989	August 31	243	12816	26856	75° S	20° S

SECTION 9

TAPE FORMATS

9.1 High Density SBUV (HDSBUV) Tape

There are a number of changes in the format of this tape from the analogous product that was previously archived, the OZONE-S tape. Software that read the OZONE-S tape is likely to need revision before it can be used to read the HDSBUV tape.

9.1.1 Overall Structure

The HDSBUV tape is a multiple-file 9-track, 6250 bpi binary tape, written in fixed-block (FB) format on an IBM 3081 OS/MVS computer. It contains a standard header file followed by data files, a trailer file, and, usually, finally a trailer documentation file.

A HDSBUV tape normally contains 13 weeks of data, starting on a Sunday. The first tape covers the period 31 October 1978 to 27 January 1979. Each data file contains ozone data for one orbit. During each orbit, the SBUV experiment measures ozone in approximately 98 fields of view. A data file therefore contains approximately 98 records. Appendix F contains a complete catalog, listing the number of files on each tape and the day range.

The first file of each tape is a special file called the standard header, which is written in a format common to all archivable tapes produced by the Nimbus Operational Processing System (NOPS). Data files follow the standard header file. The first record of each data file contains processing information about the data records it contains. Data records follow, each containing total ozone and profile information from a single 32-second scan of the SBUV instrument. The last data record on the file contains a processing summary of the preceding orbit of data. Following this "last" record will be dummy records to fill the last block. These dummy records keep all blocks the same length and should be ignored.

The record type can be identified from word 2 of each record, which contains the logical sequence number of records within the file. It is set to 1 for the first (processing information) record of the file and is incremented by 1 for each successive record. For the last record, which contains the file processing summary (and dummy records following), the negative of the logical sequence number is written.

The last data file on the tape is called the trailer file. It contains 20 identical copies of a special trailer record (to fill one block). This trailer record contains a logical sequence number of -1 in word 2 and is provided as a convenient means of locating the end of data files on a tape.

Following the trailer file, many tapes have a trailer documentation file written in the same format as the first file on the tape, the standard header file. Column 1 of the standard header file contains an indicator of whether or not a trailer documentation file is present.

Detailed descriptions of all file types appear in Section 9.1.2.

Tape Specifications:

Data Files and Trailer File

Logical Record Length (LRECL): 828 bytes

Block Size (BLKSIZE): 16560 bytes

Record Format (RECFM): FB (fixed block)

Content: Primarily IBM 32-bit real numbers in binary

Header File and Trailer Documentation File

LRECL: 504 bytes

BLKSIZE: 2520 bytes

RECFM: FB (fixed block)

Content: Standard 126 character lines

9.1.2 Detailed Description

Standard Header File

The standard header file contains two identical blocks (physical records) of 630 characters written in EBCDIC. Each block consists of five 126-character lines. Lines 1 and 2 are written according to a standardized format called the NOPS Standard Header Record.

Line 1:

Columns	Description
1	An indicator to show whether the tape contains a Trailer Documentation File (TDF) blank = No TDF * = TDF present
2-24	Label: NIMBUS-7bNOPSbSPECbNo T
25-30	Tape specification number
31-37	Label: bSQbNO b
38-39	Production Definition Standard Header File description (PDF) Code: FL for HDSBUV
40-45	Tape sequence number defined as follows:
40	The last digit of the year in which the data were acquired
41-43	Day of the year (1-366) in which the data were acquired
44	Used to remove decade ambiguities in character 40. Set to 2 starting 24 October 1988; set to 1 earlier
45	Letter B
46	Copy number: 1 = original 2 = copy
47	Spare
48-52	Subsystem ID (with leading and trailing blank) For HDSBUV: SBUV

HDSBUV Standard Header File

Columns	Description
53- 56	General (Source) facility for HDSBUV: SACC (Science and Applications Computing Center)
57- 60	Label: bTOb
61- 64	Destination facility: for HDSBUV, this is IPD _b (Information Processing Division, Goddard)
65- 67	Start year, day of year, hour, minute, second for data coverage on this tape, in the form bSTART _b 19YY _b DDD _b HHMMSS
88-106	End year, day of year, hour, minute, second for data coverage on this tape in the form TO _b 19YY _b DDD _b HHMMSS _b In order to avoid unnecessary processing complications, the true ending date does not appear in the header record. Instead a fill date is used: 1999 _b 365 _b 240000
107-126	Generation year, day of year, hour, minute, second that the tape was created, in the form GEN _b 19YY _b DDD _b HHMMSS
b = blank	
Line 2:	
1-126	HIGH DENSITY OZONE (HDOZ) PROG. VERSION 2.0, AUG. 1985
Lines 3-5:	Information about processing software (e.g., program name, software version number, version date)

See example below:

```
*NIMBUS-7 NOPS SPEC NO T634416 SQ NO FL33101B2 SBUV SACC TO IPD START 1983 310 002057 TO 1999 365 240000 GEN 1985 247 204408
HIGH DENSITY OZONE(HDOZ) PROG. VERSION 2.0, AUG. 1985
USE VERSION 5.0 OZONE-S (JULY 85);NEW STANDARD OZONE PROFILE; NEW ABSORPTION & SCATTERING COEFFS.;NEW ALGORITHMS & CALIBRATION
```

HDSBUV

Format of First Record on Data Files

4-Byte Words	Description
1	Block identifier.
2	Logical sequence number (1).
3	Orbit number.
4- 7	Date of job run, (e.g., MON DEC 10, 1978).
8	Day of first good scan on tape.
9	GMT of first good scan (seconds).
10	Year of first good scan.
11	Subsatellite latitude (degrees) for first scan.
12	Subsatellite longitude (degrees) for first scan.
13	GMT of ascending node of orbit.
14- 17	Processing limits for latitude and solar zenith angles.
18- 30	Solar irradiance values (13; 1 for each wavelength).
31- 67	Radiance conversion factors (37).
68- 80	Instrument wavelengths (13).
81- 93	Ozone absorption coefficients for instrument wavelengths.
94-106	Rayleigh scattering coefficients (atm ⁻¹).
107-126	Processing options.
127-207	Spare (-77.).

Word 1 contains hexadecimal data; words 4-7 contain EBCDIC data, and the remaining words contain data in IBM floating-point format (REAL*4).

HDSBUV

Detailed Description of First Record on Data Files

Words	Comment						
1	Bits	1-2	13-16	17	18	19-24	25-32
		block number on file	spare on file; otherwise 0	1 for last block	1 for last file; otherwise 0	record id (in decimal) 05-first block on data file 20-intermediate blocks on data file 55-last block on data file 61-all blocks trailer file	spare
		Most of the information contained in the block identifier is more easily tracked using the logical sequence number (Section 9.1.1).					
11	Latitudes	range from -90° to $+90^\circ$, southern latitudes being negative.					
12	Longitudes	range from -180° to $+180^\circ$, western longitudes being negative.					
14-17	The following processing options are currently available:						
		Maximum solar zenith angle					(word 14)
		Minimum latitude					(word 15)
		Maximum latitude					(word 16).
18-30	The solar irradiance for the current day is given in units of $\text{watts/cm}^2/1 \text{ a.u.}$ in the following order: word 18:255.5 nm,..., 29:339.8 nm, 30: photometer (343 nm).						
31-67	The count-to-radiance conversion factors are in units of $\text{watt/cm}^2/\text{steradian}/\text{count}$ and are given for each monochromator wavelength for each of the three gain ranges in the following order: words 31-33:255.5,...,64-66:339.8 nm; word 67 has the value for the photometer.						
68-80	Instrument wavelengths are given in nm in the same order as the solar irradiance.						
81-93	The ozone absorption coefficients for each of the wavelengths are in units of $(\text{atm-cm})^{-1}$ and are in the same order as the solar irradiance.						

Detailed Description of First Record on HDSBUV Data Files (continued)

Words	Comment
107-126	<p data-bbox="399 317 1448 380">These words are reserved for up to 20 possible processing options; six are currently available (0 - disabled, 1 - enabled):</p> <ul data-bbox="496 415 1448 604" style="list-style-type: none"><li data-bbox="496 415 867 443">Word 107 - THIR processing<li data-bbox="496 447 1448 474">Word 108 - Check remaining central processing unit and input/output time<li data-bbox="496 478 878 506">Word 112 - Profile processing<li data-bbox="496 510 1292 537">Word 113 - Do not use 301.9 nm channel in profile processing<li data-bbox="496 541 1292 569">Word 114 - Do not use 255.5 nm channel in profile processing<li data-bbox="496 573 1300 600">Word 115 - Do not use 312.5 nm channel in profile processing.

Data Record Format for HDSBUV Tape

4-Byte Words	Description
1	Block identifier (ZX0 800); X = block number.
2	Logical sequence number (n+1) for n th data record.
3	Orbit number.
4	Day of year (1-366) at the start of scan.
5	GMT (seconds).
6	Subsatellite latitude at beginning of scan (degrees, -90° to +90°, southern latitudes negative).
7	Subsatellite longitude at beginning of scan (degrees, -180° to +180°, western longitudes negative).
8	View latitude -- average for total ozone (degrees).
9	View longitude -- average for total ozone (degrees).
10	Solar zenith angle -- average for total ozone (degrees).
11- 14	Four photometer N-values (339.8 nm, 331.2 nm, 317.5 nm, 312.5 nm).
15- 18	Four monochromator N-values (339.8 nm, 331.2 nm, 317.5 nm, 312.5 nm).
19	Gain selection flags for each of four wavelengths.
20	THIR processing code.
21	THIR Best total ozone (matm-cm).
22	Cloud top pressure (reported by THIR).
23	Pressure of reflecting surface (estimated using THIR).
24	THIR average reflectivity.
25	THIR percent cloudiness.
26	THIR error flag for total ozone.
27	A-pair total ozone (matm-cm).

Data Record Format for HDSBUV Tape (continued)

4-Byte Words	Description
28	A-pair sensitivity.
29	A-pair average reflectivity.
30	A-pair weight.
31	B-pair total ozone (matm-cm).
32	B-pair sensitivity.
33	B-pair average reflectivity.
34	B-pair weight.
35	Best total ozone (matm-cm).
36	C-pair total ozone (matm-cm).
37	Pressure of reflecting surface estimated without THIR.
38	Average reflectivity.
39	C-pair sensitivity.
40	Error flag for total ozone.
41	Table selection scheme index.
42	Snow/Ice Code 1 : Snow/Ice 2 : No Snow/Ice -1 : No information.
43	Photometer-monochromator reflectivity difference.
44	Terrain pressure (atm).
45	Spare (-77.).
46	SOI (sulfur dioxide index).
47	Spare (-77.).
48	View latitude -- average for profile (degrees).
49	View longitude -- average for profile (degrees).

Data Record Format for HDSBUV Tape (continued)

4-Byte Words	Description
50	Solar zenith angle -- average for profile (degrees).
51- 58	Eight photometer N-values (profile wavelengths 255.5 nm, 273.5 nm, 283.0 nm, 287.6 nm, 292.2 nm, 297.5 nm, 301.9 nm, and 305.8 nm).
59- 66	Eight monochromator N-values (profile wavelengths).
67- 68	Gain selection flags for each of eight wavelengths (one REAL*8 word).
69- 80	<i>A priori</i> profile individual ozone amounts (matm-cm) in 12 layers (see Appendix A).
81	Total ozone (matm-cm) for <i>a priori</i> profile.
82- 91	Q-values corrected for multiple scattering and surface reflectivity (255.5 nm through 317.5 nm).
92-101	Initial residues (255.5 nm through 317.5 nm) in percent.
102-106	Multiple-scattering and reflectivity correction to Q-values for five longer wavelength channels (297.5 nm through 317.5 nm).
107-111	Monochromator reflectivities for five longer wavelength channels (297.5 nm through 317.5 nm).
112-116	Sensitivity of multiple-scattering correction to total ozone for five longer wavelength channels (297.5 nm through 317.5 nm).
117-121	Multiple-scattering mixing fraction for five longer wavelength channels (297.5 nm through 317.5 nm).
122-131	Final residues (255.5 through 317.5 nm) in percent.
132-143	Solution profile individual ozone amounts (matm-cm) in 12 layers (see Appendix A).
144-155	Standard deviations for solution profile individual ozone amounts (%) in 12 layers, SBUV layer 1 first.
156	Total ozone (matm-cm) for solution profile.
157	Profile error code.

Data Record Format for HDSBUV Tape (continued)

4-Byte Words	Description
158-159	Parameters C and sigma (σ).
160-178	Solution mixing ratio ($\mu\text{gm/gm}$) at 19 pressure levels; 0.3 mbar first.
179-190	Standard deviations for <i>a priori</i> profile individual ozone amounts (%) in 12 layers.
191-200	Standard deviations for Q-values corrected for multiple scattering and reflectivity (255.5 nm through 317.5 nm) in %.
201	Number of iterations for profile solution.
202	VCI (Volcano Contamination Index).
203-205	Spares (-77.).
206	Solar zenith angle at start of scan (radians x 10^4).
207	Solar zenith angle at end of scan (radians x 10^4).

All words are in IBM floating-point format (REAL*4) except word 1, which contains hexadecimal data. Any word in the record may contain -77., indicating fill data.

HDSBUV

Detailed Description of Selected Words of Data Record

Word	Comment
2	Contains positive value 2 or larger for data record.
11- 18	N-value is computed from each measurement as $N = -100 \log_{10}(I/F),$ where I = measured radiance and F = measured solar irradiance.
19	Gain selection flags are packed into a 4-byte REAL word, with the 339.8 nm gain being the most significant byte.
20	Cloud processing code (describes quality of THIR data): <ul style="list-style-type: none"> <0 - Quality information not available; THIR data not used. 0-3 - Describes quality of THIR cloud data used by algorithm; a larger number signifies poorer quality: 0 is best, 3 is lowest quality acceptable for use by algorithm. >3 - Quality of THIR data extremely poor; THIR data not used by algorithm.
21- 26	Final output of total ozone processing using the cloud information from the THIR instrument -- total ozone is value above actual terrain height; Contains -77. if THIR data not available.
28, 32, 39	Sensitivity of a pair is defined as $\Delta N_p / \Delta \Omega$ where ΔN_p is the difference in the N-value of pair wavelengths and $\Delta \Omega$ is the difference in the total ozone.
30, 34	Weighting factor given to pair in Best ozone computation using equation (19), $W_C = 1 - W_A - W_B$.
35, 37, 38, 40	Final output of total ozone processing using the cloud information as provided indirectly from the measured reflectivity. Total ozone is value above actual terrain height.
26, 40	Error flags are defined as follows (further discussion of the error codes appears in Sections 3.4 and 6.5.3): <ul style="list-style-type: none"> 0 - Low path length, good scan. 1 - High path length, good scan. 2 - Very high path length, good scan. 3 - Spare. 4 - Inconsistency between Best ozone and largest weighted ozone pair value. 5 - Inconsistency between Best ozone and profile total ozone (difference $>3\sigma$)

HDSBUV

Detailed Description of Selected Words of Data Record (continued)

Word	Comment
	6 - Spare. 7 - Photometer and monochromator reflectivities differ by more than 0.15. 8 - Reflectivity out of range (-0.05,1.05). 9 - Best total ozone exceeds the dynamic range of the tables. The dynamic ranges are as follows: Latitude $\leq 15^\circ$ 180 to 350 DU Latitude 15° to 45° 180 to 600 DU Latitude $> 45^\circ$ 180 to 650 DU. (10 is added to the error flags for descending orbit data).
41	Table selection scheme index is a real number valued 1.0 - 3.0 indicating the relative weight given to standard profiles from 1.0 Equatorial profiles 2.0 Mid-latitude, and 3.0 High latitude.
46	Sulfur dioxide index; has not proved to be a reliable measure of SO ₂ for SBUV. (See Section 8.1 for additional discussion.)
59- 66	N-values for eight wavelengths in the following order -- word 59: 255.5, ..., 66: 305.8 nm.
67- 68 (one REAL*8 word)	Packed as in word 19, 305.8 being the most significant digit. NB: Must be read as a single REAL*8 word, not two REAL*4 words.
69- 80	<i>A priori</i> profile amounts in SBUV layers, layer 1 first.
81	Total ozone above 1 atm for <i>a priori</i> profile, not necessarily above actual terrain height.
82-131	The following comments apply to these words: Q-values for wavelengths are as defined in equation (4); that is, $Q = 4\pi I/F\beta P(\theta_0)$ where I = intensity of the backscattered radiation β = Rayleigh scattering coefficient F = solar flux P(θ_0) = Rayleigh scattering phase functions.

HDSBUV

Detailed Description of Selected Words of Data Record (continued)

Word	Comment
	<p>The residue is defined as follows:</p> $100(Q_{\text{obs}} - Q_{\text{calc}})/Q_{\text{calc}}, \quad (30)$ <p>where</p> <p style="margin-left: 40px;">Q_{obs} = Q-value calculated from an assumed radiance and solar flux</p> <p style="margin-left: 40px;">Q_{calc} = Q-value calculated from an assumed profile</p> <p style="margin-left: 40px;">Q_{msr} = Q-value that refers only to the multiple-scattered and reflected component of the total intensity (obtained from a lookup table).</p> <p>The Q-values and other related quantities are given in order from the shorter to the longer wavelengths. In words 102 through 121, values for wavelengths shorter than 297.5 nm are assumed to be zero.</p> <p>Words reserved for 312.5 nm contain valid data only when this wavelength is used.</p>
82- 91	$Q_{\text{corrected}} = Q_{\text{obs}} - Q_{\text{msr}}. \quad (31)$
92-101	Residue derived using Q_{calc} obtained from first guess profile.
102-106	Q_{msr} .
122-131	Residue derived using Q_{calc} obtained from final solution profile.
156	Total ozone above 1 atm for solution profile.
157	<p>Error flags are defined as follows: (Further discussion of the error codes appears in Sections 3.4 and 6.6.5).</p> <ul style="list-style-type: none"> 0 - No error. 1 - Lower level anomaly; probable aerosol contamination. 2 - Inconsistent total ozone and profile total ozone ($>3\sigma$). 3 - Final residue $> 3\sigma$. 4 - Measured Q-value differs by more than 60% from Q-value calculated with <i>a priori</i> profile. 5 - C greater than 3.0 matm-cm or less than 0.5 matm-cm. 6 - Sigma greater than 0.8 or less than 0.3.

HDSBUV

Detailed Description of Selected Words of Data Record (continued)

Word	Comment
	<p>7 - Reflectivity less than -0.05 or greater than 1.05, or changes by more than 0.05 from wavelength to wavelength.</p> <p>8 - No Best total ozone available.</p> <p>9 - Missing measurements or bad counts. (10 is added to the error flag for descending orbit data.)</p>
158-159	<p>Parameters determined by assuming an ozone profile of the form</p> $x(p) = Cp^{1/\sigma}, \quad (32)$ <p>where p = pressure in mbar, x = cumulative ozone at pressure level p, and C = ozone at 1 mbar (matm-cm).</p>
160-178	<p>Values of the solution profile mass mixing ratios are given in order of increasing atmospheric pressure at the 19 pressure levels: 0.3, 0.4, 0.5, 0.7, 1.0, 1.5, 2.0, 3.0, 4.0, 5.0, 7.0, 10, 15, 20, 30, 40, 50, 70, and 100 mbar. Volume mixing ratio (ppmv) = mass mixing ratio/1.657.</p>
202	<p>Volcano Contamination Index can be used to identify whether the derived profiles below 5 mbar are incorrect because of scattering by aerosols (See Section 8.1 for derivation and comments on usage).</p>

HDSBUV

Format of Last Record on Data Files

4-Byte Words	Description
1	Block identifier (ZX03500); X = block number.
2	Negative of logical sequence number $-(N+2)$, where N = number of data records.
3	Orbit number.
4	Day of last scan on file.
5	GMT (seconds) of last scan on file.
6	Subsatellite latitude (degrees) at the beginning of last scan.
7	Subsatellite longitude (degrees) at the beginning of last scan.
8	View latitude -- average for total ozone on last scan (degrees).
9	View longitude -- average for total ozone on last scan (degrees).
10	Number of tape read errors.
11	Number of scans read.
12	Number of scans written.
13- 27	Total ozone processing counters.
28- 38	Profile processing counters.
39-207	Spare.

All words are in IBM floating-point format except for word 1, which contains hexadecimal data.

HDSBUV

Detailed Description of Last Record on Data Files

Word	Comment
13-27	The following counters have been defined for total ozone processing:
13	Total number of unprocessed scans written to tape.
14	Zenith angle too large.
15	(not used.)
16	Bad counts.
17	Total number of scans with error codes 4-9 or 14-19.
18	Total number of scans with error code 9 or 19.
19	Total number of scans with error code 8 or 18.
20	Total number of scans with error code 7 or 17.
21	(not used.)
22	Total number of scans with error code 5 or 15.
23	Total number of scans with error code 4 or 14.
24	(not used.)
25	Total number of scans with error code 2 or 12.
26	Total number of scans with error code 1 or 11.
27	Total number of scans with error code 0 or 10.
28-37	The following counters have been defined for profile processing:
28	Total number of scans with error code 0 or 10.
29	Total number of scans with error code 1 or 11.
30	Total number of scans with error code 2 or 12.
31	Total number of scans with error code 3 or 13.
32	Total number of scans with error code 4 or 14.

HDSBUV

Detailed Description of Last Record on Data Files (continued)

Word	Comment
33	Total number of scans with error code 5 or 15.
34	Total number of scans with error code 6 or 16.
35	Total number of scans with error code 7 or 17.
36	Total number of scans with error code 8 or 18.
37	Total number of scans with error code 9 or 19.
38	Total number of scans for which a good profile could not be calculated.

HDSBUV

Format of Trailer File Record

4-Byte Words	Description
1	Block identifier.
2	Trailer file identifier (-1.0).
3-207	Spares.

9.2 Compressed Ozone (CPOZ) Tape

9.2.1 Overall Structure

The SBUV CPOZ tape is a 9-track, 6250 bpi binary tape generated on an IBM 3081 OS/MVS computer. The first header file of the CPOZ tape contains the Nimbus Ozone Processing System (NOPS) standard header record, written twice. Following it are the ozone data files. A trailer file and a trailer documentation file follow the last data file. Figure 9.1 summarizes the format of a CPOZ tape.

A CPOZ tape normally contains one year of data, covering the period of 1 October - 30 September. The tape for the first year covers the period from 31 October 1978, the date of the first measurements, to 30 September 1979. Each data file contains ozone data for one day. A day begins at 00 hours GMT. All data for a given orbit appear on a single file; the day to which an orbit is assigned depends on the GMT time at the beginning of the orbit. For example, if an orbit begins at 23:59 GMT on day 11, the data for it will be found in the file for day 11, even though most of the data were collected after 00 hours of day 12. Nimbus-7 makes 13 or 14 orbits per day. During each orbit, the SBUV experiment measures ozone in approximately 98 fields of view, for a total of up to approximately 1375 per day. As each logical record contains ozone data from one field of view, there may be up to approximately 1375 logical records in a data file.

Tape specifications:

Density: 6250 bpi

Data files and trailer files

LRECL: 288 bytes

BLKSIZE: 18432 bytes for yearly tape

9216 bytes for quarterly tape

RECFM: FB

Content: Primarily IBM 32-bit REAL numbers in binary

Header file and trailer documentation file

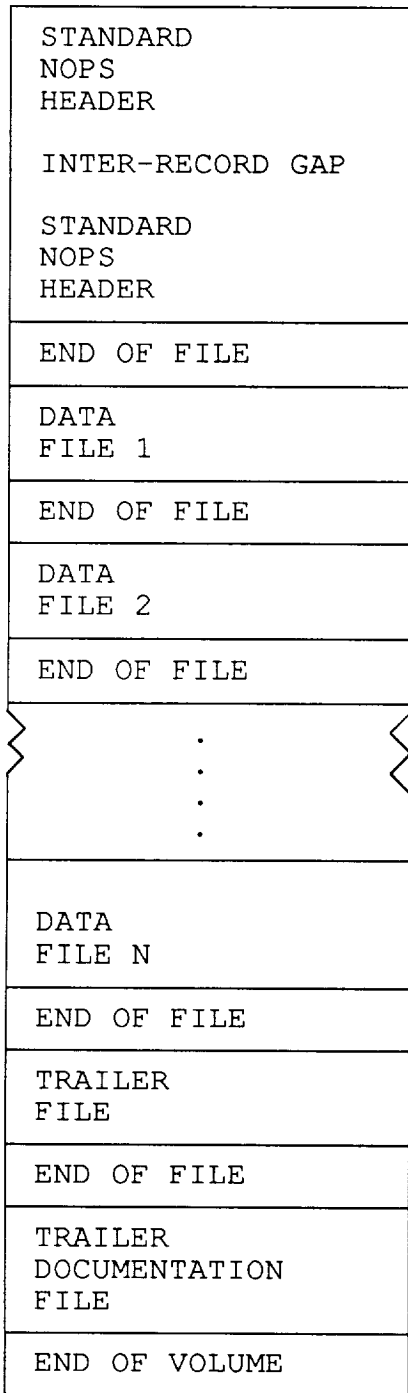
LRECL: 630

BLKSIZE: 630

RECFM: FB

Content: Standard 126 character lines

GROSS FORMAT



NOTE: Each data file contains a header record, N data records and a trailer record.

Figure 9.1. CPOZ tape structure - overview.

9.2.2 Detailed Format

CPOZ Standard Header File

The standard header file contains two identical blocks (physical records) of 630 characters written in EBCDIC. Each block consists of five 126-character lines. Lines 1 and 2 are written according to a standardized format called the NOPS Standard Header Record.

Line 1:

Columns	Description
1	An indicator to show whether a TDF will be found at the end of a tape: blank = No TDF * = TDF present
2-24	Label: NIMBUS-7bNOPSbSPECbNObT
25-30	Tape specification number
31-37	Label: bSQbNOb
38-39	Product Definition File (PDF) Code: FK for CPOZ
40-45	Tape sequence number defined as follows:
40	The last digit of the year in which the data were acquired
41-43	Day of the year (1-366) in which the data were acquired
44	Used to remove decade ambiguities in character 40. Set to 2 on or after 24 October 1988; set to 1 earlier
45	The existing hyphen remains unless there is a remake of the tape for any reason. In this case, an ascending alpha character will replace the hyphen, and reasons for the most recent remake will be recorded in logical record 4 of the header
46	Copy number: 1 = original 2 = copy

CPOZ Standard Header File

Columns	Description
47	Spare
48- 52	Subsystem ID (with leading and trailing blank) For CPOZ: SBUV
53- 56	General (Source) Facility: For CPOZ: SACC (Science and Applications Computing Center)
57- 60	Label: bTOb
61- 64	Destination Facility: for CPOZ, this is IPDb (Information Processing Division, Goddard)
65- 67	Start year, day of year, hour, minute, second for data coverage on this tape, in the form bSTARTb19YYbDDDbHHMMSS
88-106	End year, day of year, hour, minute, second for data coverage on this tape in the form bTOb19YYbDDDbHHMMSS In order to avoid unnecessary processing complications, the true ending date does not appear in the header record; instead, a fill date is used: 1999b365b240000
107-126	Generation year, day of year, hour, minute, second that the tape was created, in the following form: GENb19YYbDDDbHHMMSS
b = blank	
Line 2:	
1-126	VERSION 5 OZ-S ALGORITHMS FOR TOTAL OZ & PROFILE ; USE NEW CALIBRATIONS, STANDARD PROFILES, ABSORPTION & SCATTERING COEFFICIENTS
Lines 3-5:	USE VERSION 5.0 OZONE-S (JULY 85); NEW STANDARD OZONE PROFILE; NEW ABSORPTION & SCATTERING COEFFS.;NEW ALGORITHMS & CALIBRATION

See example below:

```
*NIMBUS-7 NOPS SPEC NO T634441 SQ NO FK40921B2 SBUV SACC TO IPD START 1984 092 001928 TO 1999 365 240000 GEN 1985 254 190001
VERSION 5 OZ-S ALGORITHMS FOR TOTAL OZ & PROFILE ; USE NEW CALIBRATIONS, STANDARD PROFILES, ABSORPTION & SCATTERING COEFFICIENTS
USE VERSION 5.0 OZONE-S (JULY 85); NEW STANDARD OZONE PROFILE; NEW ABSORPTION & SCATTERING COEFFS.; NEW ALGORITHMS & CALIBRATION
```


Description of Header Record of CPOZ Data File
(72 REAL*4 words)

Word	Description					
1	Block identifier.					
Bits	1-2	13-16	17	18	19-24	25-32
	block number on file	spare on file; otherwise 0	1 for last block	1 for last file; otherwise 0	record id (in decimal) 05-first block on data file 20-intermediate blocks on data file 55-last block on data file 61-all blocks trailer file	spare

Most of the information contained in the block identifier is easily tracked using the logical sequence number (Section 9.1.1).

- 2 Logical sequence number.
- 3 Orbit number. Orbits are numbered sequentially from the launch date (23 October 1979).
- 4 Year of first good scan on file.
- 5 Day of first good scan on file.
- 6 GMT (seconds) of first good scan on file.
- 7-8 Subsatellite latitude and longitude (degrees) for first scan.
- 9 Spare (filled).
- 10-13 Date of job run (example: MON DEC 13, 1983).
- 14-26 13 instrument wavelengths.
- 27-39 Solar flux at 13 wavelengths (watts/cm³).
- 40-52 Absorption coefficients at 13 wavelengths (atm-cm)⁻¹.
- 53-65 Count to radiance conversion constants (see Table 5.2) for gain range 2, at 13 wavelengths.
- 66-72 Spare (filled).

Description of Data Record of CPOZ Data File
(72 REAL*4 Words)

Word	Description					
1	Block identifier					
Bits:	1-12	13-16	17	18	19-24	25-32
	block number on file	spare	1 for last on file; other-wise 0	1 for last file; other-wise 0	record id (in decimal) 05-first block on data file 20-intermediate blocks on data file 55-last block on data file 61-all blocks trailer file	spare

Most of the information contained in the block identifier is easily tracked using the logical sequence number (Section 9.1.1).

- 2 Logical sequence number.
- 3 Orbit number.
- 4 Year.
- 5 Day.
- 6 GMT time of day (seconds).
- 7 View latitude (degrees; -90° to $+90^{\circ}$, north is positive).
- 8 View longitude (degrees; -180° to $+180^{\circ}$, east is positive).
- 9 Solar zenith angle (degrees).

Data Record of CPOZ Data File (continued)

Word	Description															
10	Data quality flag (3 digits): <table border="1" data-bbox="454 357 1429 798"> <thead> <tr> <th><u>Hundreds digit</u></th> <th><u>Tens digit</u></th> <th><u>Units digit</u></th> </tr> </thead> <tbody> <tr> <td>0 - ascending part of orbit</td> <td>0 - aerosol contamination not likely (but see Section 8.1)</td> <td>0 - low path</td> </tr> <tr> <td>1 - Descending part of orbit</td> <td>1 - contamination by aerosols</td> <td>1 - high path</td> </tr> <tr> <td></td> <td></td> <td>2 - very high path</td> </tr> <tr> <td></td> <td></td> <td>4 - pairs inconsistent</td> </tr> </tbody> </table>	<u>Hundreds digit</u>	<u>Tens digit</u>	<u>Units digit</u>	0 - ascending part of orbit	0 - aerosol contamination not likely (but see Section 8.1)	0 - low path	1 - Descending part of orbit	1 - contamination by aerosols	1 - high path			2 - very high path			4 - pairs inconsistent
<u>Hundreds digit</u>	<u>Tens digit</u>	<u>Units digit</u>														
0 - ascending part of orbit	0 - aerosol contamination not likely (but see Section 8.1)	0 - low path														
1 - Descending part of orbit	1 - contamination by aerosols	1 - high path														
		2 - very high path														
		4 - pairs inconsistent														
11	Reflectivity.															
12	Total ozone (matm-cm) (not using THIR infrared cloud height information).															
13	Total ozone (matm-cm) (using THIR infrared cloud height information).															
14	Volcano Contamination Index (values exceeding 5 indicate significant aerosol contamination; clusters of values between 2 and 5 indicate contamination likely).															
15-26	Monochromator N-values (255 nm - 340 nm).															
27-38	Ozone amounts - in 12 layers (matm-cm) - layer boundaries are in Appendix A. Note: Umkehr measurements report ozone amounts in <i>nanobars</i> .															
39-50	Estimated uncertainty of the 12 layer ozone amounts (percent for 67% confidence).															
51-69	Mixing ratios at 19 levels (0.3 mbar to 100 mbar) solution mixing ratio (microgram/gm) at 19 pressure levels: 0.3,0.4,0.5,0.7,1.0,1.5,2.0,3.0,4.0,5.0,7.0,10,15,20,30,40,50,70,100.															
70	Spare.															
71	Starting solar zenith angle for scan.															
72	Ending solar zenith angle for scan.															

Last Record in CPOZ Data File

Word	Description
1	IPD word (same as word 1 of header record of data file).
2	Logical record number.
3-72	Spare (filled).

Format of CPOZ Trailer File Record

4-Byte Words	Description
1	Block identifier.
2	Trailer file identifier (-1.0).
3-207	Spares.

9.3 Zonal Means Tape (ZMT)

9.3.1 Overview

The SBUV Zonal Means Tape (ZMT) is a 9-track, 1600 bpi, no-label, IBM 370/3081 compatible binary tape. It was produced on an IBM 3081 under OS/MVS. Each tape contains data for one year, starting in October. The October 1978 monthly averages on the tape for the first year are based on only one day of measurements. The tape for the year starting October 1986 is based on data only through 12 February 1987; the ZMT tapes end on that date.

The first file of the tape contains a standard header record, written twice. It is followed by 12 data files containing zonal means in geodetic coordinates. Each data file contains data for one calendar month, in the following order: daily, weekly, monthly, and, at the end of each calendar quarter, quarterly averages. Thus, the maximum number of records in any one file is 421 (366 days, 53 weeks, 1 month, 1 quarter). Records are written only for time periods where data exist. Weeks are seven-day periods, starting 1 January of each year. The average for a week appears in the file for the month in which the week ends. Because of computational complications, averages for weeks that span two quarters may not contain data for the earlier quarter. The zones are 10° in width, centered at the equator and at 10° intervals to the pole. The highest latitude, "80°" zones, use data only for 75°-81°. The data files are followed by a trailer file, which contains only one record, with a trailer file identification and fill values. The tapes also contain a Trailer Documentation File (TDF), which contains information on those tapes used in creating the current ZMT. Figure 9.2 provides a summary of the format of a ZMT. Section 9.3.2 begins with a summary of the contents of the files of each type on the tapes. A detailed description follows.

Tape specifications:

Density: 1600 bpi

Data files and trailer files

Logical Record Length (LRECL): 720 bytes

Block Size (BLKSIZE): 21600 bytes

Record Format (RECFM): FB

Content: Primarily IBM 32-bit REAL and INTEGER numbers in binary

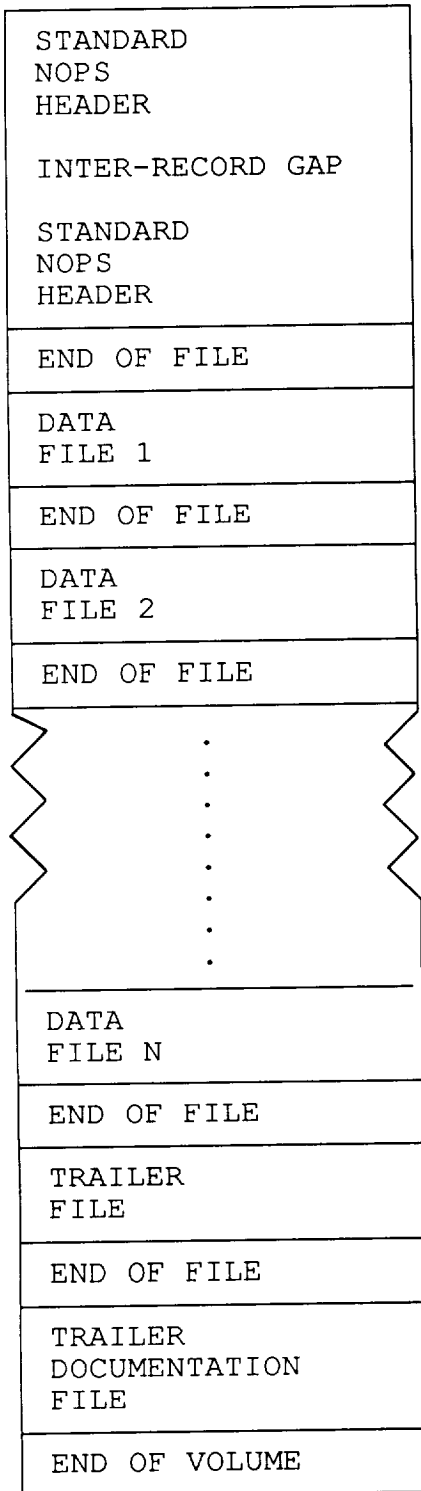
Header file and trailer documentation file

LRECL: 630

BLKSIZE: 630

RECFM: FB

Content: Standard 126 character lines



Standard Header Record
Standard Header Record
(duplicate)

First day zonal means record
⋮
Last day zonal means record
First week zonal means record
⋮
Last week zonal means record
Month 1 zonal means record
⋮
Quarterly zonal means record
(present for last month of
each quarter)

Trailer Record(s)

Figure 9.2. ZMT-T structure - overview.

9.3.2 Detailed Format

ZMT Standard Header File

The standard header file contains two identical blocks (physical records) of 630 characters written in EBCDIC. Each block consists of five 126-character lines. Lines 1 and 2 are written according to a standardized format called the NOPS Standard Header Record.

Line 1:

Columns	Description
1	An indicator of whether there is a Trailer Documentation File (TDF) at the end of a tape: blank = No TDF * = TDF present
2-24	Label: NIMBUS-7 _b NOPS _b SPEC _b NO _b T
25-30	Tape specification number
31-37	Label: _b SQ _b NO _b
38-39	Production Definition File (PDF) Code: FH for ZMT
40-45	Tape sequence number, defined as follows:
40	The last digit of the year in which the data were acquired
41-43	Starting day of year for tape
44	Used to remove decade ambiguities in character 40. Set to 2 on or after 24 October 1988; to 1 before
45	The existing hyphen remains unless there is a remake of the tape for any reason. In this case, an ascending alpha character will replace the hyphen, and reasons for the most recent remake will be recorded in logical record 4 of the header
46	Copy number: 1 = original 2 = copy
47	Spare

ZMT Standard Header File (continued)

Columns	Description
48- 52	Subsystem ID (with leading and trailing blank) For ZMT: SBUV
53- 56	General (Source) Facility For ZMT: SACC (Science and Applications Computing Center)
57- 60	Label: bTOb
61- 64	Destination Facility; for derivative products, this is IPDb (Information Processing Division, Goddard).
65- 67	Start year, day of year, hour, minute, second for data coverage on this tape, in the form bSTARTb19YYbDDDbHHMMSS
88-106	End year, day of year, hour, minute, second for data coverage on this tape in the form bTOb19YYbDDDbHHMMSS In order to avoid unnecessary processing complications, the true ending date does not appear in the header record. Instead a fill date is used: 1999b365b240000
107-126	Generation year, day of year, hour, minute, second that the tape was created in the form GENb19YYbDDDbHHMMSS
Line 2:	
1-126	SBUV/TOMS ZONAL MEANS TAPES VERSION NO. 3.0 10/85 (NEW INPUT & OUTPUT FORMATS, AND MORE LEVELS)
Lines 3-5:	USE VERSION 5.0 OZONE-S INPUT AND VERS. 3 ZMT SOFTWARE.

See example below:

Description of Data Record of ZMT Data File

Word	Type	Description of Data Items
1	-	Physical record number (12 bits) - sequence number of this record within a file.
1	-	Spare (4 bits).
1	-	File control (2 bits) - Last record in file indicator (1) - bit 17 is set to "1" to indicate last record in file, otherwise, it is 0.
1	-	Record ID (6 bits) - This field identifies the data record type: 34 = Daily means 35 = Monthly means 36 = Seasonal (Quarterly) means 62 = Weekly means.
1	-	Spares (8 bits).
2	I*4	Logical sequence number - Count of logical records in a file: Data Records: Greater than or equal to 1 Trailer Records: Less than -1.
3	I*4	Time span counter - Day (1-366), week (1-53), month (1-12), or season (1-4) depending on the time span (item 7).
4	I*4	Latitude zone - (-80, ..., 0, +10, +20, ..., +80).
5	I*4	Current year.
6	I*4	Terminator flag: +1 = terminator in zone, 0 = otherwise. On the weekly or longer means, the flag will be set if the terminator is in this zone at any time during the period.
7	I*4	Time span: 1 = daily, 2 = weekly, 3 = monthly, 4 = seasonal.
8	R*4	Pressure level in millibars: 0.3 mbar.
9	R*4	Zonal mean 0.3 mbar mixing ratio in microgm/gm. A zero average signifies that no mean could be calculated.
10	R*4	Standard deviation of zonal mean, in microgm/gm. Zero indicates no value computed.

Description of Data Record of ZMT Data File (continued)

Word	Type	Description of Data Items
11	R*4	Minimum ozone -- lowest value found while computing mean. Zero indicates no data in zone.
12	R*4	Maximum ozone -- highest value found while computing mean. Zero indicates no data in zone.
13	I*4	Number of data points used in computing mean.
14	I*4	Days (orbits) in period: actual number of days (for weekly, monthly, or quarterly data) or orbits (for daily averages) which had valid data.
15	R*4	Pressure level: 0.4 mbar.
16- 21		Same as 10-15, but for 0.4 mbar.
22-140		Same as 8-14, for 0.5, 0.7, 1.0, 1.5, 2.0, 3.0, 4.0, 5.0, 7.0, 10.0, 15.0, 20.0, 30.0, 40.0, 50.0, 70.0, and 100.0 mbar.
141	R*4	Pressure level for total ozone, 1000.0 mbar.
142	R*4	Zonal mean for Best total ozone computed without use of infrared cloud height information, in milliatmosphere-centimeters (matm-cm). A zero average signifies that no mean could be calculated.
143	R*4	Standard deviation of zonal mean, also in matm-cm. Zero signifies no value computed.
144	R*4	Minimum ozone: lowest total ozone value found while computing mean. Zero signifies no data in zone.
145	R*4	Maximum ozone: highest total ozone value while computing mean. Zero signifies no data in zone.
146	I*4	Number of data points used in computing mean.
147	I*4	Days (orbits) in period: actual number of days (weekly, monthly, or quarterly data) or orbits (for daily averages) that had valid total ozone values.
148-154		Same as 141-147, but for Best total ozone calculated using infrared cloud height information.
155-161		Same as 141-147, but for total ozone values used in deriving profiles.
162	R*4	1000.0 (mbar).
163	R*4	Zonal mean reflectivity (zero if no data in zone).

Description of Data Record of ZMT Data File

Word	Type	Description of Data Items
164	R*4	Standard deviation of zonal average reflectivity (zero if not computed).
165	R*4	Minimum reflectivity: lowest value found while computing mean (zero if no data in zone).
166	R*4	Maximum reflectivity: highest value found while computing mean (zero if no data in zone).
167	I*4	Number of data points used to compute mean.
168	I*4	Days (orbits) in period: number of days (for weekly, monthly, or quarterly average) or orbits (for daily average) with valid reflectivities.
169	I*4	Coordinate system = -1 for geodetic.
170-180		Spares.

Format of ZMT Trailer File Record

4-Byte Words	Description
1	Block identifier (ZX03500); X = block number.
2	Negative of logical sequence number. $-(N+2)$, where N = number of data records.
3	Orbit number.
4	Day of last scan on file.
5	GMT (seconds) of last scan on file.
6	Subsatellite latitude (degrees) at the beginning of last scan.
7	Subsatellite longitude (degrees) at the beginning of last scan.
8	View latitude - average for total ozone on last scan (degrees).
9	View longitude - average for total ozone on last scan (degrees).
10	Number of tape read errors.
11	Number of scans read.
12	Number of scans written.
13- 27	Total ozone processing counters.
28- 38	Profile processing counters.
39-207	Spare.

All words are in IBM floating-point format except for word 1, which contains hexadecimal data.

ZMT Trailer Documentation File

The Trailer Documentation File (TDF) is the last file on each volume (tape). It has the same structure as the standard header and contains a collection of standard headers (non-duplicated) from all input tapes that were used to produce the tape. The TDF is written in EBCDIC and is used to identify the genealogy of each tape. It is present only for tapes with an * in the first byte (character) of the NOPS standard header file. Since the TDF capability was implemented only after the data processing system was operational, not all tapes have such a file. The first record identifies the file as the TDF:

```
Characters  1-10:  *****  
  
            11-116:  NOPS TRAILER DOCUMENTATION FILE FOR  
                    TAPE PRODUCT T(SPEC NO. #(6 DIGIT)  
                    GENERATED ON YYY DDD HHMM.
```

The second physical record will be a repeat of the Standard Header File for the ZMT tape, except that data referring to end time are correct. Subsequent physical records contain the standard header records from the various input tapes in the production stream leading to the ZMT.

REFERENCES

- Bates, D. R., Rayleigh scattering by air, *Planet. Sp. Sci.*, 32, 785-790, 1984.
- Bhartia, P. K., K. F. Klenk, V.G. Kaveeshwar, S. Ahmad, A. J. Fleig, R. D. McPeters, and C. L. Mateer, Algorithm for vertical ozone profile determination for the Nimbus-4 BUV data set, *Proceedings, Fourth Conference on Atmospheric Radiation*, Toronto, Ont., Canada, pp. 27-32, 1981.
- Bhartia, P. K., D. Silberstein, B. Monosmith, and Albert J. Fleig, Standard profiles of ozone from ground to 60 km obtained by combining satellite and ground based measurements, in *Atmospheric Ozone*, edited by C. S. Zerefos and A. Ghazi, pp. 243-247, D. Reidel, Dordrecht, 1985.
- Cebula, R. P., H. Park, and D. F. Heath, Characterization of the Nimbus-7 SBUV radiometer for the long-term monitoring of stratospheric ozone, *J. Atm. Ocean. Tech.*, 5, 215-227, 1988.
- Chapman, S., The absorption and dissociative or ionizing effect of monochromatic radiation in an atmosphere on a rotating earth, *Proc. Phy. Soc. (London)*, 43, 483-501, 1931.
- Chubachi, S., A special ozone observation at Syowa station, Antarctica, from February 1982 to January 1983, in *Atmospheric Ozone*, edited by C. S. Zerefos and A. Ghazi, pp. 285-289, D. Reidel, Dordrecht, 1985.
- Dave, J. V., Meaning of successive iteration of the auxiliary equation of radiative transfer, *Astrophys. J.*, 140, 1292-1303, 1964.
- Dave, J. V., Effect of aerosols on the estimation of total ozone in an atmospheric column from the measurement of its ultraviolet radiance, *J. Atmos. Sci.*, 35, 899-911, 1978.
- DeLuisi, John J., Umkehr profile errors caused by the presence of stratospheric aerosols, *J. Geophys. Res.*, 84, 1766-1770, 1979.
- DeLuisi, J. J., T. DeFoor, K. Coulson, and F. Fernald, Lidar observations of stratospheric aerosol Over Mauna Loa, 1982-1983, *NOAA Data Report ERL ARL-5*, 1985.
- DeLuisi, J. J., C. L. Mateer, and W. D. Komhyr, Effects of the El Chichon stratospheric cloud on Umkehr measurements at Mauna Loa, Hawaii, in *Atmospheric Ozone*, edited by C. S. Zerefos and A Ghazi, pp. 316-320, D. Reidel, Dordrecht, 1985.
- Environmental Science Services Administration, National Aeronautics and Space Administration, and United States Air Force, U. S. standard atmosphere supplements, 1966, U. S. Government Printing Office, Washington, D. C., 1966.
- Fleig, Albert J., Pawan K. Bhartia., and David S. Silberstein, An assessment of the long-term drift in SBUV total ozone data, based on comparison with the Dobson network, *Geophys. Res. Lett.*, 13, 1359-1362, 1986.

- Fleig, A. J., D. F. Heath, K. F. Klenk, N. Oslak, K. D. Lee, H. Park, P. K. Bhartia, and D. Gordon, User's guide for the Solar Backscattered Ultraviolet (SBUV) and the Total Ozone Mapping Spectrometer (TOMS) RUT-S and RUT-T data sets, October 31, 1978 to November 1, 1980, *NASA Reference Publication 1112*, National Aeronautics and Space Administration, Washington, D. C., 1983.
- Fleig, A. J., K. F. Klenk, P. K. Bhartia, D. Gordon, and W. H. Schneider, User's guide for the Solar Backscattered Ultraviolet (SBUV) Instrument first-year Ozone-S data set, *NASA Reference Publication 1095*, National Aeronautics and Space Administration, Washington, D. C., 1982.
- Fleig, Albert J., David S. Silberstein, Charles G. Wellemeyer, Richard P. Cebula, and Pawan K. Bhartia, An assessment of the long-term drift in TOMS total ozone data, based on comparison with the Dobson network, *Geophys. Res. Lett.*, 15, 1133-1136, 1988.
- Fleig, A. J., C. Wellemeyer, N. Oslak, K. D. Lee, A. J. Miller, and R. Nagatani, User's guide for SBUV/TOMS ozone derivative products, *NASA Reference Publication 1116*, National Aeronautics and Space Administration, Washington, D. C., 1984.
- Fraser, R. S., and Z. Ahmad, The effect of surface reflection and clouds on the estimation of total ozone from satellite measurements. Fourth NASA Weather and Climate Program Science Review, *NASA Conf. Publ. 2076*, [NTIS N7920633] pp. 247-252, 1978.
- Heath, D. F., A. J. Krueger, and H. Park, in *The Nimbus-7 User's Guide*, edited by C. R. Madrid, pp. 175-187, NASA Goddard Space Flight Center, Greenbelt, MD, 1978.
- Heath, D. F., A. J. Krueger, H. A. Roeder, and B. D. Henderson, The Solar Backscatter Ultraviolet and Total Ozone Mapping Spectrometer (SBUV/TOMS) for Nimbus G, *Opt. Eng.*, 14, 323-331, 1975.
- Klenk, K. F., P. K. Bhartia, A. J. Fleig, V. G. Kaveeshwar, R. D. McPeters and P. M. Smith, Total ozone determination from the Backscattered Ultraviolet (BUV) experiment, *J. Appl. Meteor.*, 21, 1672-1684, 1982.
- Klenk, K. F., P. K. Bhartia, A. J. Fleig, and C. L. Mateer, Vertical ozone profile determination from Nimbus-7 SBUV measurements, in *Proceedings, Fifth Conference on Atmospheric Radiation*, Baltimore, MD, 1983.
- Krueger, A. J., Detection of volcanic eruptions from space by their sulfur dioxide clouds, *Proceedings AIAA 23rd Aerospace Sciences Meeting*, January 14-17, 1985.
- Logan, Jennifer A., and Volker W. J. H. Kirchhoff, Seasonal variations of tropospheric ozone over Natal, Brazil, *J. Geophys. Res.*, 91, 7879-7881, 1986.
- McPeters, R. D., The behavior of ozone near the stratopause from two years of BUV observations, *J. Geophys. Res.*, 85, 4545-4550, 1980.
- McPeters, R. D., R. D. Hudson, P. K. Bhartia, and S. L. Taylor, The vertical ozone distribution in the Antarctic ozone minimum measured by SBUV, *Geophys. Res. Lett.*, 13, 1213-1216, 1986.

- NASA, Nimbus-7 Solar Backscattered Ultraviolet and Total Ozone Mapping Spectrometer (SBUV/TOMS): Tape format for the Nimbus-7 Solar Backscattered Ultraviolet (SBUV) instrument CPOZ dataset (version 5), Goddard Space Flight Center, Greenbelt MD, 1986.
- NASA, Nimbus-7 Solar Backscattered Ultraviolet and Total Ozone Mapping Spectrometer (SBUV/TOMS); Third and fourth year addendum to the "User's guide for the Solar Backscattered Ultraviolet (SBUV) instrument first-year Ozone-S data set", Goddard Space Flight Center, Greenbelt MD., 1984.
- Ozone Data for the World; Atmospheric Environmental Service, Ontario Canada, Station #101, Syowa.
- Paur, R. J., and A. M. Bass, The ultraviolet cross-sections of ozone: II. Results and temperature dependence, in *Atmospheric Ozone*, edited by C. S. Zerefos and A Ghazi, pp. 611-616, D. Reidel, Dordrecht, 1985.
- Rodgers, C. D., Retrieval of atmospheric temperature and composition from remote measurements of thermal radiation, *Rev. Geophys. Sp. Phys.*, 14, 609-624, 1976.
- Taylor, S. L., P. K. Bhartia, V. G. Kaveeshwar, K. F. Klenk, A. J. Fleig, C. L. Mateer, Role of multiple scattering in ozone profile retrieval from satellite measurements in ultraviolet, *Remote Sensing of Atmospheres and Oceans*, Williamsburg Va., Academic Press, pp 219-231. 1980.
- Watson, R.T. and Ozone Trends Panel, M.J. Prather and Ad Hoc Theory Panel, and M.J. Kurylo and NASA Panel for Data Evaluation, Present state of knowledge of the atmosphere 1988: an assessment report, NASA Reference Publication 1208, 1988.

RELATED LITERATURE

- Bhartia, P. K., K. F. Klenk, A. J. Fleig, C. G. Wellemeyer and D. Gordon, Intercomparison of Nimbus-7 Solar Backscattered Ultraviolet (SBUV) ozone profile with rocket, balloon and Umkehr profiles, *J. Geophys. Res.*, 89, 227-5238, 1984.
- Bhartia, P. K., K. F. Klenk, C. K. Wong, and D. Gordon, Intercomparison of the Nimbus-7 SBUV/TOMS total ozone data sets with Dobson and M83 results, *J. Geophys. Res.*, 89, 5239-5247, 1984.
- Chandra, S., and R. D. McPeters, The intercomparison of ozone measured from the SME and Nimbus-7 satellites on short and long time scales, *Geophys. Res. Lett.*, 13, 1387-1390, 1986.
- Dave, J. V., Multiple scattering in a non-homogeneous, Rayleigh atmosphere, *J. Atmos. Sci.*, 22, 273-279, 1964.
- Dave, J. V., and Carlton L. Mateer, A preliminary study on the possibility of estimating total atmospheric ozone from satellite measurements, *J. Atmos. Sci.*, 24, 414-427, 1967.
- DeLuisi, John J., Carlton Mateer, and Pawan K. Bhartia, On the correspondence between standard Umkehr, short Umkehr, and Solar Backscattered Ultraviolet vertical ozone profiles, *J. Geophys. Res.*, 90, 3845-3849, 1985.
- Klenk, K. F., P. K. Bhartia, E. Hilsenrath, and A. J. Fleig, Standard ozone profiles from balloon and satellite data sets, *J. Climate Appl. Meteorol.*, 12, 2012-2022, 1983.
- Madrid, C. L. (Ed.), *The Nimbus-7 Users' Guide*, National Aeronautics and Space Administration, 1978.
- McPeters, R. D., D. F. Heath, and P. K. Bhartia, Average ozone profiles for 1979 from the Nimbus-7 SBUV instrument, *J. Geophys. Res.*, 89, 5199-5214, 1984.
- McPeters, R. D., D. F. Heath, and B. M. Schlesinger, Satellite observation of SO₂ from El Chichon: identification and measurement, *Geophys. Res. Lett.*, 11, 1203-1206, 1984.
- Schneider, W. H., P. K. Bhartia, K. F. Klenk, and C. L. Mateer, An optimum statistical technique for ozone profile retrieval from backscattered UV radiances, in *Proceedings, Fourth Conference on Atmospheric Radiation*, Toronto, Ont., Canada, pp. 33-37, 1981.
- Twomey, Sean, On the deduction of the vertical distribution of ozone by ultraviolet spectral measurements from a satellite, *J. Geophys. Res.*, 66, 2153-2162, 1961.
- Yarger, D. N., An evaluation of some methods of estimating the vertical atmospheric ozone distribution from the inversion of spectral ultraviolet radiation, *J. Appl. Meteor.*, 9, 921-928, 1970.

PRECEDING PAGE BLANK NOT FILMED

LIST OF ACRONYMS, INITIALS, AND ABBREVIATIONS

a.u.	astronomical units
atm.	atmospheres
bpi	bits per inch
BUV	Backscatter Ultraviolet
CPOZ	Compressed Ozone
EBCDIC	Extended Binary Coded Decimal Interchange Code
FB	Fixed Block
FOV	Field of View
FWHM	Full Width at Half Maximum
GMT	Greenwich Mean Time
HDOZ	High Density Ozone
HDSBUV	High-Density SBUV
Ifov	Instantaneous Field of View
IPD	Information Processing Division
M. R.	Mixing ratio
MSR	Multiple Scattering and Reflectivity
NBS	National Bureau of Standards
NET	Nimbus Experiment Team
NMC	National Meteorological Center
NOAA	National Oceanic and Atmospheric Administration
NOPS	Nimbus Operational Processing System
NSSDC	National Space Science Data Center
OPT	Ozone Processing Team
PDF	Product Definition File
PMT	Photomultiplier Tube
rms	Root-mean-square

RSS	Root sum of squares
RUT	Raw Unit Tape
SACC	Science and Applications Computing Center
SBUV	Solar Backscatter Ultraviolet
SOI	SO ₂ Index
SPAN	Space Physics Analysis Network
SUNC	Spectral scan solar irradiance tape
TDF	Trailer Documentation File
THIR	Temperature Humidity Infrared Radiometer
TOMS	Total Ozone Mapping Spectrometer
UV	ultraviolet
VCI	Volcano Contamination Index
VIP	Versatile Information Processor
ZMT	Zonal Means Tape

APPENDIX A

DEFINITION OF SBUV PROFILE LAYER AND LEVELS

SBUV ozone profiles are reported in two separate ways:

1. as ozone amounts (matm-cm) in 12 atmospheric layers with their 1σ uncertainties expressed as a percentage of the layer amounts.
2. as ozone mass mixing ratios at 19 selected pressure levels from 0.3 mbar to 100 mbar.

Error bars are not reported for mixing ratios because they are virtually the same as those for layer amounts for a vertically smooth ozone profile.

Table A.1 defines the layers for which SBUV layer ozone amounts are reported. Most of these layers are similar to those used by operational Umkehr technique, except that they are numbered differently and that the Umkehr layer 1 spans 253-507 mbar.

Table A.1 also gives the pressure and altitude of the layer midpoints (defined in terms of altitude). These are useful quantities since the layer mean partial pressure reported by Umkehr is often very close to the true partial pressure at the layer midpoint for a vertically smoothed ozone profile. Layer ozone amounts (matm-cm), reported by SBUV, can be easily converted to layer mean partial pressures (nb) by multiplying by 1.828 for layers 2 through 11, and by 0.914 for layer 1.

Ozone mixing ratios O_3 are obtained from the following equation

$$O_3 = [(2.096/p)(dx/d \log p)], \quad (33)$$

where O_3 is the ozone mixing ratio in micrograms/gram, p is the pressure in millibars, and x is the cumulative ozone amount above pressure p in matm-cm, obtained by summing the layer amounts.

To obtain the necessary derivative, a cubic spline is fit to the x -log p curve. Simulation results show that this procedure does not increase the retrieval errors provided the x -log p curve is smooth, as it is for SBUV retrieval. The values of the solution profile mass mixing ratios are given in order of increasing atmospheric pressure at the 19 pressure levels: 0.3, 0.4, 0.5, 0.7, 1.0, 1.5, 2.0, 3.0, 4.0, 5.0, 7.0, 10, 15, 20, 30, 40, 50, 70, and 100 mbar.

Finally, it should be mentioned that ozone mixing ratios are often expressed as parts per million by volume (ppmv), which can be obtained by dividing the SBUV mixing ratio values (given in parts per million by mass) by 1.6547. Partial pressure (nbar) is obtained by multiplying the mixing ratio (ppmv) by the pressure (mbar).

Table A.1.
Standard Layers Used for Ozone Profiles

SBUV Layer No.	Corresponding Umkehr Layer No.	Layer Pressure (mb)	Pressure at Altitude at Midpoint (mb)	Layer Midpoint (km)
1	-	0.0	0.247	-
2	-	0.247	0.495	56.5
3	-	0.495	0.990	51.0
4	9	0.990	1.98	45.5
5	8	1.98	3.96	40.2
6	7	3.96	7.92	35.2
7	6	7.92	15.8	30.4
8	5	15.8	31.7	25.8
9	4	31.7	63.3	21.3
10	3	63.3	127.0	17.0
11	2	127.0	253.0	12.5
12	-	253.0	1013.0	5.5

APPENDIX B

FORTTRAN PROGRAMS TO READ HDSBUV, CPOZ, AND ZMT TAPES HDSBUV

```
//ZMPVRPV3 JOB (      ,910,15),'READ HDSBUV-TAPE ',TIME=(0,30),
// CLASS=A,MSGCLASS=X
// EXEC FORTRANV
//SYSIN DD *
C
C GENERAL PROGRAM TO READ DATA FILES OF HDSBUV TAPE
C
C FT05 INPUT
C
C     HDTAP = HIGH DENSITY TAPE NAME
C     IFILE = FIRST DATA FILE NUMBER
C     NFILE = NUMBER OF DATA FILES TO BE READ
C
REAL*8 HDTAP
REAL*4  BUFF(207)
INTEGER IBUFF(207)
EQUIVALENCE (BUFF(1),IBUFF(1))
C
C READ TAPE NAME, FIRST FILE # AND # OF FILES
READ(5,1000)HDTAP,IFILE,NFILE
1000 FORMAT(A8,I4,I4)
WRITE(6,2005) HDTAP,IFILE,NFILE
2005 FORMAT(5X,'HDTAP-',2X,A8,2X,'IFILE-',2X,I2,2X,'NFILE-',
12X,I2)
C
C MOUNT TAPE
CALL MOUNT(1,20,HDTAP,1)
C
C READ FILES
DO 200 NF=1,NFILE
IDF = NF + IFILE
CALL POSN(1,20,IDF)
100 CONTINUE
CALL FREAD(BUFF,20,LEN,*200,*910)
C SKIP FIRST RECORD
IF(BUFF(2).EQ. 1.) GO TO 100
C READ NEXT FILE IF AT END OF FILE
IF(BUFF(2).LT.-1.) GO TO 200
C WRITE DATA RECORD #, TOTAL OZONE LATITUDE AND LONGITUDE
WRITE(6,2000)BUFF(2),BUFF( 8),BUFF( 9)
2000 FORMAT(1X,F4.0,F6.1,F7.1)
GO TO 100
200 CONTINUE
GO TO 920
910 WRITE(6,1200)IDF
1200 FORMAT(' READ ERROR ON FILE',I6)
920 STOP
END
/*
// EXEC LINKGO,REGION.GO=256K
//GO.FT06F001 DD SYSOUT=X
//GO.FT20F001 DD UNIT=(9TRACK,,DEFER),LABEL=(,NL,,IN),DISP=OLD,
// DCB=(RECFM=FB,LRECL=828,BLKSIZE=16560,DEN=4),VOL=SER=HDTAP
//GO.DATA5 DD *
N21509      1  1

/*
// EXEC NOTIFYTS
//
```

CPOZ

```
//ZMPVRPVI JOB (      ,910,15),'READ CPOZ-TAPE ',TIME=(0,30),
// CLASS=A,MSGCLASS=X
// EXEC FORTRANV
//SYSIN DD *
```

```
C*****GENERAL PROGRAM EXAMPLE TO READ CPOZ TAPE ON
C*****IBM 3081 AND ACQUIRE SELECTED DATA FROM THE
C*****TAPE
C*****
C*****VARIABLE DEFINITIONS(ONLY THOSE VARIABLES
C*****WHOSE MEANING IS NOT OBVIOUS ARE DEFINED IN
C*****THIS SECTION).
C*****          CPOZ:CPOZ TAPE NAME
C*****          IFILE: FIRST FILE TO BE READ
C*****          NFILE : LAST FILE TO BE READ
C*****
```

```
REAL *8 CPOZ
REAL *4 BUFF(72)
REAL SEQ,ORBN,DAY,YEAR,SZA,XLAT,XLONG,TIME
REAL REFL,OZONET,OZONE
REAL OZ(12),RATIO(19),RATIO1(19)
INTEGER IFILE,NFILE
```

```
C*****
C*****READ TAPE NAME, FIRST FILE TO BE READ AND LAST
C*****FILE TO BE READ
```

```
5   CONTINUE
    READ(5, 1000,END= 940) CPOZ ,IFILE,NFILE
1000 FORMAT(A8,I4,I4)
    WRITE(6,2060) CPOZ,IFILE,NFILE
2060 FORMAT(5X,'CPOZ-',2X,A8,2X,'IFILE-',2X,I2,
           12X,'NFILE-',2X,I2)
```

```
C*****MOUNT THE TAPE
    CALL MOUNT (1,20,CPOZ,1)
C*****SKIP STANDARD HEADER FILE
```

```
    IF(IFILE.EQ.1)IFILE=2
C*****POSITION TAPE TO A FILE
    DO 200 NF = IFILE,NFILE
      CALL POSN(1,20,NF)
100 CONTINUE
C*****READ ONE LOGICAL RECORD FROM UNIT 20
    CALL FREAD(BUFF,20,LEN,*200,*910)
C*****IF SEQUENCE = -1, IT IS TRAILER FILE
C*****ON TAPE. GO READ NEXT TAPE.
    IF(BUFF(2).EQ.-1.) GO TO 5
C*****IF SEQUENCE IS 1 ; GET YEAR, DAY,ORBIT
C*****NUMBER
    IF(BUFF(2).NE.1.)GO TO 20
    SEQ = BUFF(2)
    ORBN = BUFF(3)
    DAY = BUFF(5)
    YEAR = BUFF(4)
```

CPOZ

```

        WRITE(6,2000) SEQ,ORBN,DAY,YEAR
2000   FORMAT(5X,'SEQUENCE:',2X,F8.2,2X,'ORBIT:',2X,
1      F8.2,2X,'DAY:',2X,F7.2,2X,'YEAR:',2X,F8.2)
        GO TO 100
20    CONTINUE
C*****IF SEQ IS LT -1 IT IS LAST RECORD ON A FILE.
C*****GO READ NEXT FILE
        IF(BUFF(2).LT.-1.)GO TO 200
C*****SEQUENCE IS GT 1. IT IS A DATA RECORD.
C*****GET TIME OF DAY, LATITUDE, LONGITUDE, SOLAR
C*****ZENITH ANGLE.
        SEQ = BUFF(2)
        TIME = BUFF(6)
        XLAT = BUFF(7)
        XLONG = BUFF(8)
        SZA = BUFF(9)
        WRITE(6,2005) SEQ,TIME,XLAT,XLONG,SZA
2005   FORMAT(5X,'SEQ:',2X,F8.2/10X,F8.2,2X,F8.2,2X,
1F8.2,2X,F8.2)
C*****CHECK DATA QUALITY FLAG (WORD(10)). IF FLAG
C*****IS 0,1,2, 11,12,13 ACCEPT DATA.
C*****GET REFLECTIVITY,TOTAL OZONE(NOT USING INFRARED
C*****CLOUD HEIGHT INFORMATION),TOTAL OZONE USING
C*****INFRARED CLOUD HEIGHT INFORMATION.
        IF(BUFF(10).LT.13.) THEN
            IF(BUFF(10).LT.3..OR.BUFF(10).GT.9.)THEN
                REFL = BUFF(11)
                OZONET = BUFF(12)
                OZONE = BUFF(13)
                WRITE (6,2015) REFL,OZONET,OZONE
2015   FORMAT(5X,F8.2,2X,F8.2,2X,F8.2)
            ENDIF
C*****IF FLAG IS 0, 1, OR 2 GET OZONE AMOUNTS IN 12
C*****LAYERS AND MIXING RATIOS IN 19 LAYERS
            IF( BUFF(10).LT.3.)THEN
                DO 210 J = 1,12
                    OZ(J) =BUFF(26 + J)
210     CONTINUE
                    WRITE(6,2020)(OZ(I), I =1 ,12)
2020   FORMAT(4(5X,F8.2))
                    DO 220 L = 1,19
                        RATIO(L) = BUFF(50+L)
220     CONTINUE
                    WRITE(6,2025)(RATIO(L1),L1=1,19)
2025   FORMAT(4(5X,F8.2))
            ENDIF
C*****IF FLAG EQUALS 10,11,12 THEN LOWER LAYERS ARE
C*****AFFECTED BY VOLCANIC CONTAMINATION. GET MIXING
C*****RATIOS FOR FIRST TEN LAYERS.
            IF(BUFF(10).GT.9.)THEN
                DO 230 J1= 1,10
                    RATIO1(J1)= BUFF(50+J1)
230     CONTINUE
                    WRITE(6,2025)(RATIO1(K1),K1=1,10)
            ENDIF
        ENDIF
        GO TO 100
200   CONTINUE
C*****
        GO TO 5

```

ZMT

```
//ZMPVRPV2 JOB ( ' ' .910,15), 'READ ZMT-TAPE ', TIME=(0,30),  
// CLASS=A,MSGCLASS=X  
// EXEC FORTRANV  
//SYSIN DD *
```

```
REAL*8 ZMT  
REAL*4   BUFF(180)  
REAL PRESS(19),ZMEAN(19),STDEV(19),DPT(19)  
REAL TOTPRE,ZMTOT,SIGTOT,REFL,SIGREF  
INTEGER*4 IBUFF(180)  
INTEGER IFILE,NFILE,IXLAT,IYEAR,IFLAG,ISPAN  
INTEGER NF,NDPT  
EQUIVALENCE (BUFF(1),IBUFF(1))  
  
C  
C*****  
5 CONTINUE  
  
C*****READ TAPE NAME, STARTING FILE ,ENDING FILE TO  
C*****BE READ.  
READ(5,1000,END=940)ZMT,IFILE,NFILE  
1000 FORMAT(A8,I4,I4)  
WRITE(6,2005) ZMT,IFILE,NFILE  
2005 FORMAT(5X,'ZMT:',2X,A8,2X,'IFILE:',2X,I4,2X,  
1'NFILE:',2X,I4)  
C*****MOUNT THE TAPE  
CALL MOUNT(1,20,ZMT,1)  
C*****SKIP THE STANDARD HEADER FILE  
IF (IFILE.EQ.1)IFILE=2  
DO 200 NF=IFILE,NFILE  
CALL POSN(1,20,NF )  
100 CONTINUE  
C*****READ ONE LOGICAL RECORD  
CALL FREAD(BUFF,20,LEN,*200,*910)  
C*****IF SEQ = -1 LAST FILE ON TAPE,GO READ NEXT TAPE  
IF(BUFF(2).EQ.-1.) GO TO 5  
C*****IF SEQ IS LESS THAN -1 LAST RECORD ON FILE. GO  
C*****READ NEXT FILE  
IF(BUFF(2).LT.-1.)GO TO 200  
C*****IF SEQ GREATER THAN OR EQUAL TO 1 IT IS A DATA  
C*****RECORD. GET LATITUDE, YEAR, TERMINATOR FLAG  
C*****GET ONLY MONTHLY DATA  
IF(IBUFF(7).NE.3)GO TO 100  
IXLAT = IBUFF(4)  
IYEAR = IBUFF(5)  
IFLAG = IBUFF(6)  
ISPAN = IBUFF(3)  
WRITE(6,2010)  
2010 FORMAT(5X, 'WRITING LATITUDE , YEAR TERMI-  
INATOR FLAG AND TIME SPAN')  
WRITE(6,2015) IXLAT,IYEAR,IFLAG,ISPAN  
2015 FORMAT(5X,I5,2X,I5,2X,I5,2X,I5)  
  
C*****GET PRESSURE, ZONAL MEANS, STD DEV, AND NUMBER  
C*****OF DATA POINTS AT VARIOUS PRESSURE LEVELS.  
DO 210 LEVEL = 1,19  
PRESS(LEVEL) = BUFF(7*LEVEL + 1)
```

ZMT

```

                ZMEAN(LEVEL) = BUFF(7*LEVEL + 2)
                STDEV(LEVEL) = BUFF(7*LEVEL + 3)
                DPT(LEVEL)   = BUFF(7*LEVEL + 6)
210  CONTINUE
C*****WRITE PRESSURE, STD DEV, ZONAL MEAN, NO. OF
C*****DATA POINTS FOR PRESSURE LEVELS OF 1.5 AND
C*****15.0 MBARS
        WRITE(6,2065)PRESS(6),ZMEAN(6),STDEV(6),DPT(6)
        WRITE(6,2065)PRESS(13),ZMEAN(13),STDEV(13),
        1DPT(13)
2065  FORMAT(5X,F8.3,2X,F8.3,2X,F8.3,2X,F8.3)
C*****GET PRESSURE , ZONAL MEAN, STD DEV, NUMBER OF
C*****DATA POINTS FOR TOTAL OZONE(PRESS OF 1000
C***** MBARS)
        TOTPRE = BUFF(141)
        ZMTOT  = BUFF(142)
        SIGTOT = BUFF(143)
        WRITE(6,2035) TOTPRE,ZMTOT,SIGTOT,NDTPT
2035  FORMAT(5X,F8.3,2X,F8.3,2X,F8.3,2X,I5)
C*****GET ZONAL MEAN REFLECTIVITY AND STD DEV OF
C*****ZONAL AVERAGE REFLECTIVITY
        REFL = BUFF(163)
        SIGREF = BUFF(164)
        WRITE(6,2040) REFL,SIGREF
2040  FORMAT(5X,F8.3,2X,F8.3)
        GO TO 100
200  CONTINUE
        GO TO 5
910  CONTINUE
        WRITE(6,2045) NF
2045  FORMAT(5X,'ERROR IN READING FILE',2X,I4)
        GO TO 920
940  CONTINUE
        WRITE(6,2050)
2050  FORMAT(5X,'LAST TAPE READ EXIT NOW')
920  CONTINUE
        STOP
        END

/*
// EXEC LINKGO,REGION.GO=256K
//GO.FT06F001 DD SYSOUT=X
//GO.FT20F001 DD UNIT=(9TRACK,,DEFER),LABEL=(,NL,,IN),DISP=OLD,
// DCB=(RECFM=FB,LRECL=720,BLKSIZE=21600,DEN=4),VOL=SER=HDTAP
//GO.DATAS DD *
ZMTS03      1  5
/*
// EXEC NOTIFYTS
//

```

ZMT

```
910 CONTINUE
    WRITE(6,2030) NF
2030 FORMAT(5X,'READ ERROR IN FILE',2X,I6)
    GO TO 920
940 CONTINUE
    WRITE(6,2040)
2040 FORMAT(5X,'LAST TAPE READ,EXIT NOW')
920 CONTINUE
    STOP
    END
```

```
/*
// EXEC LINKGO,REGION.GO=256K
//GO.FT06F001 DD SYSOUT=X
//GO.FT20F001 DD UNIT=(9TRACK,,DEFER),LABEL=(,NL,,IN),DISP=OLD,
// DCB=(RECFM=FB,LRECL=288,BLKSIZE=28800,DEN=4),VOL=SER=HDTAP
//GO.DATAS DD *
CPOZ01      1  2
/*
// EXEC NOTIFYTS
//
```

APPENDIX C

COEFFICIENTS FOR TEMPERATURE DEPENDENCE OF OZONE ABSORPTION

WAVELENGTH CHANNEL	C ₀	C ₁	C ₂
2557	309.60	-2.0994 X 10 ⁻²	-9.3894 X 10 ⁻⁵
2736	170.08	3.7852 X 10 ⁻²	18.251 X 10 ⁻⁵
2831	80.072	2.6479 X 10 ⁻²	-16.413 X 10 ⁻⁵
2877	48.650	3.3314 X 10 ⁻²	8.7041 X 10 ⁻⁵
2923	28.175	2.6358 X 10 ⁻²	6.3807 X 10 ⁻⁵
2976	14.053	2.0086 X 10 ⁻²	1.0029 X 10 ⁻⁴
3020	7.8066	1.3295 X 10 ⁻²	4.8393 X 10 ⁻⁵
3059	4.6220	9.8596 X 10 ⁻³	4.1681 X 10 ⁻⁵
3126	1.8264	5.45055 X 10 ⁻³	2.8263 X 10 ⁻⁵
3175	0.97295	3.0592 X 10 ⁻³	1.8348 X 10 ⁻⁵
3313	0.16543	7.2305 X 10 ⁻³	3.9015 X 10 ⁻⁶
3349	0.036449	3.7215 X 10 ⁻³	2.7058 X 10 ⁻⁶

ATMOSPHERIC TEMPERATURE PROFILES (°Kelvin)

LAYER PRESSURE (MB)	LATITUDE BAND		
	LOW	MID	HIGH
0-0.247	271	268	261
0.247-0.495	271	268	261
0.99-1.98	270	265	256
1.98-3.96	261	254	243
3.96-7.92	248	240	235
7.92-15.8	234	229	227
15.8-31.7	222	222	221
31.7-63.3	210	217	222
63.3-127	201	214	222
127-253	214	216	221
253-506	251	239	228
506-1013	283	273	260

$$\text{OZONE ABSORPTION} = C_0 + C_1 (T - 273.16) + C_2 (T - 273.16)^2$$

APPENDIX D

CLIMATOLOGICAL PROFILES USED FOR TOTAL OZONE TABLES
(matm-cm)

LOW LATITUDE (15°)

TOTAL OZONE

SBUV LAYER	225	275	325
12	26.0	26.0	26.0
11	5.0	6.0	10.0
10	7.0	16.0	31.0
9	25.0	52.0	71.0
8	62.2	75.2	87.2
7	57.0	57.0	57.0
6	29.4	29.4	29.4
5	10.9	10.9	10.9
4	3.2	3.2	3.2
1,2,3	1.3	1.3	1.3

MID-LATITUDE (45°)

SBUV LAYER	225	275	325	375	425	475	525
12	27.0	28.0	30.0	32.0	34.0	38.0	42.0
11	7.0	15.0	26.0	39.0	54.0	72.0	91.0
10	14.0	29.0	45.0	64.0	84.0	107.7	131.7
9	42.0	58.0	74.7	85.7	97.7	101.0	108.0
8	55.1	63.7	66.9	71.1	71.7	72.6	68.8
7	39.2	40.6	41.7	42.5	42.9	43.0	42.8
6	24.5	24.5	24.5	24.5	24.5	24.5	24.5
5	11.1	11.1	11.1	11.1	11.1	11.1	11.1
4	3.7	3.7	3.7	3.7	3.7	3.7	3.7
1,2,3	1.4	1.4	1.4	1.4	1.4	1.4	1.4

HIGH LATITUDE (75°)

SBUV LAYER	225	275	325	375	425	475	525
12	25.0	26.0	29.0	33.0	38.0	45.0	54.0
11	22.2	30.5	40.8	53.2	68.7	85.0	104.1
10	56.4	67.1	78.6	89.8	100.9	114.1	128.1
9	46.2	59.2	71.2	82.2	91.2	99.0	105.0
8	29.0	38.5	45.7	51.9	56.9	59.8	60.2
7	19.1	24.6	28.8	32.5	35.6	37.5	38.2
6	13.4	15.4	17.2	18.7	20.0	20.9	21.7
5	8.9	8.9	8.9	8.9	8.9	8.9	8.9
4	3.4	3.4	3.4	3.4	3.4	3.4	3.4
1,2,3	1.4	1.4	1.4	1.4	1.4	1.4	1.4

APPENDIX E

A PRIORI INFORMATION

The form of the first guess profile equation is as follows:

$$X_k = A_k + B_k(\text{Oz} - 300) + C_k(\text{Oz} - 300)^2; \text{ layers 10-12} \quad (34)$$

$$X_k = D_k + E_k \cos 2\pi/365(d - F_k); \text{ layers 1-7,} \quad (35)$$

where

A_k = layer ozone when total ozone = 300 matm-cm

B_k = linear coefficient of total ozone dependence

C_k = quadratic coefficient of total ozone dependence

D_k = seasonal mean layer ozone

E_k = amplitude of the annual wave for layer k

F_k = day of the peak of the annual variation in layer k

d = day of the year

Oz = total ozone (in matm-cm)

k = layer number.

Coefficients in First Guess Profile Equations

SBUV LAYER	75 COEF.	45 NORTH	15 NORTH	15 NORTH	45 SOUTH	75 SOUTH	SOUTH
12	A	27	29	24	24	29	27
	B	0.05	0.03	0	0	0.03	0.05
	C	0.0003	0.0001	0	0	0.0001	0.0003
11	A	35	20	8	8	20	35
	B	0.21	0.21	0.08	0.08	0.21	0.21
	C	0.0004	0.0004	0.0006	0.0006	0.0004	0.0004
10	A	72	37	23	23	37	72
	B	0.22	0.33	0.30	0.30	0.33	0.22
	C	0.0001	0.0004	0.0012	0.0012	0.0004	0.0001
7	D	31.4	42.5	56.4	56.6	42.1	29.8
	E	4.5	4.0	2.7	2.9	4.5	4.8
	F	54	173	179	1	-10	-45
6	D	17.9	24.5	29.2	29.6	24.4	18.1
	E	1.8	2.4	0.5	1.6	2.2	3.2
	F	90	173	181	1	-15	-27
5	D	9.0	10.9	10.8	10.9	11.2	8.8
	E	0.9	0.6	0.2	0.2	1.2	0.5
	F	87	0.0	-87	-54	-177	2
4	D	3.4	3.6	3.2	3.2	3.8	3.4
	E	1.0	0.8	0.1	0.1	1.2	1.1
	F	-2	-11	-89	-150	175	151
3	D	1.05	1.00	0.94	0.94	1.06	1.02
	E	0.38	0.16	0.027	0.33	0.26	0.40
	F	-5	-13	-144	-154	173	153
2	D	0.284	0.269	0.273	0.273	0.278	0.282
	E	0.84	0.017	0.008	0.005	0.034	0.085
	F	-1	-4	-171	-151	175	160
1	D	0.102	0.103	0.113	0.113	0.106	0.099
	E	0.018	0.003	0.004	0.001	0.002	0.013
	F	11	145	180	-101	-114	168

*A Priori Profile Covariance Matrix**

Layer Number	1	2	3	4	5	6	7	8	9	10	11	12
1	40.00	9.00	0	0	0	0	0	0	0	0	0	0
2		22.50	7.20	0	0	0	0	0	0	0	0	0
3			14.40	6.00	0	0	0	0	0	0	0	0
4				10.00	4.00	0	0	0	0	0	0	0
5					6.40	2.56	0	0	0	0	0	0
6						6.40	2.40	0	0	0	0	0
7							10.00	2.00	-4.50	0	0	0
8								10.00	3.00	-7.50	0	0
9									22.50	7.50	-15.75	0
10										62.50	0	-18.75
11											122.50	
12												62.50

* All elements must be multiplied by 10^{-3} .

APPENDIX F

INVENTORY OF HDSBUY TAPES

<u>Year of Satellite Lifetime</u>	<u>Time Span</u>	<u>Files</u>
1	10/31/78 - 01/27/79	1002
	01/28/79 - 04/28/79	1052
	04/29/79 - 07/28/79	897
	07/29/79 - 11/03/79	957
2	11/05/79 - 02/03/80	812
	02/03/80 - 05/03/80	884
	05/04/80 - 08/03/80	891
	08/03/80 - 11/01/80	910
3	11/04/80 - 01/31/81	885
	02/01/81 - 05/02/81	877
	05/03/81 - 07/31/81	885
	08/02/81 - 10/31/81	901
4	11/02/81 - 01/31/82	884
	01/31/82 - 05/01/82	885
	05/02/82 - 07/30/82	899
	08/01/82 - 11/06/82	985
5	11/07/82 - 02/05/83	873
	02/06/83 - 05/08/83	902
	05/08/83 - 08/13/83	975
	08/21/83 - 11/05/83	1024
6	11/06/83 - 01/14/84	912
	01/15/84 - 03/24/84	927
	03/25/84 - 06/02/84	931
	06/03/84 - 08/18/84	1021
	08/19/84 - 11/03/84	1025
7	11/04/84 - 01/27/85	1089
	01/27/85 - 04/13/85	1023
	04/14/85 - 06/29/85	1022
	06/30/85 - 09/14/85	1011
	09/15/85 - 11/02/85	655
8	11/03/85 - 01/19/86	1014
	01/19/86 - 04/05/86	1018
	04/06/86 - 06/22/86	1015
	06/22/86 - 09/06/86	1013
9	11/02/86 - 01/18/87	997

APPENDIX G

DATA AVAILABILITY AND COST

The derivative tape products defined in this User's Guide are archived and available from the National Space Science Data Center (NSSDC). The NSSDC will furnish limited quantities of data to qualified users without charge. The NSSDC may establish a nominal charge for production and dissemination if a large volume of data is requested. Whenever a charge is required, a cost estimate will be provided to the user prior to filling the data request.

Domestic requests for data should be sent to the following address:

National Space Science Data Center
NASA/Goddard Space Flight Center
Code 633
Greenbelt, MD 20771
Telephone: (301) 286-6695
Telex: 89675NASCOMGBLT
TWX Number: 7108289716

All requests from foreign researchers must be specifically addressed to:

Director, World Data Center A for
Rockets and Satellites
NASA/Goddard Space Flight Center
Code 630.2
Greenbelt, MD 20771 USA
Telephone: (301) 286-6695
Telex: 89675NASCOMGBLT
TWX Number: 7108289716

When ordering data from either NSSDC or the World Data Center, a user should specify why the data are needed, the subject of the work, the name of the organization with which the user is connected, and any Government contracts under which the study is being performed. Each request should specify the experiment data desired, the time period of interest, and any other information that would facilitate the handling of the data request.

A user requesting data on magnetic tapes should provide additional information concerning the plans for using the data (i.e., what computers and operating systems will be used). In this context, the NSSDC is compiling a library of routines that can unpack or transform the contents of many of the data sets into formats that are appropriate for the user's computers. NSSDC will provide, upon request, information concerning its services. When requesting data on magnetic tape the user must specify whether he or she will supply new tapes prior to the processing, or return the original NSSDC tapes after the data have been copied.

Data product order forms may be obtained from NSSDC/World Data Center A.

NSSDC is a node on SPAN (Space Physics Analysis Network), and it can be reached in two additional ways. Electronic Mail can be directed to NCS::REQUEST. If Telemail is used, the current addresses are JLGREEN, JVETTE, or JKING.



Report Documentation Page

1. Report No. NASA RP-1234		2. Government Accession No.		3. Recipient's Catalog No.	
4. Title and Subtitle NIMBUS 7 SOLAR BACKSCATTER ULTRAVIOLET (SBUV) OZONE PRODUCTS USER'S GUIDE				5. Report Date January 1990	
				6. Performing Organization Code 636	
7. Author(s) Albert J. Fleig, R. D. McPeters, P. K. Bhartia, Barry M. Schlesinger, Richard P. Cebula, K. F. Klenk, Steven L. Taylor, and Donald F. Heath				8. Performing Organization Report No.	
				10. Work Unit No.	
9. Performing Organization Name and Address Goddard Space Flight Center Greenbelt, Maryland 20771				11. Contract or Grant No. NAS5-29386	
				13. Type of Report and Period Covered Reference Publication	
12. Sponsoring Agency Name and Address National Aeronautics and Space Administration Washington DC 20546-0001				14. Sponsoring Agency Code	
				15. Supplementary Notes Albert J. Fleig, R. D. McPeters, and Donald F. Heath: Goddard Space Flight Center, Greenbelt, Maryland P. K. Bhartia, Barry M. Schlesinger, Richard P. Cebula, K. F. Klenk, and Steven L. Taylor: ST Systems Corporation (STX), Lanham, Maryland.	
16. Abstract <p>Three ozone tape products from the Solar Backscatter Ultraviolet (SBUV) experiment aboard Nimbus 7 have been archived at the National Space Science Data Center. The experiment measures the fraction of incoming radiation backscattered by the Earth's atmosphere at 12 wavelengths. In-flight measurements have been used to monitor changes in the instrument sensitivity. Total column ozone is derived by comparing the measurements with calculations of what would be measured for different total ozone amounts. The altitude distribution is retrieved using an optimum statistical technique for the inversion. The estimated initial error in the absolute scale for total ozone is 2%, with a 3% drift over 8 years. The profile error depends on latitude and height, smallest at 3-10 mbar; the drift increases with increasing altitude. Three tape products are described. The High Density SBUV (HDSBUV) tape contains the final derived information generated during the retrieval process. The Compressed Ozone (CPOZ) tape contains only that subset of HDSBUV information, including total ozone and ozone profiles, considered most useful for scientific studies. The Zonal Means Tape (ZMT) contains daily, weekly, monthly and quarterly averages of the derived quantities over 10° latitude zones.</p>					
17. Key Words (Suggested by Author(s)) Ozone Nimbus 7 SBUV Stratosphere			18. Distribution Statement Unclassified - Unlimited Subject Category 46		
19. Security Classif. (of this report) Unclassified		20. Security Classif. (of this page) Unclassified		21. No. of pages 128	22. Price A07